CHAPTER 1 INTRODUCTION

1.1 Motivation and Background

In the 3G/4G (the third/fourth-generation) digital cellular systems, wireless networks and devices will support not only voice communication but also other high-speed data and multimedia services including facsimile, file transfer, e-mail and video teleconferencing. These services require the high data rate with low delay and bit error rate (BER). Supporting these requirements is challenging since wireless systems are subjected to many major constraints such as a complex and harsh fading channel, a scare useable radio spectrum, and limitations on the power and size of hand-held terminals [77]. Although increasing the transmitted power and channel bandwidth may improve the data rate in wireless systems, these radio resources are very scarce and expensive in a practical communication link [77], [79]. Moreover, increasing the transmitted power leads to raise the power of interference and reduces the battery lifetime of mobile transmitters. Therefore to obtain a high data rate together with reliable transmission in wireless systems, the effective spectral and power efficient fading mitigation techniques are required. In this dissertation, two particular techniques such as diversity combining techniques and cooperation communications to improve the performance of wireless systems are presented. In these techniques, the improvement is achieved without an increase in the transmitted bandwidth and power but at the expense of a higher system complexity.

1.2 Diversity Combining Techniques

For point-to-point wireless communications, various diversity combining techniques such as selection combining (SC), maximum ratio combining (MRC), and equal gain combining (EGC) have been proposed to mitigate the detrimental effects of multipath

fading in the wireless channels [3], [4], [11], [17], [19], [66-69]. In the absence of interference, MRC offers the best performance improvement but comes at the expense of complexity since it requires the knowledge of all channel fading parameters [36], [77]. Alternative combining techniques such as EGC and SC are often used in the practice because of their reduced complexity relative to the MRC. However, since many practical wireless systems suffer from both interference and noise, attention has also turned recently to the analysis of a communication link with the presence of channel noise as well as multiple co-channel interferers (CCI) [1], [23]. In this case, the optimum combining (OC) that maximizes the output signal-to-interference-plus-noise ratio (SINR) has been widely studied in the literature [2], [23], [29], [34-35], [72-73], [89].

1.3 Cooperative Communications

Although diversity combining techniques can unfold their huge benefit in cellular base stations, they may face limitations which come from the deployment in mobile handsets. In particular, the typically small size and low power of mobile handsets make them impractical to deploy multiple antennas. An innovative approach to apply the diversity combining without deploying multiple antennas is the cooperative communications [44], [65]. The cooperative communications through multi-hop relaying technology has emerged as an effective tool to enhance the spectral efficiency and extend the coverage of cellular and ad hoc wireless networks [21], [56]. In particular, multi-hop relaying can enable the source and destination nodes to communicate through a set of cooperating relay nodes in which the transmitted signals propagate through cascaded relay nodes, with the aim of extending coverage and improving the performance of the network. For example, idle mobile stations between

the source and destination may be employed as relay nodes to provide extra diversity links [51]. Recently, the two main types of relaying protocols which are widely studied in the literature are amplify-and-forward (AF), and decode-and-forward (DF) relaying protocol.

1.3.1 Amplify-and-Forward (AF) Relaying Protocol

In the most commonly used signal processing technique at the relay, the information from the previous node is simply amplified and forwarded to the next node as shown in Figure 1.1; this is known as amplify-and-forward relaying protocol. In Figure 1.1, G_n^2 denotes the gain at the nth relay node. AF relaying protocol is very simple to implement as the relaying node essentially acts as an analog repeater. The resulting end-to-end SINR of AF relaying depends on the choice of gain adopted at relay node [40-42], [45], [51], [71].
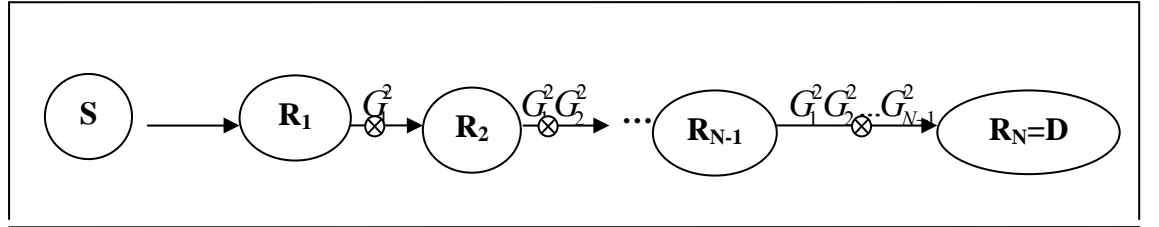

Figure 1.1 Multi-hop AF relaying systems

- **Optimum Channel-state Information (CSI)**

The optimal choice of the relay gain called the optimum channel-state information (CSI) assisted relay that maximizes the end-to-end SINR inverts a linear combination of the instantaneous channel gain and interference and noise powers at the relay node. The CSI gain at the nth relay node G_n^2 is given by [45], [51], [71]

$$G_n^2 = \frac{1}{\alpha_n^2 + \sigma_n^2 + \sum_{i=1}^{L_n} Z_{i,n}} \ , \tag{1.1}$$

where α_n is the fading amplitude of the desired signal at the nth node, and σ_n^2 is the noise power. The instantaneous power of the ith interferer at relay node n is denoted by $Z_{i,n}$, $i=1,2,...,L_n$, where L_n is the number of interferers.

- **Suboptimum Channel-state Information (suboptimum CSI)**

The suboptimal choice of the relay gain ignores the presence of interference and noise information and is given by [40], [71]

$$G_n^2 = \frac{1}{\alpha_n^2}.$$ (1.2)

- **Fixed Gain Relay**

For the simplification, the fixed or constant gain relay is chosen as [42], [71]

$$G_n^2 = \mathbf{E}\left[\frac{1}{\alpha_n^2 + \sigma_n^2 + \sum_{i=1}^{L_n} Z_{i,n}}\right],$$ (1.3)

where $\mathbf{E}[-]$ is the expected value operator.

1.3.2 Decode-and-Forward (DF) Relaying Protocol

In large networks with many geographically distributed nodes, AF relaying may be difficult to scale due to the strict synchronization requirement [65]. Alternatively, the receiving node may first decode the information in the received signal and then re-encodes it before forwarding it to the next node; this relaying format is referred to as decode-and-forward relaying protocol. DF relaying provides the possibility to vary the communication rate and prevents error propagation, but leads to higher decoder complexity.

In addition, there are other relay processing techniques that have also been studied in the literature. For example, the decode-amplify-and-forward (DAF) in which the relay performs soft decoding and forwards the reliability information at the output of the

decoder instead of that extracted directly from the raw channel, to the destination. The DAF protocol combines the merit of both AF and DF [15]. Also, the estimate-and-forward relay (EF) transmits a hyperbolic tangent function of the received signal to the destination [52]; the piecewise-and-forward (PF) provides a fine segment approximation of the EF protocol [84], while in several other protocols the relays provide more complicated functions of the received signals to the destination [37].

1.4 Objective

In this dissertation, we study the performance of OC technique and multi-hop AF&DF relaying systems operating over multipath fading channels in the presence of interference and thermal noise. The main dessertation objective is to provide easy-to-compute analytical expressions that allow the researcher or system designer to perform the comparison and tradeoff (performance versus complexity) studies among various communication types and OC technique/ multi-hop AF&DF relaying systems so as to determine the optimum choice in the face of his/her available constraints.

1.5 Outline

The remainder of the dissertation is organized as follows. In Chapter 2, a brief review of the principal characteristics and models of wireless fading channels are presented while in Chapter 3 the derivations for several system performance measures such as moment generating function (MGF), outage probability, average symbol error rate (ASER) for digital modulation schemes, amount of fading (AoF), and channel capacity are shown. Then in Chapter 4 the performance of OC combining technique operating over Generalized Gamma (GG) fading environment in the presence of co-channel interference is investigated. Also several performance measures such as outage

probability, MGF, and ASER for digital modulation schemes are derived in this chapter. In addition, the performance of dual-hop AF relaying system operating over Raleigh fading environment in the presence of co-channel interference and noise is studied in Chapter 5. Moreover, the outage probability in terms of the incomplete Weber function, which can be easily evaluated numerically is derived. An approximate expression for the outage probability, which is quite accurate for moderate and large average signal powers along the source-relay and relay-destination links is also provided. Based on this approximation the average bit error rate for both coherent and non-coherent/differentially coherent binary modulations are then derived as well. In Chapter 6, the performance of multi-hop AF&DF relay transmission systems operating in a Rayleigh fading environment in the presence of both CCI and thermal noise are evaluated. Several performance measures for these multi-hop relay systems such as the outage probability, the average symbol error rate, and the average channel capacity are obtained. Moreover in Chapter 7, the outage performance of multi-hop AF&DF relay transmission systems in the interference-limited Nakagami-m fading channels are also obtained in terms of the Lauricella multivariate hypergeometric function of the second kind which can be easily and accurately computed by the software programs e.g., MAPLE and MATHEMATICA. The accuracy of the analytical results is then verified and depicted by computer simulation. Finally, the concluding remarks and future work are given in Chapter 8.

CHAPTER 2 MODELING OF WIRELESS FADING CHANNELS

Radio-wave propagation through wireless channel is a complicated phenomenon characterized by various effects, such as multipath and shadowing. A precise mathematical description of this phenomenon is either unknown or too complex for tractable wireless system analyses. However, considerable efforts have been devoted to the statistical modeling and characterization of these different effects. The result is range of relatively simple and accurate statistical models for fading channels which depend on the particular propagation environment and the underlying communication scenario. In this chapter, the three common effects that are often encountered in wireless systems such as multipath fading, shadowing and composite multipath/shadowing are presented. The simple and accurate statistical models for characterization of these different effects are then provided.

2.1 Multipath Fading

Multipath fading is due to the constructive and destructive combination of randomly delayed, reflected, scattered, and diffracted signal components [36], [70], [77], [83]. Depending on the nature of radio propagation environments, there are two main statistical models that can be used to describe behavior of multipath fading envelope, namely, Gaussian and non-Gaussian model.

2.1.1 Gaussian Model

A Gaussian model is commonly used in modelling wireless communication channels due to the mathematical tractability. Two well-known distributions of Gaussian model that are widely used to characterize behavior of multipath fading envelope in both outdoor and indoor environment are Rayleigh and Rice distribution [18].

- **Rayleigh Distribution**

Rayleigh distribution is frequently used to model signal multipath fading with no direct line-of-sight (LOS) path. In this case, the channel amplitude α is distributed according to

$$f_\alpha(\alpha) = \frac{2\alpha}{\Omega} \exp\left(-\frac{\alpha^2}{\Omega}\right), \tag{2.1}$$

where Ω is average mean-square value, $\Omega = \left|\alpha^2\right|$.

Using [77, eq. (2.3)], the probability density function (pdf) of the instantaneous signal-to-noise (SNR) ratio, γ can be given by

$$f_\gamma(\gamma) = \frac{f_\alpha\left(\sqrt{\Omega\gamma/\bar{\gamma}}\right)}{2\sqrt{\gamma\bar{\gamma}/\Omega}}, \tag{2.2}$$

where $\bar{\gamma} = \Omega/\sigma^2$ is average signal-to-noise ratio and σ^2 is the power of noise.

Substituting (2.1) in (2.2), the pdf of γ can then be shown as

$$f_\gamma(\gamma) = \frac{1}{\bar{\gamma}} \exp(-\gamma/\bar{\gamma}). \tag{2.3}$$

- **Rice Distribution**

Rice distribution is often used to model propagation paths consisting one strong direct LOS component and many random weak components [18]. In this case, the channel amplitude α is given by

$$f_\alpha(\alpha) = \frac{2\alpha(1+K)}{\Omega} e^{-K} \exp\left(-\frac{(1+K)\alpha^2}{\Omega}\right) I_0\left(2\alpha\sqrt{\frac{K(1+K)}{\Omega}}\right), \tag{2.4}$$

where K is the Rician factor and $I_0(.)$ is the modified Bessel function of the first kind and zero order [7].

Using (2.2), the pdf of the instantaneous signal-to-noise (SNR) ratio is given by

$$f_\gamma(\gamma) = \frac{(1+K)}{\overline{\gamma}} e^{-K} \exp\left(-\frac{(1+K)\gamma}{\overline{\gamma}}\right) I_0\left(2\sqrt{\frac{K(1+K)}{\overline{\gamma}}\gamma}\right). \qquad (2.5)$$

2.1.2 Non-Gaussian Model

Recall that the Gaussian distribution is commonly used to describe the multipath fading in an environment where there are a large number of received radio wave paths. Hence, Rayleigh and Rice model are derived theoretically by using a central limit theorem (CLT) argument [18]. However, when the number of incoming radio paths is limited, these distributions may not be the appropriate fading models since the conditions for validity of the CLT may not hold [18], [32]. In this situation, some evidence indicates that the signal amplitude can be well described by a non-Gaussian model such as Nakagami, and Weibull distribution [77].

- **Nakagami Distribution**

The pdf of Nakagami distribution is given by [77]

$$f_\alpha(\alpha) = \frac{2m^m \alpha^{2m-1}}{\Omega^m \Gamma(m)} \exp\left(-m\frac{\alpha^2}{\Omega}\right), \qquad (2.6)$$

where m is the Nakagami-m fading parameter.

Applying (2.2) shows that the average SNR is distributed according to gamma distribution given by

$$f_\gamma(\gamma) = \left(\frac{m}{\overline{\gamma}}\right)^m \frac{\gamma^{m-1}}{\Gamma(m)} \exp(-m\gamma/\overline{\gamma}). \qquad (2.7)$$

- **Weibull Distribution**

For Weibull distribution, the pdf of average SNR can be expressed as [26]

$$f_\gamma(\gamma) = \frac{b}{\overline{\gamma}} \gamma^{b-1} \exp\left(-\gamma^b/\overline{\gamma}\right), \qquad (2.8)$$

where b is the Weibull fading parameter with the range from 0 to ∞.

2.2 Shadowing

In terrestrial and satellite land-mobile system, the link quality is also affected by slow variation to the mean signal level due to the shadowing from terrain, building and trees. The communication system performance will be interrupted only on shadowing if the receiver is able to average out the fast multipath fading or using an efficient micro-diversity system eliminates the effect of multipath. The well-known distribution which can be model shadowing for various indoor and indoor environments is log-normal distribution [77], [82].

2.2.1 Log-normal Distribution

For log-normal distribution, the pdf of average SNR can be given by [77], [82]

$$f_\gamma(\gamma) = \frac{\varepsilon}{\sqrt{2\pi}\sigma\gamma} \exp\left(-\frac{\{10\log_{10}\gamma - \mu\}^2}{2\sigma^2}\right), \qquad (2.9)$$

where $\varepsilon = 10/\ln 10 = 4.3429$, μ and σ are the mean and the standard derivation of $10\log_{10}\gamma$, respectively.

2.3 Composite Multipath/Shadowing

A composite multipath/shadowed fading environment consists of multipath fading superimposed on log-normal shadowing. This environment is often encountered in the communication systems whose receiver does not average out the envelope fading due to multipath but rather, reacts to the instantaneous composite multipath/shadowed signal such as congested downtown areas with slow-moving pedestrian and vehicles, and mobile satellite systems [16], [27], [57], [77]. There are several composite models that were proposed in literatures such as Raleigh-lognormal [38], Nakagami-lognormal distribution [43], Generalized-K distribution [6], [62] and Generalized Gamma

distribution [78], [90]. The main concept of the composite model is that the instantaneous SNR, γ due to multipath fading is averaged over the conditional diversity of average SNR, $\bar{\gamma}$ due to shadowing. Therefore, the pdf of instantaneous SNR in the composite multipath/shadowed channel is given by [39], [77]

$$f_\gamma(\gamma) = \int_0^\infty f_\gamma(\gamma|\bar{\gamma}) f_{\bar{\gamma}}(\bar{\gamma}) d\bar{\gamma} .$$

(2.10)

2.3.1 Nakagami-lognormal Distribution

For Nakagami-lognormal distribution, the pdf of instantaneous SNR, γ is gamma distribution given in (2.7) while the pdf of average SNR, $\bar{\gamma}$ is log-normal distribution given by

$$f_{\bar{\gamma}}(w) = \frac{\varepsilon}{\sqrt{2\pi}\sigma w} \exp\left(-\frac{\{10\log_{10} w - \mu\}^2}{2\sigma^2}\right).$$

(2.11)

Substituting (2.7) and (2.11) in (2.10), the pdf of instantaneous SNR, γ in a Nakagami-lognormal fading channel can be given by

$$f_\gamma(\gamma) = \frac{m^m \varepsilon}{\Gamma(m)\sqrt{2\pi}\sigma} \gamma^{m-1} \int_0^\infty \frac{1}{w^{m+1}} \exp\left(-\frac{\{10\log_{10} w - \mu\}^2}{2\sigma^2}\right) dw .$$

(2.12)

Note that replacing $m=1$ in (2.12), (2.12) becomes Rayleigh-lognormal distribution. It is unfortunate that the result of (2.12) is not in closed form, thereby making the performance evaluation of communication links over this channel cumbersome. Therefore other tractable composite distributions such as Generalized-K and Generalized Gamma distribution are alternatively introduced in the literature.

2.3.2 Generalized-K Distribution

In Generalized-K distribution, the log-normal shadowing was approximated by a gamma shadowing which has the pdf given by [6], [62]

$$f_{\bar{\gamma}}(w) = \left(\frac{k}{\bar{\gamma}}\right)^{k} \frac{w^{k-1}}{\Gamma(k)} \exp(-kw/\bar{\gamma}), \tag{2.13}$$

where k is the Nakagami parameter for shadowing.

Substituting (2.7) and (2.13) in (2.10) yields

$$f_{\gamma}(\gamma) = \frac{m^{m}\gamma^{m-1}}{\Gamma(m)\Gamma(k)} \left(\frac{k}{\bar{\gamma}}\right)^{k} \int_{0}^{\infty} w^{k-m-1} \exp\left(-\left\{\frac{m\gamma}{w} + wk/\bar{\gamma}\right\}\right) dw. \tag{2.14}$$

Using the identity in [38, eq.(3.471.9)], the pdf of instantaneous SNR, γ in a Generalized-K fading channel can be given by

$$f_{\gamma}(\gamma) = \frac{\nu^{\beta+1}}{2^{\beta}\Gamma(m)\Gamma(k)} \gamma^{\frac{\beta-1}{2}} K_{k-m}\left(\nu\sqrt{\gamma}\right), \tag{2.15}$$

where now $\nu = \sqrt{4km/\bar{\gamma}}$, $\beta = k + m - 1$, and $K_m(.)$ is the modified Bessel function of the second kind and m^{th} order [7], [61].

2.3.3 Generalized Gamma Distribution

The other composite distribution which includes many well-known channel models for both multipath as well as shadowing is the Generalized Gamma distribution. This model includes the Rayleigh, Nakagami and Weibull as special cases, the log-normal distribution as a limiting case, and can also appropriately approximate the Suzuki distribution. The pdf of instantaneous SNR in a GG fading channel is given by [78]

$$f_{\gamma}(\gamma) = \left(\frac{k}{\bar{\gamma}}\right)^{a/c} \frac{c}{\Gamma(a/c)} \gamma^{a-1} \exp\left(-k\gamma/\bar{\gamma}\right)^{c}, \tag{2.16}$$

where k, a and c are GG fading parameters. These fading parameters can be chosen to introduce the different distributions for multipath fading and shadowing as shown in Table 2.1.

Table 2.1 The envelope distributions derived by GG distribution

Distributions	a	c	k
Generalized Rayleigh	2		
Rayleigh	2	2	1
Gamma			1
Chi	$2v$	2	
Nakagami-m	$2m$	2	m
Weibull		$a=c$	
Chi-square	$d/2$	1	1/2
Half-Gaussian	1	2	
One-sided exponential	1	1	
Log-normal		$c \to 0$	$k \to \infty$

CHAPTER 3 SYSTEM PERFORMANCE MEASURES

As the performance of wireless communication systems is degraded by several detrimental effects e.g. multipath fading, shadowing, co-channel interference and noise, it is important for the system designer to have the analytical measures that allow easy and accurate performance evaluation. In this chapter, the wireless system performance measures are presented including moment generating function, outage probability, average symbol error rate for digital modulation schemes, amount of fading (AoF), and channel capacity.

3.1 Moment Generating Function (MGF)

The moment generating function of output SINR is given by [58], [77]

$$M_\gamma(t) = \int_0^\infty e^{-t\gamma} f_\gamma(\gamma) d\gamma, \tag{3.1}$$

where $f_\gamma(\gamma)$ is the pdf of instantaneous SINR. Moreover, the MGF may be alternatively expressed as

$$M_\gamma(t) = 1 - \int_0^\infty e^{-t\gamma} \bar{F}_\gamma(\gamma) d\gamma, \tag{3.2}$$

where $\bar{F}_\gamma(\gamma)$ is the complementary cumulative density function (ccdf) of the SINR, defined as $\bar{F}_{\gamma_{eq_1}}(\gamma) = 1 - F_\gamma(\gamma)$. Note that the (3.2) is obtained from (3.1) by using integration by parts.

3.2 Outage Probability

The outage probability is defined as the probability that the output SINR γ falls below a predetermined protection ratio γ_{th} and is given by

$$P_{out} = \int_0^{\gamma_{th}} f_\gamma(\gamma)d\gamma = F_\gamma\left(\gamma_{th}\right), \tag{3.3}$$

where $F_\gamma(.)$ is the cumulative density function (cdf) of instantaneous SINR.

Furthermore, using the MGF-based approach, the outage probability can be evaluated as [5]

$$P_{out} = \mathcal{L}^{-1}\left[\frac{M_\gamma(t)}{t}\right]\Bigg|_{x=\gamma_{th}}, \tag{3.4}$$

where $\mathcal{L}^{-1}(.)$ is the inverse Laplace transform [38].

3.3 Average Symbol Error Rate (ASER)

The ASER which is an important performance study of digital communication systems with fading channel can be derived by averaging the conditional SER $P_s(\varepsilon|\gamma)$ over the instantaneous SINR γ as

$$\bar{P}_s = \int_0^\infty P_s(\varepsilon|\gamma)f_\gamma(\gamma)d\gamma. \tag{3.5}$$

The conditional SER $P_s(\varepsilon|\gamma)$ can be shown in a generic form as [63], [77], [87],

$$P_s(\varepsilon|\gamma) = \sum_{\tilde{z}=1}^{\tilde{Z}} \int_0^{\theta_{\tilde{z}}} \lambda_{\tilde{z}} \exp\left(-\frac{\phi_{\tilde{z}}\gamma}{\sin^2\theta}\right)d\theta, \tag{3.6}$$

where parameters $\tilde{Z}$, $\lambda_{\tilde{z}}$, $\phi_{\tilde{z}}$ and $\theta_{\tilde{z}}$ are used to represent the various modulation schemes as shown in Table 3.1.

Substituting (3.6) in (3.5), the average symbol error rate can be given by

$$\bar{P}_s = \sum_{\tilde{z}=1}^{\tilde{Z}} \int_0^{\theta_{\tilde{z}}} \lambda_{\tilde{z}} \int_0^\infty \exp\left(-\frac{\phi_{\tilde{z}}\gamma}{\sin^2\theta}\right)f_\gamma(\gamma)d\gamma d\theta,$$

$$= \sum_{\tilde{z}=1}^{\tilde{Z}} \int_0^{\theta_{\tilde{z}}} \lambda_{\tilde{z}} M_\gamma \left(\frac{\phi_{\tilde{z}}}{\sin^2 \theta} \right) d\theta , \qquad (3.7)$$

where $M_\gamma(t)$ is the MGF given in (3.1).

Table 3.1 The parameters of a generic form for several modulation schemes

Modulation Schemes	$\tilde{Z}$	$\lambda_{\tilde{z}}$	$\phi_{\tilde{z}}$	$\theta_{\tilde{z}}$
MPSK	1	$1/\pi$	$\sin^2(\pi/M)$	$\pi(1-1/M)$
MQAM	2	$4/\pi\left(1-1/\sqrt{M}\right)$	$3/2(M-1)$	$\dfrac{\pi}{2}$
		$-4/\pi\left(1-1/\sqrt{M}\right)^2$	$\dfrac{3}{2}(M-1)$	$\pi/4$
MPAM	1	$2/\pi(1-1/M)$	$3/\left(M^2-1\right)$	$\dfrac{\pi}{2}$
MSK	2	$\dfrac{2}{\pi}$	1	$\pi/2$
		$-\dfrac{1}{\pi}$	1	$\dfrac{\pi}{4}$
DE-BPSK	2	$2/\pi$	1	$\pi/2$
		$-2/\pi$	1	$\pi/4$
DE-QPSK	4	$-4/\pi$	1	$\dfrac{\pi}{2}$
		$-8/\pi$	$\dfrac{1}{2}$	$\pi/4$
		$\left(4/\pi^2\right)\cos^{-1}\left[(3\cos 2\theta-1)/(3\cos^3 2\theta-1)\right]$	$1/2$	$\dfrac{\pi}{6}$
		$\left(4/\pi^2\right)\left[\pi-\cos^{-1}\left((3\cos 2\theta-1)/(2\cos^3 2\theta)\right)-1\right]$	$1/2$	$\sin^{-1}\left(1/\sqrt{3}\right)/\pi^2$
			$1/2$	

3.4 Amount of Fading (AoF)

The AoF, or "fading figure," is a unified measure of the severity of the fading and is defined as [77],

$$\text{AoF} = \frac{\mathbf{E}\left[\gamma^2\right] - \left(\mathbf{E}[\gamma]\right)^2}{\left(\mathbf{E}[\gamma]\right)^2} , \qquad (3.8)$$

where $\mathbf{E}[.]$ is the expected value operator defined as $\mathbf{E}[x^n] = \int_0^\infty x^n f_x(x)dx$ [58]. In addition, using the MGF-based approach, $\mathbf{E}[.]$ may be defined as

$$\mathbf{E}\left[\gamma^n\right] = \frac{d^n}{dt^n} M_\gamma(t)\bigg|_{t=0} . \qquad (3.9)$$

3.5 Channel Capacity

Channel capacity is the tightest upper bound on the amount of information that can be

reliably transmitted over a communications channel which can be defined by

$$\bar{C} = W \int_0^\infty \log_2(1+\gamma) f_\gamma(\gamma) d\gamma, \qquad (3.10a)$$

$$= W \int_0^\infty \frac{\bar{F}_\gamma(\gamma)}{1+\gamma} d\gamma, \qquad (3.10b)$$

where W is the channel bandwidth.

CHAPTER 4 OPTIMUM COMBINING TECHNIQUE IN GENERALIZED GAMMA FADING CHANNELS

4.1 Introduction

As a consequence of the growing interest in wireless communication systems, much effort is being devoted to the channel characterization and modeling. This is obvious since the performance depends fundamentally on the channels under consideration, so a communication system design must be preceded by the study of channel characteristics. Wireless communication channels are mainly described by considering three separable phenomena, namely, multipath, shadowing, and composite multipath fading/shadowing [77]. There are different fading-shadowing distributions that have been used to model these composite fading such as Rayleigh-lognormal, and Nakagami-lognormal distribution. However as shown in Chapter 2, the main drawback of these composite fading models is their complicated mathematical forms which make the analytical performance evaluation very difficult. A relatively simple and versatile envelope distribution that generalizes many of the commonly used models for multipath and shadow fading is the Generalized Gamma distribution [28], [89]. The GG distribution can be used to account for both multipath fading and shadowing conditions and includes the Rayleigh, Nakagami and Weibull distributions as special cases, the lognormal distribution as a limiting case, and can appropriately approximate the Suzuki distribution as well [28], [89].

The GG distribution was originally introduced by Stacy [78] as a generalization of the gamma distribution. Due to the highly flexible form of the probability density function, it has applications in many areas. For example, in teletraffic analysis, Zonoozi and Dassanayake [94] have shown that the GG distribution is adequate to characterize the cell residence time of both new and handover calls in cellular mobile networks. In radar

applications it has been shown that the GG distribution, as a clutter model, encompasses a wide range of distributions ranging from the Rayleigh distribution to the Weibull distribution and other pdfs with longer tails based on the statistical moments and goodness-of-fit tests [12], [49]. In speech signal processing, Shin et al. [74] have shown that a two-sided GG distribution models speech signals better than the generalized Gaussian, Laplacian, or gamma distributions. In the context of image and video processing, it is important to know the pdf of the image signal in the discrete cosine transform (DCT) domain. The same authors showed that the DCT coefficients based on the GG distribution gives the best performance [75]. In the field of wireless communications, Coulson et al. [28] have shown, via simulation, that the GG pdf (like the Suzuki pdf) can characterize the behavior of multipath/shadowing fading. As a result the performance evaluation of digital mobile receivers in the presence of GG composite fading is of practical importance.

Although the Generalized Gamma distribution has been shown to adequately characterize the wireless channel in many practical fading environments, the study of performance results in such channels have so far limited to the case of no interferers. For example with the absence of interference, the performance of ASER for digital modulation schemes with no diversity in GG fading channel was studied in [4], [28]. Moreover the outage probability and the ASER of MRC, EGC, SC, and SWC receivers were obtained in [3], [66], [68]. However many wireless systems suffer both effects of interference and noise. In this case, the OC technique that maximizes the output signal-to-interference-plus-noise ratio should be employed at the receiver to mitigate the effects of CCI and noise. To the best our knowledge, the performance of OC receivers over GG fading channels with CCI is still not available in the open literature.

In this chapter, we investigate the system performance of OC operating over a GG fading channel in the presence of co-channel interference. The closed-form expressions for the important performance measures such as the outage probability, moment generating function, and average symbol probability for various digital modulation schemes are then derived.

4.2 System Model

In this section, we consider a wireless communication system employing optimum combining receivers in an interference-limited environment as shown in Figure 4.1.
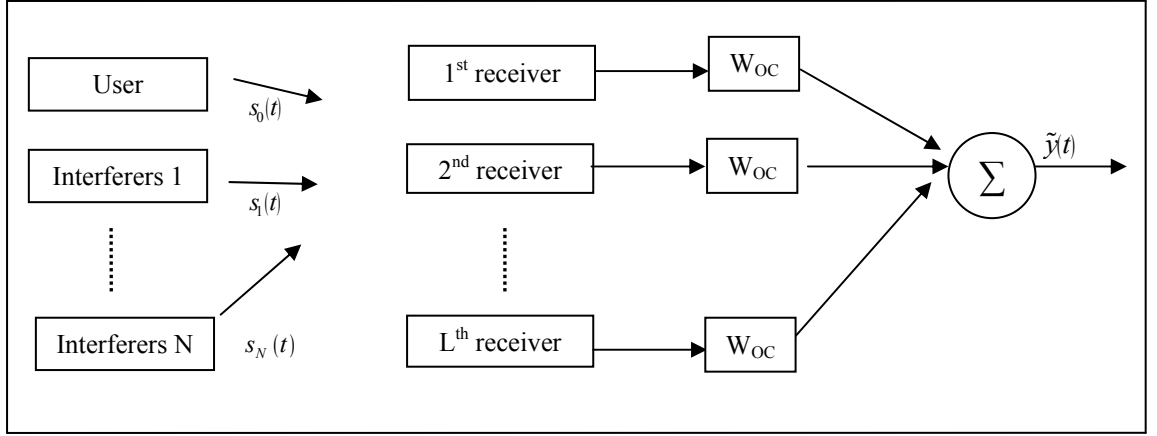
Figure 4.1 Optimum combining receivers with N interferers

In Figure 4.1, the system is dominated by the main effect of CCI. The received signal at the output OC receivers is then given by

$$\tilde{y}(t) = W_{OC}^{H} \left(\sqrt{\Omega_0} X_0 s_0(t) + \sum_{j=1}^{N} \sqrt{\Omega_j} X_j s_j(t) \right), \tag{4.1}$$

where X_0 and Ω_0 are the complex fading gain and power for desired signal $s_0(t)$, and $s_j(t)$ is the jth co-channel interference signal at the output with complex channel gain X_j and power Ω_j. The OC weighted vector gain is denoted by W_{oc} and a superscript H is the Hermitian transpose.

Also assuming that the complex fading gains X_0 and X_j follow the spherically invariant random process (SIRP) so-called the spherically invariant random vector (SIRV) [24], [64], [86]. Therefore, they can be characterized by the product of a non-negative random vector (u) and a Gaussian random vector (z), as $X_0 = u_0 Z_0$ and $X_j = u_j Z_j$ [92]. It is noted that the pdf of u which is used to classify the types of the SIRP is called the characteristic pdf (Cpdf) of an SIRP [86].

The weight vector W_{oc} that maximizes the output signal-to-interference ratio (SIR) is given by [89]

$$W_{OC} = \tilde{R}^{-1} X_0 = \left[\sum_{i=1}^{N} \Omega_i X_i X_i^H \right]^{-1} X_0,$$ (4.2)

where $\tilde{R}$ is the interference covariance matrix given by [72], [73].

Noting that all interference signals have equal power $\Omega = \Omega_1 = ,...,\Omega_N$ and are modulated by the same independent positive random variable $\tilde{u}$, which is independent of u_0 that modulates the desired signal [24]. Therefore, the interference covariance matrix $\tilde{R}$ may be expressed as

$$\tilde{R} = \left[\sum_{i=1}^{N} X_i X_i^H \right] = \tilde{u}^2 \Omega \left[\sum_{i=1}^{N} Z_i Z_i^H \right].$$ (4.3)

Substituting (4.2) and (4.3) in (4.1), the output SIR γ of OC combiners can be written as

$$\gamma = X_0^H \tilde{R}^{-1} X_0,$$

$$= \frac{\Omega_0}{\Omega} \left(u_0 / \tilde{u} \right)^2 Z_0^H \left[\sum_{i=1}^{N} Z_i Z_i^H \right]^{-1} Z_0.$$ (4.4)

Conditioning on the positive random variable u_0 and $\tilde{u}$, the random variable γ has the Hotelling T^2 statistic and can be written as the ratio of two independent central Chi-square random variables [72], i.e,

$$\gamma = \frac{\chi_{2L}}{\tilde{\chi}_{2(N-L+1)}},$$ (4.5)

where χ_{2L} and $\tilde{\chi}_{2(N-L+1)}$ are the central Chi-square random variables with degree of freedom (DOF) $=2L$ and $2(N-L+1)$, respectively. Therefore, the pdf of SIR γ, conditioned on u_0^2 and $\tilde{u}^2$, $f_\gamma\left(\gamma \mid u_0^2, \tilde{u}^2\right)$ can be expressed as

$$f_\gamma\left(\gamma \mid u_0^2, \tilde{u}^2\right) = \left(\frac{1}{u_0^2\Omega_0}\right)^L \left(\frac{1}{\tilde{u}^2\Omega}\right)^{N-L+1} \frac{\gamma^{L-1}}{\Gamma(L)\Gamma(N-L+1)} \int_0^\infty \tilde{\chi}^N \exp\left(-\tilde{\chi}\left[\frac{\gamma}{u_0^2\Omega_0}+\frac{1}{u^2\Omega}\right]\right) d\tilde{\chi}.$$ (4.6)

Using [38, eq.(3.3814)] and [8], the integral term in (4.6) may be expressed as

$$f_\gamma\left(\gamma \mid s\right) = \frac{(s\Lambda)^{-L}\gamma^{L-1}}{\Gamma(L)\Gamma(N-L+1)} G_{1,1}^{1,1}\left(\frac{s\Lambda}{\gamma} \middle| \begin{matrix} 1 \\ N+1 \end{matrix}\right),$$ (4.7)

where $G(.)$ is the Meijer-G function [38], [53], $\Lambda = \Omega_0/\Omega$ is the average SIR and $s = u_0^2/\tilde{u}^2$ is the random variable that depends on the chosen Cpdfs of SIRP. Therefore the pdf of the output SIR γ for OC receivers in an SIRP fading channel can be obtained by

$$f_\gamma(\gamma) = \frac{\Lambda^{-L}\gamma^{L-1}}{\Gamma(L)\Gamma(N-L+1)} \int_0^\infty s^{-L} G_{1,1}^{1,1}\left(\frac{s\Lambda}{\gamma} \middle| \begin{matrix} 1 \\ N+1 \end{matrix}\right) f_S(s)\,ds.$$ (4.8)

4.2.1 The Characteristic pdf (Cpdf) of SIRP Envelope Distribution

The envelope of SIRV can be given by $R_X = uR_Z$ where $R_Z = \left[Z_c^2 + Z_s^2\right]^{1/2}$ is the envelope component of zero-mean Gaussian vector.

The pdf of R_X is given by [64], [86]

$$f_{R_X}(r) = r\int_0^\infty u^{-2}\exp\left(-\frac{r^2}{2u^2}\right) f_u(u)\,du,$$ (4.9)

where $f_u(u)$ is the Cpdf of SIRP envelope distribution.

On the other hand, the pdf of the non-negative random, u may be expressed as

$$f_u(u) = \int_0^\infty r_Z f_{R_X}(ur_Z|r_Z) f_{R_Z}(r_Z) dr_Z. \tag{4.10}$$

Note that (4.10) requires the knowledge of $f_{R_X}(r_X)$ and $f_{R_Z}(r_Z)$. For the case of $f_{R_X}(r_X)$ being the Generalized Gamma distribution which includes many useful distributions for modeling wireless fading channels such as Rayleigh, Nakagami, Weibull and lognormal distribution as shown in Chapter 2. Moreover in the case of no direct LOS path, $f_{R_Z}(r_Z)$ is modeled by Rayleigh distribution.

Therefore substituting (2.3) and (2.16) in (4.10) and using [8, eq.(11)], yields

$$f_u(u) = \frac{k^{a/c} c u^{a-1}}{\Gamma(a/c)} \int_0^\infty r^{a+1} G_{0,1}^{1,0}\left(\frac{r^2}{2}\bigg|\begin{matrix}-\\0\end{matrix}\right) G_{0,1}^{1,0}\left((kur)^c\bigg|\begin{matrix}-\\0\end{matrix}\right) dr, \tag{4.11}$$

where the fading parameters a, c, and k are given in Table 2.1.

Next using the identity in [30] and some mathematical manipulations, the closed-form Cpdf expression for Generalized Gamma distribution can be expressed as

$$f_u(u) = \frac{k^{a/c} c u^{a-1} (2\pi)^{(c/2-1)/2} 2^{a/2}}{\Gamma(a/c)(c/2)^{(1-a)/2}} G_{c/2,1}^{1,0}\left((ku)^c c^{c/2}\bigg|\begin{matrix}\Delta(c/2,1-a/2)\\0\end{matrix}\right), \tag{4.12}$$

where $\Delta(t,h) = \frac{h}{t}, \frac{h+1}{t}, ..., \frac{h+t-1}{t}$, and c is a non-negative even number due to the integer term of $c/2$ in the Meijer-G function.

4.2.2 Generalized Gamma Fading Channel

Applying the Cpdf of Generalized Gamma envelope distribution in (4.12), $f_S(s)$, $s = u_0^2/\tilde{u}^2$ can be given by

$$f_S(s) = \left(\frac{k^{a/c-a} a}{\Gamma(a/c)c}\right)^2 (2\pi)^{c/2-1} s^{a/2-1} G_{\frac{c}{2}+1,\frac{c}{2}+1}^{1,1}\left(s^{c/2}\bigg|\begin{matrix}1-\frac{2a}{c}, \Delta\left(\frac{c}{2},1-\frac{a}{2}\right)\\0, 1-\frac{2a}{c}-\Delta\left(\frac{c}{2},1-\frac{a}{2}\right)\end{matrix}\right). \tag{4.13}$$

Note that the number of terms of $1-\frac{2a}{c}-\Delta\left(\frac{c}{2},1-\frac{a}{2}\right)$ is depended on the specific value of $c/2$

(e.g., when $a = 2$ and $c = 4$, we find $1-\frac{2a}{c}-\Delta\left(\frac{c}{2},1-\frac{a}{2}\right)=0-\Delta(2,0)=0-\left\{\frac{0}{2},\frac{1}{2}\right\}=0,-0.5$).

Thus, substituting (4.13) in (4.8), the pdf of output SIR γ of OC diversity in the GG

fading channels can be expressed as

$$f_\gamma(\gamma)=\left(\frac{k^{a/c-a}a}{\Gamma(a/c)c}\right)^2\frac{(c/2)^N\Lambda^{-a/2}\gamma^{a/2-1}}{\Gamma(L)\Gamma(N-L+1)}$$
$$\times G_{c+1,c+1}^{\frac{c}{2}+1,\frac{c}{2}+1}\left(\left(\frac{\gamma}{\Lambda}\right)^{c/2}\left|\begin{array}{c}1-\frac{2a}{c},\Delta\left(\frac{c}{2},1-\frac{a}{2}-(N-L+1)\right),\Delta\left(\frac{c}{2},1-\frac{a}{2}\right)\\0,\Delta\left(\frac{c}{2},L-\frac{a}{2}\right),1-\frac{2a}{c}-\Delta\left(\frac{c}{2},1-\frac{a}{2}\right)\end{array}\right.\right). \quad (4.14)$$

Note that replacing the parameters $a=2$, $c=2$ and $k=1$ in (4.14) yields

$$f_\gamma(\gamma)=\frac{\Lambda^{-1}}{\Gamma(L)\Gamma(N-L+1)}\times G_{1,1}^{1,1}\left(\frac{\gamma}{\Lambda}\left|\begin{array}{c}-(N-L+1)\\L-1\end{array}\right.\right),$$

$$=\frac{\Lambda^{-1}}{\Gamma(L)\Gamma(N-L+1)}\times G_{1,1}^{1,1}\left(\frac{\gamma}{\Lambda}\left|\begin{array}{c}-(N-L+1)\\L-1\end{array}\right.\right),$$

$$=\frac{\Gamma(N+1)}{\Gamma(L)\Gamma(N-L+1)}\Lambda^{N-L+1}\frac{\gamma^{L-1}}{(\gamma+\Lambda)^{N+1}}\quad, \quad (4.15)$$

which is the Rayleigh fading channel agreed with the result in [73, eq.(13)].

4.3 Performance Analysis

4.3.1 Outage Probability

The outage probability is defined as the probability that the output SIR falls below a

predetermined protection ratio (t).

Substituting (4.14) in (3.3), we have

$$P_{out}=\left(\frac{k^{a/c-a}a}{\Gamma(a/c)c}\right)^2\frac{(c/2)^N\Lambda^{-a/2}}{\Gamma(L)\Gamma(N-L+1)}$$

$$\times \int_0^t \gamma^{a/2-1} G_{c+1,c+1}^{\frac{c}{2}+1,\frac{c}{2}+1} \left(\left(\frac{\gamma}{\Lambda}\right)^{c/2} \middle| \begin{array}{l} 1-\frac{2a}{c}, \Delta\left(\frac{c}{2},1-\frac{a}{2}-(N-L+1)\right), \Delta\left(\frac{c}{2},1-\frac{a}{2}\right) \\ 0, \Delta\left(\frac{c}{2}, L-\frac{a}{2}\right), 1-\frac{2a}{c}-\Delta\left(\frac{c}{2},1-\frac{a}{2}\right) \end{array} \right) d\gamma. \quad (4.16)$$

Using the identity in [8, eq.(26)], the outage probability of output SIR in the Generalized Gamma fading channel can then be shown to be given by

$$P_{out} = \left(\frac{k^{a/c-a}a}{\Gamma(a/c)c}\right)^2 \frac{(c/2)^{N-1}\Lambda^{-a/2}t^{a/c}}{\Gamma(L)\Gamma(N-L+1)}$$

$$\times G_{c+2,c+2}^{\frac{c}{2}+1,\frac{c}{2}+2} \left(\frac{t}{\Lambda^{c/2}} \middle| \begin{array}{l} 1-\frac{2a}{c}, \Delta\left(\frac{c}{2},1-\frac{a}{2}-(N-L+1)\right), 1-\frac{a}{c}, \Delta\left(\frac{c}{2},1-\frac{a}{2}\right) \\ 0, \Delta\left(\frac{c}{2}, L-\frac{a}{2}\right), -\frac{a}{c}, 1-\frac{2a}{c}-\Delta\left(\frac{c}{2},1-\frac{a}{2}\right) \end{array} \right). \quad (4.17)$$

Note that (4.17) can be accurately computed by the software program of Maple or Mathematica. For the case of Rayleigh fading channel ($a=2,c=2$ and $k=1$), (4.17) reduces to

$$P_{out} = \frac{t/\Lambda}{\Gamma(L)\Gamma(N-L+1)} G_{4,4}^{2,3}\left(\frac{t}{\Lambda} \middle| \begin{array}{l} -1, -(N-L+1), 0, 0 \\ 0, L-1, -1, -1 \end{array} \right),$$

$$= \frac{t/\Lambda}{\Gamma(L)\Gamma(N-L+1)} G_{2,2}^{1,2}\left(\frac{t}{\Lambda} \middle| \begin{array}{l} -(N-L+1), 0 \\ L-1, -1 \end{array} \right),$$

$$= \frac{\Gamma(N+1)(t/\Lambda)^L}{\Gamma(L)\Gamma(N-L+1)} {}_2F_1\left(N+1,L; 1+L;-\frac{t}{\Lambda} \right), \quad (4.18)$$

which agrees with the result in [73, eq. (16)].

4.3.2 Moment Generating Function (MGF)

Substituting (4.14) in (3.1), MGF $M_\gamma(t)$ can be obtained as

$$M_\gamma(t) = \left(\frac{k^{a/c-a}a}{\Gamma(a/c)c}\right)^2 \frac{(c/2)^{N+(a-1)/2}\Lambda^{a/2}t^{-a/2}}{\Gamma(L)\Gamma(N-L+1)}$$

$$\times G_{\frac{3c}{2}+1,c+1}^{\frac{c}{2}+1,c+1} \left(\left(\frac{\Lambda c}{2t}\right)^{c/2} \middle| \begin{array}{l} 1-\frac{2a}{c}, \Delta\left(\frac{c}{2},1-\frac{a}{2}-(N-L+1)\right), \Delta\left(\frac{c}{2},1-\frac{a}{2}\right), \Delta\left(\frac{c}{2},1-\frac{a}{2}\right) \\ 0, \Delta\left(\frac{c}{2}, L-\frac{a}{2}\right), 1-\frac{2a}{c}-\Delta\left(\frac{c}{2},1-\frac{a}{2}\right) \end{array} \right). \quad (4.19)$$

4.3.3 Average Symbol Error Rate (ASER)

Using the MGF-based approach, the ASER can be given by

$$\bar{P}_s = \sum_{\tilde{z}=1}^{\tilde{Z}} \int_0^{\theta_{\tilde{z}}} \lambda_{\tilde{z}} M_\gamma \left(\frac{\phi_{\tilde{z}}}{\sin^2 \theta} \right) d\theta , \qquad (4.20)$$

where parameters $\tilde{Z}$, $\lambda_{\tilde{z}}$, $\phi_{\tilde{z}}$ and $\theta_{\tilde{z}}$ are given in Table 3.1.

For the case of binary phase-shift keying (BPSK), we have $\tilde{Z} = 1$, $\theta_1 = 1$, $\lambda_1 = 1/\pi$, and

$\phi_1 = \pi/2$ in (4.20); making a change variable $t = \sin^2 \theta$, the integral in (4.20) may be

evaluated as

$$\bar{P}_b = \frac{1}{\pi} \int_0^{\pi/2} M_X \left(\frac{1}{\sin^2 \theta} \right) d\theta,$$

$$= \frac{1}{2\pi} \int_0^1 s^{-1/2} (1-s)^{-1/2} M_X \left(\frac{1}{s} \right) ds , \qquad (4.21)$$

Substituting (4.19) in (4.21) and introducing $a=c=2$, $k=1$(Rayleigh fading channel), we

have

$$\bar{P}_b = \frac{\Lambda}{2\sqrt{\pi}\Gamma(L)\Gamma(N-L+1)} G_{3,2}^{1,3} \left(\Lambda \left| \begin{matrix} -1/2, -(N-L+1), 0 \\ (L-1), -1 \end{matrix} \right. \right), \qquad (4.22)$$

which agrees with the result in [73,eq.(21)].

4.4 Numerical Results

In this section, some numerical results for outage probability and ASER of OC receivers in Generalized Gamma fading channel have been present. In Figure 4.2, outage probability in (4.17) is plotted when the threshold (t) is set at 7 dB, $L=$ [1, 2, 3, 4] and $N=8$. All interferers are assumed to have the equal power ($\Omega = 5$ dB) and the GG fading parameters are set as follows $a = 2.2$, $c = 2$ and $k = 1.1$. As expected, increasing the

number of OC receivers decreases the outage probability. In Figure 4.3, the outage probability with fading parameters $a = 2m,\ c = 2$ and $k = m$ (Nakagami-m fading as shown in Table 2.1) when $L=1$ and $N=8$ is depicted. It is shown that the Generalized Gamma fading channel represents a Rayleigh faded environment when fading parameters $a=c=2$ and $k=1$. In Figure 4.4, the performance of ASER for coherent 8-PSK for OC receivers (L=1, 2, 3, 4) with the presence of eight equal-power interferers ($\Omega=5$ dB) in Generalized Gamma fading channel is shown. Similar to the Figure 4.2, the ASER is also decreased when the number of antenna array increases. Finally in Figure 4.5, the performance for BPSK in Generalized Gamma fading channel is provided. The fading parameters are also set as $a = 2m,\ c = 2$ and $k = m$. The result shows the GG fading channel reduces to a Rayleigh fading when $a=c=2$ and $k=1$.
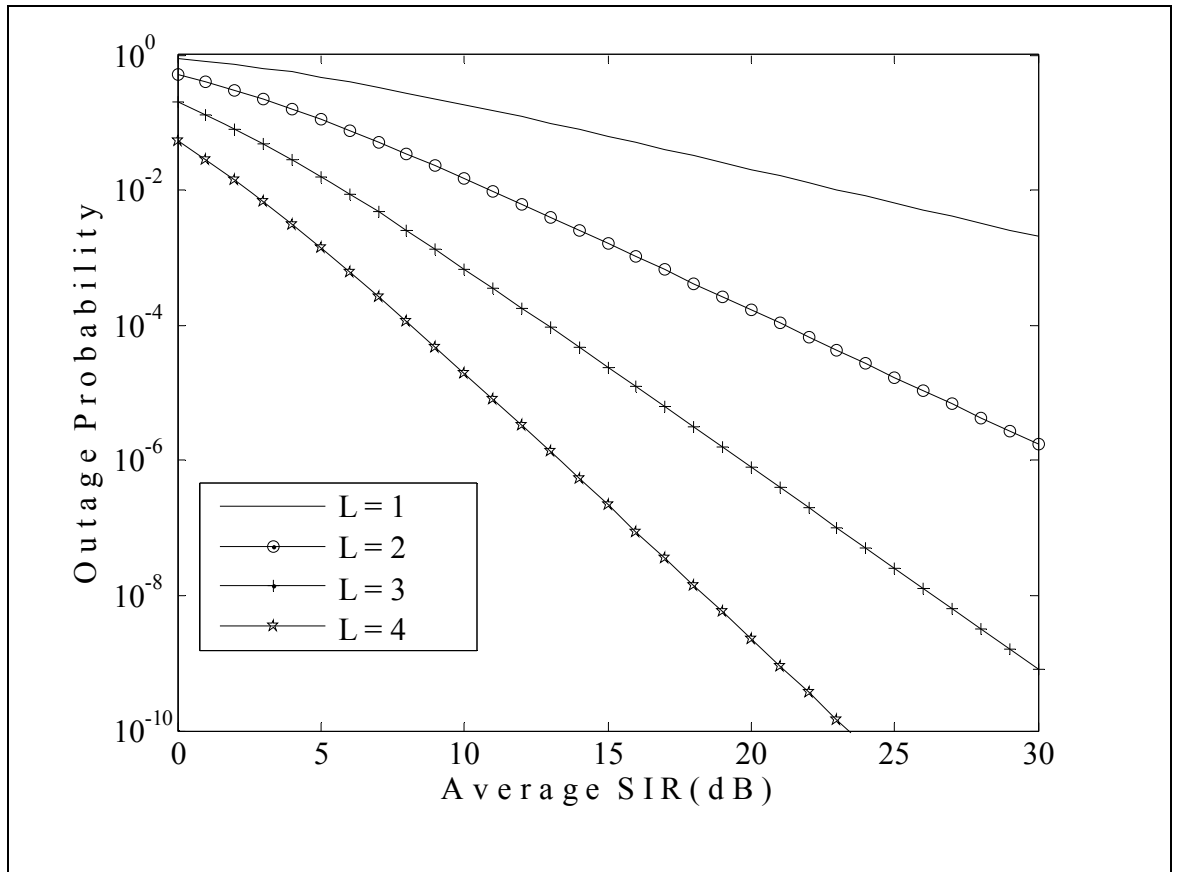
Figure 4.2 The outage probability of OC receivers with 8 equal mean-power interferers in Generalized Gamma fading channel
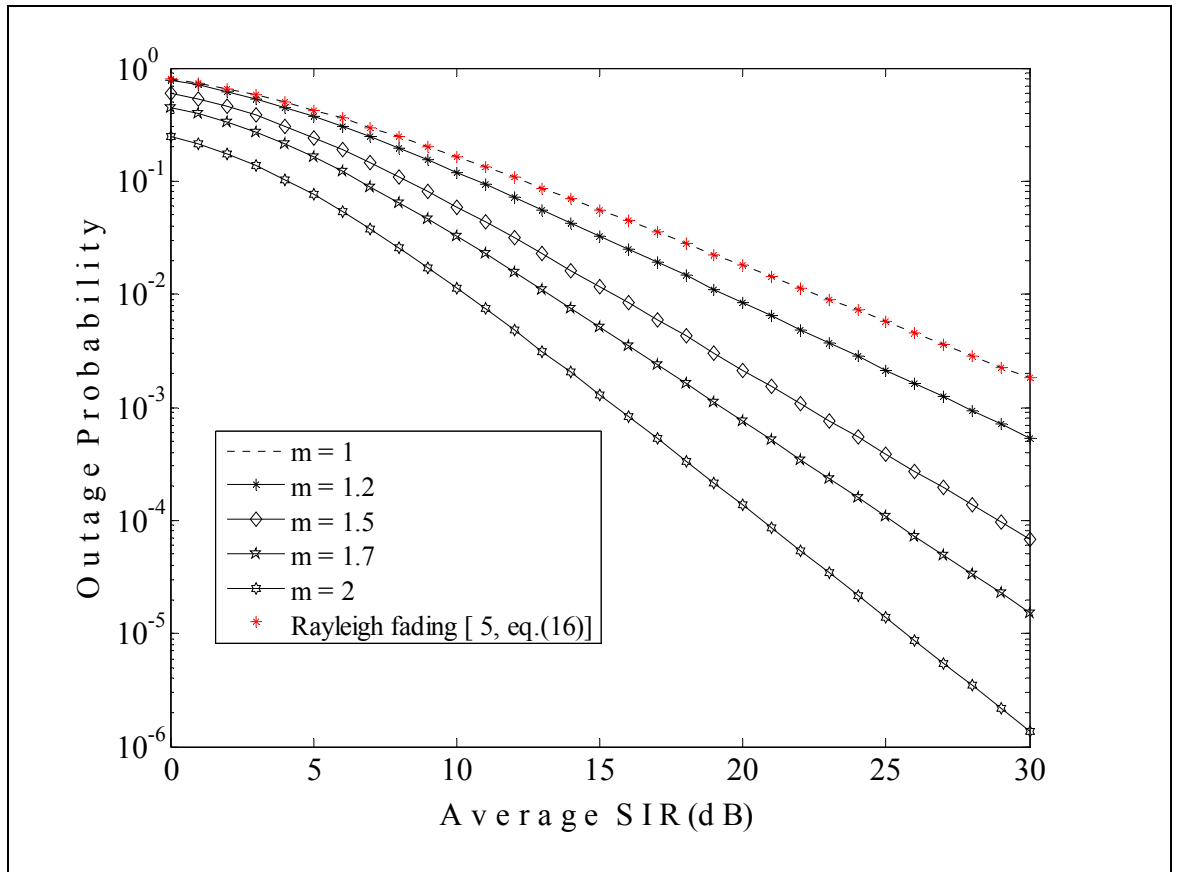
Figure 4.3 The outage probability of an OC receiver (no diversity) with 8 equal mean-power interferers in Generalized Gamma fading channel ($a = 2m$, $c = 2$ and $k = m$)
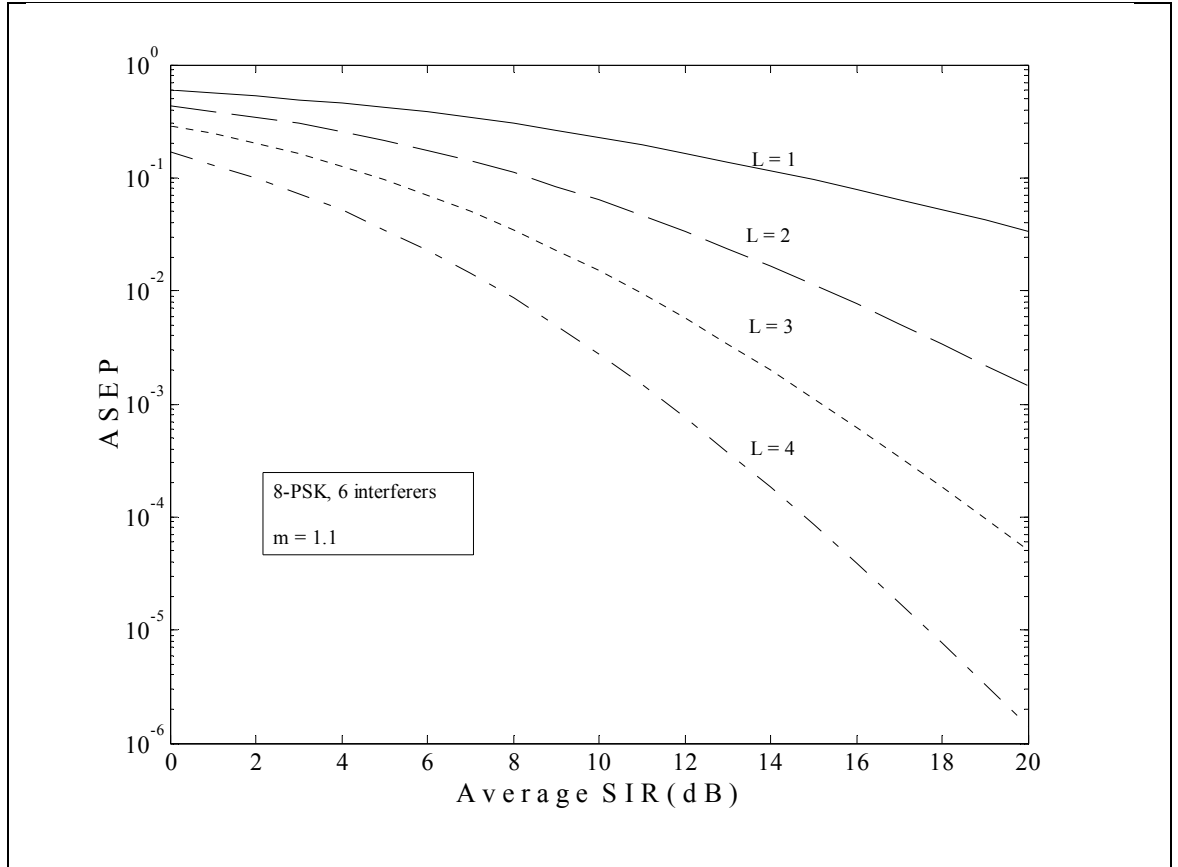
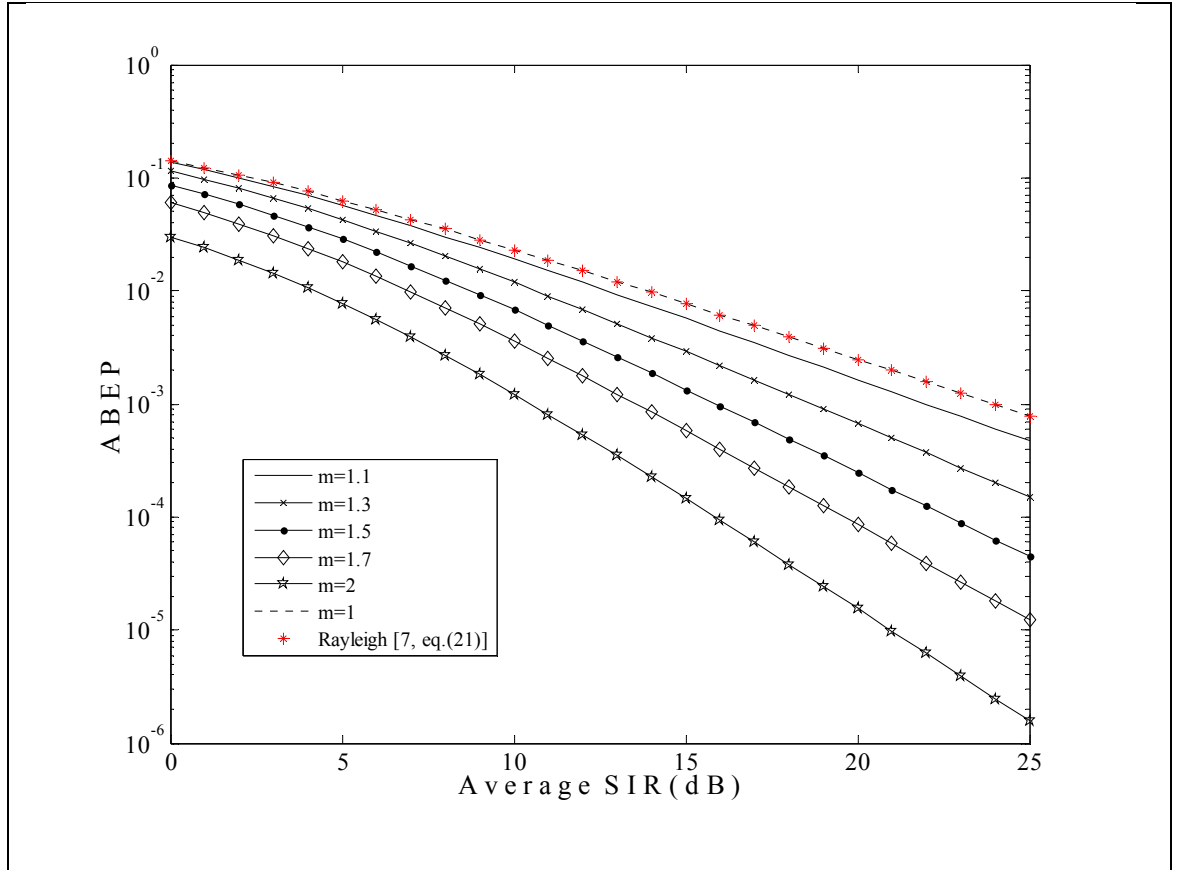**Figure 4.4** The ASER of 8-PSK for OC receivers with 8 equal mean-power interferers in Generalized Gamma fading channel.

Figure 4.5 The ABER of BPSK of an OC receiver (no diversity) with 8 equal mean-power interferers in Generalized Gamma fading channel ($a = 2m$, $c = 2$ and $k = m$)

CHAPTER 5 DUAL-HOP RELAY SYSTEMS IN RAYLEIGH FADING CHANNELS

5.1 Introduction

Signal transmission via intermediate relays has the potential of improving the performance and extending the coverage of many wireless communication systems. In particular, the dual hop relaying transmission has received considerable attention in the recent literature as it can provide increased link quality and reliability, and can mitigate channel impairments in next generation wireless systems [10], [21], [56]. Two relaying policies that have been widely investigated are the decode-and-forward and the amplify-and-forward [65]. As mentioned in Chapter 1, DF relays are regenerative, i.e., the received signal is first decoded and then re-transmitted to the destination node, whereas in an AF relay system, the signal received at the relay node is simply amplified and forwarded to the destination node. The resulting end-to-end SNR of AF relays depends on the choice of the gain adopted at the relay node [40]. The performance of dual-hop relaying has been investigated in various wireless environments that include Rayleigh [40], Nakagami-m, Nakagami-n (Rice) and Nakagami-q (Hoyt) [46] channel fading models.

Until recently, the performance of dual-hop relaying systems has been limited to systems that are noise-limited [40], [46]. However, since many practical wireless systems suffer from both interference and noise, attention has turned recently to dual-hop relay transmission in the presence of co-channel interference, which in many cases may be more detrimental to system performance than thermal noise [20], [25], [45], [50], [55], [76], [80], [91], [94]. In [50], the performance of relay selection with AF relays having a single interferer at each relay was investigated. In [20] and [92], the outage probability of DF relaying was derived in the presence of multiple interferers at

the relays and the destination nodes. The outage probability for the DF protocol under the same interference model was also investigated in [76] for different combining methods at the destination. Furthermore, the outage performance of dual-hop AF (employing sub-optimum gain policy [40]) and DF relaying systems with multiple interferers at both the relay and the destination was obtained in [55]. For the case of AF relaying with optimum gain policy [4], Ikki and Aissa in [45] derived the outage and error probabilities assuming a tight upper bound for the end-to-end SINR. A lower bound and an asymptotic expression for the outage probability of the AF protocol were also derived in [25], assuming Rician fading for the desired signal and Rayleigh fading for the multiple interferers at both the relay and the destination. Moreover, special cases for the performance analysis in the presence of co-channel interference include the work of [94] on the outage performance of dual-hop systems in an interference-limited destination environment and [80] on the outage and ABER of AF dual-hop systems with interference at the relay only. To the best of our knowledge, the outage performance of dual-hop AF transmission with optimum gain in the presence of interference at both the relay and destination has been limited to lower bound and approximation expressions even for the Rayleigh fading channel.

In this chapter, the presence of multiple Rayleigh faded interferers at both the relay and the destination are investigated. Also the analytical expressions for the outage probability and ABER of binary modulations for AF dual-hop relay systems are considered. Specifically, an expression for the exact outage probability of dual-hop relay transmission system in Rayleigh fading is then derive in terms of the incomplete Weber integral which can be easily evaluated numerically by several computer programs such as MATLAB, MATHEMATICA, or MAPLE and the approximate closed-form expressions for the outage as well as the ABER are provided. The special

case of an interference-limited system is also considered. The analytical results are validated by Monte Carlo simulation.

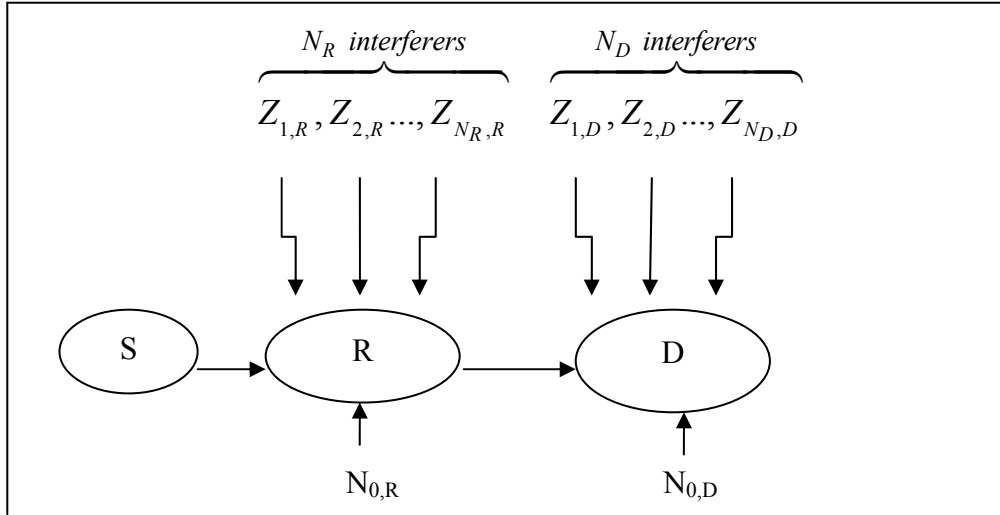## 5.2 The Presence of CCI and Noise

Figure 5.1 The dual-hop systems with the presence of interference and noise

5.2.1 System Model

We consider a wireless communication system in which the source S sends a message to a destination D via a non-regenerative relay R that simply amplifies and forwards the received signal to the destination as shown in Figure 5.1. In Figure 5.1, both the relay and destination nodes are assumed to operate in a Rayleigh-fading environment in the presence of co-channel interference and additive white Gaussian noise (AWGN). The received signal at the relay node is given by

$$y_R(t) = \sqrt{P_s}\left|h_{SR}\right|x_s(t) + \sum_{i=1}^{N_R}\sqrt{P_{R_i}}\left|h_{R_i}\right|s_{R_i}(t) + n_R(t),\tag{5.1}$$

where P_s is the transmitted power of the desired signal $x_s(t)$, P_{R_i} is the transmitted power of the ith co-channel interference signal $s_{R_i}(t)$, $\left|h_{SR}\right|$ is the complex fading gain

for the desired signal on the link between the source and the relay, N_R is the number of interfering signals at the relay, and $\left|h_{R_i}\right|$ is the complex fading gain of the ith co-channel interference signal for $i = 1,\ldots, N_R$. The AWGN term, $n_R(t)$, has zero mean and average power σ_R^2. The relay multiplies the received signal $y_R(t)$ by a gain G and then re-transmits it to the destination D. The received signal is then given by

$$y_D(t) = G\left|h_{RD}\right| y_R(t) + \sum_{i=1}^{N_D} \sqrt{P_{D_i}} \left|h_{D_i}\right| s_{D_i} + n_D(t),$$

$$= G\left|h_{RD}\right| \left\{ \sqrt{P_s} \left|h_{SR}\right| x_s(t) + \sum_{i=1}^{N_R} \sqrt{P_{R_i}} \left|h_{R_i}\right| s_{R_i} + n_R(t) \right\} + \sum_{i=1}^{N_D} \sqrt{P_{D_i}} \left|h_{D_i}\right| s_{D_i} + n_D(t), \qquad (5.2)$$

where $\left|h_{RD}\right|$ denotes the complex fading gain for the desired signal on the link between the relay and the destination, N_D is the number of interfering signals present at the destination, each with power P_{D_i} and fading amplitude $\left|h_{D_i}\right|$ $(i=1,2,\ldots,N_D)$ and σ_D^2 is the one-sided power spectral density of the noise at the destination node. In general, the choice of the node gain, G, determines the end-to-end SINR. The best choice of the node gains that maximizes the end-to-end SINR requires the knowledge of the channel-state information, which includes the signal fading level as well as the noise power *S-R* link. In such CSI-based relays, the amplification gains at each relay are chosen, with the knowledge of the channel state information, to invert the fading state of the preceding link. The corresponding relay gain is chosen as

$$G^2 = \frac{P_R}{P_S \left|h_{SR}\right|^2 + \sum_{i=1}^{N_R} P_{R_i} \left|h_{R_i}\right|^2 + \sigma_R^2}. \qquad (5.3)$$

The SINR at the destination node is given by

$$\gamma_{eq} = \frac{P_s \left| h_{SR} \right|^2 \left| h_{RD} \right|^2 G^2}{G^2 \left| h_{RD} \right|^2 \left(\sum_{i=1}^{N_R} P_{R_i} \left| h_{R_i} \right|^2 + \sigma_R^2 \right) + \sum_{i=1}^{N_D} P_{D_i} \left| h_{D_i} \right|^2 + \sigma_D^2},$$

$$= \frac{P_s \left| h_{SR} \right|^2 \left| h_{RD} \right|^2}{\left| h_{RD} \right|^2 \left(\sum_{i=1}^{N_R} P_{R_i} \left| h_{R_i} \right|^2 + \sigma_R^2 \right) + \left(\sum_{i=1}^{N_D} P_{D_i} \left| h_{D_i} \right|^2 + \sigma_D^2 \right) / G^2}. \qquad (5.4)$$

Substitute (5.3) in (5.4) to get

$$\gamma_{eq} = \frac{P_s \left| h_{SR} \right|^2 P_R \left| h_{RD} \right|^2}{P_R \left| h_{RD} \right|^2 \left(\sum_{i=1}^{N_R} P_{R_i} \left| h_{R_i} \right|^2 + \sigma_R^2 \right) + \left(\sum_{i=1}^{N_D} P_{D_i} \left| h_{D_i} \right|^2 + \sigma_D^2 \right) \left(P_S \left| h_{SR} \right|^2 + \sum_{i=1}^{N_R} P_{R_i} \left| h_{R_i} \right|^2 + \sigma_R^2 \right)}.$$

$$(5.5)$$

Divide numerator and denominator of (5.5) by $\sigma_R^2 \sigma_D^2$ gives

$$\gamma_{eq} = \frac{\dfrac{P_s \left| h_{SR} \right|^2}{\sigma_R^2} \dfrac{P_R \left| h_{RD} \right|^2}{\sigma_D^2}}{\dfrac{P_R \left| h_{RD} \right|^2}{\sigma_D^2} \left(\sum_{i=1}^{N_R} \dfrac{P_{R_i} \left| h_{R_i} \right|^2}{\sigma_R^2} + 1 \right) + \left(\sum_{i=1}^{N_D} \dfrac{P_{D_i} \left| h_{D_i} \right|^2}{\sigma_D^2} + 1 \right) \left(\dfrac{P_S \left| h_{SR} \right|^2}{\sigma_R^2} + \sum_{i=1}^{N_R} \dfrac{P_{R_i} \left| h_{R_i} \right|^2}{\sigma_R^2} + 1 \right)},$$

$$= \frac{\gamma_{SR} \gamma_{RD}}{\gamma_{RD} \left(\gamma_a + 1 \right) + \left(\gamma_b + 1 \right) \left(\gamma_{SR} + \gamma_a + 1 \right)}, \qquad (5.6)$$

where

$$\gamma_{SR} = \frac{P_s \left| h_{SR} \right|^2}{\sigma_R^2} , \ \gamma_{RD} = \frac{P_R \left| h_{RD} \right|^2}{\sigma_D^2} , \ \gamma_a = \sum_{i=1}^{N_R} \frac{P_{R_i} \left| h_{R_i} \right|^2}{\sigma_R^2} , \text{ and } \gamma_b = \sum_{i=1}^{N_D} \frac{P_{D_i} \left| h_{D_i} \right|^2}{\sigma_D^2}.$$

Next divide (5.6) by $\left(\gamma_a + 1 \right) \left(\gamma_b + 1 \right)$ to give

$$\gamma_{eq} = \frac{\dfrac{\gamma_{SR}}{\left(\gamma_a + 1 \right)} \dfrac{\gamma_{RD}}{\left(\gamma_b + 1 \right)}}{\dfrac{\gamma_{RD}}{\left(\gamma_b + 1 \right)} + \dfrac{\left(\gamma_{SR} + \gamma_a + 1 \right)}{\left(\gamma_a + 1 \right)}},$$

$$= \frac{\gamma_1 \gamma_2}{\gamma_2 + \gamma_1 + 1}, \tag{5.7}$$

where now $\gamma_1 = \dfrac{\gamma_{SR}}{(\gamma_a + 1)}$ and $\gamma_2 = \dfrac{\gamma_{RD}}{(\gamma_b + 1)}$ are the instantaneous signal-to- interference

-plus-noise ratio (SINR) at the relay and destination nodes, respectively. For a Rayleigh

fading channel

$$f_{\gamma_{SR}}(\gamma) = \frac{1}{\lambda_{SR}} e^{-\gamma/\lambda_{SR}} u(\gamma), \tag{5.8a}$$

$$f_{\gamma_{RD}}(\gamma) = \frac{1}{\lambda_{RD}} e^{-\gamma/\lambda_{RD}} u(\gamma). \tag{5.8b}$$

In (5.8a) and (5.8b), $\lambda_{SR} = \mathbf{E}\left(\left|h_{SR}\right|^2\right) P_s / \sigma_R^2$, and $\lambda_{RD} = \mathbf{E}\left(\left|h_{RD}\right|^2\right) P_D / \sigma_D^2$ are the average

SNRs at the relay and the destination, respectively. To simplify the analysis, we further

assume that the interferers at the relay and the destination have equal powers, i.e.,

$P_{R_1} = P_{R_2} = ... = P_{R_{N_R}}$ and $P_{D_1} = P_{D_2} = ... = P_{D_{N_D}}$, respectively. Then the cdf of the

instantaneous SINR at the relay is given by

$$F_{\gamma_1}(\gamma) = P\left(\gamma_1 \leq \gamma\right) = P\left(\frac{\gamma_{SR}}{\gamma_a + 1} \leq \gamma\right),$$

$$= \int_0^\infty F_{\gamma_{SR}}\left(\gamma\left(\gamma_a + 1\right)\right) f_a(x) dx. \tag{5.9}$$

In (5.9), we have

$$F_{\gamma_{SR}}(\gamma) = 1 - e^{-\gamma/\lambda_{SR}}, \tag{5.10a}$$

$$f_{\gamma_{SR}}(\gamma) = \frac{\gamma^{N_R - 1}}{\Omega_R^{N_R}(N_R - 1)!} \exp\left(-\frac{\gamma}{\Omega_R}\right). \tag{5.10b}$$

The term $\Omega_R = \dfrac{\mathbf{E}\left(\left|h_{R_i}\right|^2\right)P_{R_i}}{\sigma_R^2}$ $\forall i$ is the average interference-to-noise ratio (INR) at the

relay for each interferer. Substituting (5.10a) and (5.10b) in (5.9) and simplifying gives

[1], [45, eq. (17)],

$$F_{\gamma_1}(\gamma) = 1 - \frac{e^{-\gamma/\lambda_{SR}}}{\Omega_R^{N_R}(N_R-1)!} \int_0^\infty x^{N_R-1} \exp\left(-x\left(\frac{\gamma}{\lambda_{SR}} + \frac{1}{\Omega_R}\right)\right) dx,$$

$$= 1 - \left(\frac{\Lambda_R}{\gamma + \Lambda_R}\right)^{N_R} \exp\left(\frac{-\gamma}{\Omega_R}\right), \tag{5.11}$$

where $\Lambda_R = \dfrac{\lambda_{SR}}{\Omega_R}$ is the average SIR at the relay for each interferer. The corresponding

pdf of the instantaneous SINR at the relay may be obtained by differentiating (5.11) to

give

$$f_{\gamma_1}(\gamma) = \left[\frac{N_R \Lambda_R^{N_R}}{(\gamma + \Lambda_R)^{N_R+1}} + \frac{1}{\Omega_R}\left(\frac{\Lambda_R}{\gamma + \Lambda_R}\right)^{N_R}\right] \exp\left(\frac{-\gamma}{\Omega_R}\right). \tag{5.12}$$

In a manner similar to (5.9)-(5.12), the cdf and pdf of the SINR at the destination node

may be shown to be given by

$$F_{\gamma_2}(\gamma) = 1 - \left(\frac{\Lambda_D}{\gamma + \Lambda_D}\right)^{N_D} \exp\left(\frac{-\gamma}{\Omega_D}\right), \tag{5.13}$$

$$f_{\gamma_2}(\gamma) = \left[\frac{N_D \Lambda_D^{N_D}}{(\gamma + \Lambda_D)^{N_D+1}} + \frac{1}{\Omega_D}\left(\frac{\Lambda_D}{\gamma + \Lambda_D}\right)^{N_D}\right] \exp\left(\frac{-\gamma}{\Omega_D}\right), \tag{5.14}$$

where $\Omega_D = \mathbf{E}\left(\left|h_{D_i}\right|^2\right)P_{D_i}/\sigma_D^2$ $\forall i$ and $\Lambda_D = \dfrac{\lambda_{RD}}{\Omega_D}$ are the average INR and average SIR

at the destination node for each interferer, respectively.

5.2.1.1 CDF of End-to-End SINR System

The cdf of instantaneous end-to-end SINR $\gamma_{eq} = \dfrac{\gamma_1 \gamma_2}{\gamma_2 + \gamma_1 + 1}$ is given by

$$F_{\gamma_{eq}}(\gamma) = \Pr\left(\frac{\gamma_1 \gamma_2}{\gamma_2 + \gamma_1 + 1} \le \gamma\right) = \Pr\left(\gamma_1 \le \frac{\gamma \gamma_2 + \gamma}{\gamma_2 - \gamma}\right). \tag{5.15}$$

Conditioning on the random variables γ_2, the $F_{\gamma_{eq}}(\gamma)$ becomes

$$F_{\gamma_{eq}}(\gamma) = \int_0^\gamma \Pr\left(\gamma_1 > \frac{\gamma \gamma_2 + \gamma}{\gamma_2 - \gamma}\right) f_{\gamma_2}(\gamma_2) d\gamma_2 + \int_\gamma^\infty \Pr\left(\gamma_1 \le \frac{\gamma \gamma_2 + \gamma}{\gamma_2 - \gamma}\right) f_{\gamma_2}(\gamma_2) d\gamma_2 ,$$

$$= \int_0^\gamma f_{\gamma_2}(\gamma_2) d\gamma_2 + \int_\gamma^\infty F_{\gamma_1}\left(\frac{\gamma \gamma_2 + \gamma}{\gamma_2 - \gamma}\right) f_{\gamma_2}(\gamma_2) d\gamma_2 . \tag{5.16}$$

Using (5.11), the integral in (5.16) becomes

$$F_{\gamma_{eq}}(\gamma) = \int_0^\gamma f_{\gamma_2}(\gamma_2) d\gamma_2 + \int_\gamma^\infty f_{\gamma_2}(\gamma_2) d\gamma_2 - \int_\gamma^\infty \frac{\Lambda_R^{N_R}}{\left(\frac{\gamma \gamma_2 + \gamma}{\gamma_2 - \gamma} + \Lambda_R\right)^{N_R}} \exp\left(-\frac{\gamma(\gamma_2 + 1)}{(\gamma_2 - 1)\lambda_{SR}}\right) f_{\gamma_2}(\gamma_2) d\gamma_2 ,$$

$$= 1 - \int_\gamma^\infty \frac{\Lambda_R^{N_R}}{\left(\frac{\gamma \gamma_2 + \gamma}{\gamma_2 - \gamma} + \Lambda_R\right)^{N_R}} \exp\left(-\frac{\gamma(\gamma_2 + 1)}{(\gamma_2 - 1)\lambda_{SR}}\right) f_{\gamma_2}(\gamma_2) d\gamma_2 . \tag{5.17}$$

Substituting (5.13) and (5.14) in (5.17) and making the change of variable $x = \gamma_2 - \gamma$

gives

$$F_{\gamma_{eq}}(\gamma) = 1 - \left(\frac{\Lambda_R}{\gamma + \Lambda_R}\right)^{N_R} \frac{\Lambda_D^{N_D}}{\lambda_{RD}} \exp\left(-\gamma\left(\frac{\lambda_{SR} + \lambda_{RD}}{\lambda_{SR}\lambda_{RD}}\right)\right) \int_0^\infty \frac{G(x)}{x} \exp\left(-\frac{\gamma(\gamma + 1)}{\lambda_{SR} x} - \frac{x}{\lambda_{RD}}\right) dx ,$$

$$\tag{5.18}$$

where

$$G(x) = \frac{x^{N_R + 1}\left(x + \gamma + \Lambda_D + \lambda_{RD} N_D\right)}{\left(x + \frac{\gamma(\gamma + 1)}{\gamma + \Lambda_R}\right)^{N_R}\left(x + \gamma + \Lambda_D\right)^{N_D + 1}}. \tag{5.19}$$

A partial-fraction expansion of $G(x)$ is given by

$$G(x) = \sum_{i=1}^2 \sum_{k=1}^{\sigma_i} \frac{\Xi_{ik}}{(x + \rho_i)^k}, \tag{5.20}$$

where $\sigma_1 = N_R$, $\sigma_2 = N_D + 1$, $\rho_1 = \dfrac{\gamma(\gamma+1)}{\gamma + \Lambda_R}$, $\rho_2 = \gamma + \Lambda_D$, and the coefficients Ξ_{ik} is

given by

$$\Xi_{ik} = \frac{1}{(\sigma_i - k)!} \frac{d^{\sigma_i - k}}{dx^{\sigma_i - k}} (x + \rho_i)^{\sigma_i} \, G(x)\Big|_{x = -\rho_i}. \tag{5.21}$$

It is shown in Appendix A that the coefficients in (5.21) may be expressed in closed

form as

$$\Xi_{1k} = \frac{1}{(N_R - k)!} \left\{ \frac{\Gamma(N_R+3)(-\rho_2)^{k+2}}{\Gamma(k+3)(\rho_1 - \rho_2)^{N_D+1}} \sum_{j=0}^{N_R-k} \binom{N_R - k}{j} \frac{(-1)^j (N_D+1)_j}{(k+3)_j} \left(\frac{\rho_2}{\rho_1 - \rho_2}\right)^j \right.$$

$$\left. + \frac{(\rho_2 + \Lambda_D + \lambda_{RD}N_D)\Gamma(N_R+2)(-\rho_2)^{k+1}}{\Gamma(k+2)(\rho_1 - \rho_2)^{N_D+1}} \sum_{j=0}^{N_R-k} \binom{N_R - k}{j} \frac{(-1)^j (N_D+1)_j}{(k+2)_j} \left(\frac{\rho_2}{\rho_1 - \rho_2}\right)^j \right\},$$

$$\tag{5.22a}$$

$$\Xi_{2k} = \frac{1}{(N_D+1-k)!} \left\{ \frac{\Gamma(N_R+3)(-\rho_2)^{N_R-N_D+k+1}}{\Gamma(N_R - N_D + k + 2)(\rho_1 - \rho_2)^{N_R}} \right.$$

$$\times \sum_{j=0}^{N_D+1-k} \binom{N_D+1-k}{j} \frac{(-1)^j (N_R)_j}{(N_R - N_D + k + 2)_j} \left(\frac{\rho_2}{\rho_1 - \rho_2}\right)^j + \frac{(\rho_1 + \Lambda_D + \lambda_{RD}N_D)\Gamma(N_R+2)}{\Gamma(N_R - N_D + k + 1)}$$

$$\left. \times \frac{(-\rho_2)^{N_R-N_D+k}}{(\rho_1 - \rho_2)^{N_R}} \sum_{j=0}^{N_D+1-k} \binom{N_D+1-k}{j} \frac{(-1)^j (N_R)_j}{(N_R - N_D + k + 1)_j} \left(\frac{\rho_2}{\rho_1 - \rho_2}\right)^j \right\}, \tag{5.22b}$$

where $\binom{a}{b}$ is the Binomial coefficient. Using [38, 3.381.4], (5.20) can be rewritten as

$$G(x) = \sum_{i=1}^{2} \sum_{k=1}^{\sigma_i} \frac{\Xi_{ik}}{\Gamma(k)} \int_0^\infty t^{k-1} e^{-t(x+\rho_i)} \, dt. \tag{5.23}$$

Substituting (5.23) in (5.18) and using [38, eq. (3.3471.9)], yields

$$F_{\gamma_{eq}}(\gamma) = 1 - 2\left(\frac{\Lambda_R}{\gamma + \Lambda_R}\right)^{N_R} \frac{\Lambda_D^{N_D}}{\lambda_{RD}} \exp\left(-\gamma\left(\frac{\lambda_{SR} + \lambda_{RD}}{\lambda_{SR}\lambda_{RD}}\right)\right) \sum_{i=1}^{2} \sum_{k=1}^{\sigma_i} \frac{\Xi_{ik}}{\Gamma(k)}$$

$$\times \int_0^\infty t^{k-1} e^{-t\rho_i} K_0\left(2\sqrt{\frac{\gamma(\gamma+1)(t+1/\lambda_{RD})}{\lambda_{SR}}}\right) dt, \tag{5.24}$$

where $K_0(.)$ is the modified Bessel function of the second kind and zero order [38].

After introducing $z = 2\sqrt{\frac{\gamma(\gamma+1)(t+1/\lambda_{RD})}{\lambda_{SR}}}$, the integral term in (5.24) become

$$I = \frac{1}{2}\left(\frac{\lambda_{SR}}{\gamma(\gamma+1)}\right) e^{\frac{\rho_i}{\lambda_{RD}}} \int_A^\infty \left(\frac{z^2 \lambda_{SR}}{4\gamma(\gamma+1)} - \frac{1}{\lambda_{RD}}\right)^{k-1} e^{-Bz^2} K_0(z) dz,$$

$$= \frac{1}{2}\left(\frac{\lambda_{SR}}{\gamma(\gamma+1)}\right) e^{\frac{\rho_i}{\lambda_{RD}}} \sum_{n=0}^{k-1}\binom{k-1}{n}\left(-\frac{1}{\lambda_{RD}}\right)^{k-n-1}\left(\frac{\lambda_{SR}}{4\gamma(\gamma+1)}\right)^n \int_A^\infty z^{2n} e^{-Bz^2} K_0(z) dz, \tag{5.25}$$

where $A = 2\sqrt{\frac{\gamma(\gamma+1)}{\lambda_{SR}\lambda_{RD}}}$ and $B = \frac{\lambda_{SR}\rho_i}{4\gamma(\gamma+1)}$. Finally, simplifying (5.25) and substituting in

(5.24), the outage probability becomes

$$F_{\gamma_{eq}}(\gamma) = 1 - \left(\frac{\Lambda_R}{\gamma+\Lambda_R}\right)^{N_R} \frac{\Lambda_D^{N_D}}{\lambda_{RD}}\left(\frac{\lambda_{SR}}{\gamma(\gamma+1)}\right)\exp\left(-\gamma\left(\frac{\lambda_{SR}+\lambda_{RD}}{\lambda_{SR}\lambda_{RD}}\right)\right)\sum_{i=1}^2\sum_{k=1}^{\sigma_i}\frac{\Xi_{ik}}{\Gamma(k)}e^{\frac{\rho_i}{\lambda_{RD}}}$$

$$\times \sum_{n=0}^{k-1}\binom{k-1}{n}\left(-\frac{1}{\lambda_{RD}}\right)^{k-n-1}\left(\frac{\lambda_{SR}}{4\gamma(\gamma+1)}\right)^n\left[\frac{\Gamma(n+1/2)\Gamma(n+1/2)}{4B^{n+1/2}}\psi\left(n+\frac{1}{2}:1:\frac{1}{4B}\right) - K_{e^2_{2n,0}}(B,A)\right], \tag{5.26}$$

where

$$\psi(u;v;x) = \frac{1}{\Gamma(u)}\int_0^\infty e^{-xt}t^{u-1}(1+t)^{v-u-1}dt, \quad \mathrm{Re}\, u > 0 \tag{5.27}$$

is the confluent hypergeometric function of the second kind [38] and

$$K_{e^2_{u,v}}(p,x) = \int_0^x t^u e^{-pt^2} K_v(t) dt \tag{5.28}$$

is the incomplete Weber integral [9], [22], [60]. Note that some special cases of

$K_{e^2_{u,v}}(p,x)$ are shown in Appendix B.

In addition, using the identities in [38, eq.(8.436) and eq. (9.211.2)], and interchanging the order of integration, $K_{e^2_{u,v}}(p,x)$ can be numerically evaluated by

$$K_{e^2_{u,v}}(p,x) \cong \frac{x^{v+u+1}}{2^{v+1}(v+u+1)} \sum_{i=1}^{K} w_i y_i^{-(v+1)} {}_1F_1\left(\frac{v+u+1}{2}; 1+\frac{v+u+1}{2}; -x^2\left(p+\frac{1}{4y_i}\right)\right), \quad (5.29)$$

where ${}_1F_1(a;b;x)$ is the confluent hypergeometric function [38], the weights w_i and the roots y_i are given in [7, (25.4.33)] and the value of K is chosen to obtain a desired accuracy.

5.2.1.2 Approximate CDF of End-to-End SINR System

In order to obtain a simple approximation for the cdf of the end-to-end SINR, the expression of the integral in (5.18) can be written as

$$I = \int_0^\infty \left(x^{N_R+1} + x^{N_R}\left(\gamma + \Lambda_D + \lambda_{RD}N_D\right)\right)\left(x + \frac{\gamma(\gamma+1)}{\gamma+\Lambda_R}\right)^{-N_R}$$

$$\times(x+\gamma+\Lambda_D)^{-(N_D+1)}\exp\left(-\frac{\gamma(\gamma+1)}{\lambda_{SR}x}-\frac{x}{\lambda_{RD}}\right)dx. \quad (5.30)$$

The two terms in the denominator of (5.30) may be written as [38, eq. (3.381.4)]

$$\left(x+\frac{\gamma(\gamma+1)}{\gamma+\Lambda_R}\right)^{-N_R} = \frac{x^{-N_R}}{\Gamma(N_R)}\int_0^\infty z^{N_R-1}e^{-\left(1+\frac{\gamma(\gamma+1)}{x(\gamma+\Lambda_R)}\right)z}dz, \quad (5.31)$$

$$(x+\gamma+\Lambda_D)^{-(N_D+1)} = \frac{1}{\Gamma(N_D+1)}\int_0^\infty t^{N_D-1}e^{-t(x+\gamma+\Lambda_D)}dt. \quad (5.32)$$

Using (5.31) and (5.32) in (5.30), we have $I = I_1 + I_2$ where

$$I_1 = \frac{1}{\Gamma(N_R)\Gamma(N_D+1)}$$

$$\times\int_0^\infty z^{N_R-1}e^{-z}\int_0^\infty t^{N_D}e^{-t(\gamma+\Lambda_D)}\int_0^\infty x\exp\left(-\frac{\gamma(\gamma+1)}{x}\left(\frac{1}{\lambda_{SR}}+\frac{z}{\gamma+\Lambda_R}\right)-x\left(t+\frac{1}{\lambda_{RD}}\right)\right)dxdtdz. \quad (5.33)$$

Next performing the inner integration in (5.33) via [38, eq. (3.471.9)] gives

$$I_1 = \frac{2}{\Gamma(N_R)\Gamma(N_D+1)} \int_0^\infty z^{N_R-1} e^{-z} \int_0^\infty t^{N_D} e^{-t(\gamma+\Lambda_D)} \left(\frac{1}{\lambda_{SR}} + \frac{z}{\gamma+\Lambda_R} \right) \frac{\gamma(\gamma+1)}{(t+\lambda_{RD}^{-1})}$$

$$\times K_2 \left(2 \left\{ \gamma(\gamma+1) \left(\frac{1}{\lambda_{SR}} + \frac{z}{\gamma+\Lambda_R} \right) (t+\lambda_{RD}^{-1}) \right\}^{1/2} \right) dtdz. \tag{5.34}$$

However, the modified Bessel function may be approximated as [7, eq. (9.6.9)]

$$K_v(x) \cong \frac{\Gamma(v)}{2} \left(\frac{x}{2} \right)^{-v}. \tag{5.35}$$

Thus, (5.34) becomes

$$I_1 = \frac{1}{\Gamma(N_R)\Gamma(N_D+1)} \int_0^\infty z^{N_R-1} e^{-z} \int_0^\infty t^{N_D} e^{-t(\gamma+\Lambda_D)} (t+\lambda_{RD}^{-1})^{-2} dtdz,$$

$$= \frac{1}{\lambda_{RD}^{N_D-1}} \psi \left(N_D+1; N_D; \frac{(\gamma+\Lambda_D)}{\lambda_{RD}} \right). \tag{5.36}$$

Note that the approximation in (5.35) is valid when the argument of the modified Bessel function tends to zero; this is equivalent to assuming that the **S** - **R** link has a strong signal strength (i.e., for large λ_{SR}). The term of I_2 is given by

$$I_2 = \frac{(\gamma+\Lambda_D+\lambda_{RD}N_D)}{\Gamma(N_R)\Gamma(N_D+1)}$$

$$\times \int_0^\infty z^{N_R-1} e^{-z} \int_0^\infty t^{N_D} e^{-t(\gamma+\Lambda_D)} \int_0^\infty \exp \left(-\frac{\gamma(\gamma+1)}{x} \left(\frac{1}{\lambda_{SR}} + \frac{z}{\gamma+\Lambda_R} \right) - x \left(t + \frac{1}{\lambda_{RD}} \right) \right) dxdtdz. \tag{5.37}$$

Following a similar analysis to the one leading to (5.36), it is straightforward to show that

$$I_2 = \frac{(\gamma+\Lambda_D+\lambda_{RD}N_D)}{\lambda_{RD}^{N_D+1}} \psi \left(N_D+1; N_D+1; (\gamma_{th}+\Lambda_D)\lambda_{RD}^{-1} \right). \tag{5.38}$$

Then, substituting (5.36) and (5.38) in (5.18), the cdf of end-to-end SINR may be approximated as

$$F_{\gamma_{eq}}^{approx}(\gamma) = 1 - \left(\frac{\Lambda_R}{\gamma + \Lambda_R}\right)^{N_R} \frac{\Lambda_D^{N_D}}{\lambda_{RD}^{N_D+1}} \exp\left(-\gamma\left(\frac{1}{\lambda_{SR}} + \frac{1}{\lambda_{RD}}\right)\right)$$
$$\times \left\{\lambda_{RD}\psi\left(N_D + 1; N_D; \frac{\gamma + \Lambda_D}{\lambda_{RD}}\right) + (\gamma + \Lambda_D + \lambda_{RD}N_D)\psi\left(N_D + 1; N_D + 1; \frac{\gamma + \Lambda_D}{\lambda_{RD}}\right)\right\}.$$

(5.39)

5.3 Interference-limited (CCI only)

5.3.1 System Model

In an interference-limited Rayleigh fading environment, the dual-hop system is dominated by co-channel interference. In this case the effect of thermal noise may be neglected. Therefore, $\sigma_R^2 = \sigma_D^2 = 0$ in (5.5), the end-to-end instantaneous SIR is then given by

$$\tilde{\gamma}_{eq} = \frac{P_s |h_{SR}|^2 P_R |h_{RD}|^2}{P_R |h_{RD}|^2 \tilde{\gamma}_a + \tilde{\gamma}_b \left(P_S |h_{SR}|^2 + \tilde{\gamma}_a\right)}, \tag{5.40}$$

where $\tilde{\gamma}_a = \sum_{i=1}^{N_R} P_{R_i} |h_{R_i}|^2$, $\tilde{\gamma}_b = \sum_{i=1}^{N_D} P_{D_i} |h_{D_i}|^2$. Next dividing (5.40) by $\tilde{\gamma}_a\tilde{\gamma}_b / \tilde{\gamma}_a\tilde{\gamma}_b$ gives

$$\tilde{\gamma}_{eq} = \frac{\tilde{\gamma}_1\tilde{\gamma}_2}{\tilde{\gamma}_1 + \tilde{\gamma}_2 + 1}, \tag{5.41}$$

where $\tilde{\gamma}_1 = \dfrac{P_s |h_{SR}|^2}{\tilde{\gamma}_a}$, $\tilde{\gamma}_2 = \dfrac{P_s |h_{RD}|^2}{\tilde{\gamma}_b}$ are the instantaneous SIRs at the relay and the destination, respectively. The pdfs for $\tilde{\gamma}_1$ and $\tilde{\gamma}_2$ are given, respectively, as [73, eq. (13)]

$$f_{\tilde{\gamma}_1}(\gamma_1) = \frac{N_R\Lambda_R^{N_R}}{(\gamma_1 + \Lambda_R)^{N_R+1}}, \tag{5.42a}$$

$$f_{\tilde{\gamma}_2}(\gamma_2) = \frac{N_D\Lambda_D^{N_D}}{(\gamma_2 + \Lambda_D)^{N_D+1}}. \tag{5.42b}$$

The corresponding cdfs for $\tilde{\gamma}_1$ and $\tilde{\gamma}_2$ are given by (see Appendix C)

$$F_{\tilde{\gamma}_1}(\gamma_1) = 1 - \left(1 + \frac{\gamma_1}{\Lambda_R}\right)^{-N_R}, \qquad (5.43a)$$

$$F_{\tilde{\gamma}_2}(\gamma_2) = 1 - \left(1 + \frac{\gamma_2}{\Lambda_D}\right)^{-N_D}. \qquad (5.43b)$$

5.3.1.1 CDF of End-to-End SIR System

Similar to (5.15) and (5.16), the cdf of the end-to-end SIR can be given by

$$F_{\tilde{\gamma}_{eq}}(\gamma) = \int_0^\gamma f_{\tilde{\gamma}_2}(\gamma_2)d\gamma_2 + \int_\gamma^\infty F_{\tilde{\gamma}_1}\left(\frac{\gamma\gamma_2 + \gamma}{\gamma_2 - \gamma}\right)f_{\tilde{\gamma}_2}(\gamma_2)d\gamma_2. \qquad (5.44)$$

Substituting (5.42b) and (5.43a) in (5.44) and making the change of variables $x = \gamma_2 - \gamma$

gives

$$F_{\tilde{\gamma}_{eq}}(\gamma) = 1 - \frac{\Lambda_R^{N_R} N_D \Lambda_D^{N_D}}{(\gamma + \Lambda_R)^{N_R}} \int_0^\infty x^{N_R} \left(x + \frac{\gamma(\gamma+1)}{(\gamma + \Lambda_R)}\right)^{-N_R} (x + \gamma + \Lambda_D)^{-(N_D+2)} dx. \qquad (5.45)$$

Using the identity in [38, eq. (3.197.1)], the closed-form expression for the cdf of the

end-to-end SIR is given by

$$F_{\tilde{\gamma}_{eq}}(\gamma) = 1 - \frac{\Lambda_R^{N_R} \Lambda_D^{N_D} \Gamma(N_D + 1)\Gamma(N_R + 1)}{(\gamma + \Lambda_R)^{N_R+1}(\gamma + \Lambda_D)^{N_D+1}\Gamma(N_R + N_D + 1)}$$

$$\times {}_2F_1\left(N_R + 1, N_D + 1; N_R + N_D + 1; -\frac{\gamma(\gamma+1)}{(\gamma + \Lambda_R)(\gamma + \Lambda_D)}\right), \qquad (5.46)$$

where ${}_2F_1(a,b;c;z)$ is the Gauss hypergeometric function [38].

5.4 Performance Analysis

5.4.1 Outage Probability

In a wireless communication system with co-channel interference and thermal noise, the outage probability is the probability that the instantaneous SINR exceeds a preset threshold γ_{th} and is given by $P_{out} = \Pr\left(\gamma \le \gamma_{th}\right)$. For the dual hop relay system, the exact and the approximate outage probabilities may be obtained from (5.26) and (5.39) as $P_{out(exact)} = F_{\gamma_{eq}}\left(\gamma_{th}\right)$ and $P_{out(approx)} = F_{\gamma_{eq}^{approx}}\left(\gamma_{th}\right)$, respectively. Similarly, for an interference-limited system, the probability that the instantaneous SIR falls below a preset threshold γ_{th} can be obtained from (5.46) by $P_{out(SIR)} = F_{\tilde{\gamma}_{eq}}\left(\gamma_{th}\right)$.

5.4.2 ABER of Binary Modulations

The ABER is another useful performance measure that is usually used to characterize a wireless digital communication system. In the presence of AWGN, the conditional BER for binary phase shift keying (BPSK) and binary frequency shift keying (BFSK), with coherent (i.e., CPSK/CFSK) and non-coherent (i.e., NPSK/NFSK) detections, is given by

$$P_E\left(\gamma\right) = \frac{\Gamma\left(\beta, \alpha\gamma\right)}{2\Gamma\left(\beta\right)}, \tag{5.47}$$

where $\alpha = 1$ for BPSK, $\alpha = 1/2$ for BFSK, $\beta = 1$ for NPSK/DPSK, $\beta = 1/2$ for CFSK/CPSK [63] and $\Gamma\left(p,x\right) = \int_x^\infty t^{p-1}e^{-t}dt$ is the incomplete gamma function [38]. The ABER for binary modulations may then be obtained as

$$\bar{P}_E = \frac{1}{2\Gamma\left(\beta\right)}\int_0^\infty \Gamma(\beta,\alpha\gamma)f_{\gamma_{eq}}(\gamma)d\gamma,$$

$$= \frac{1}{2\Gamma\left(\beta\right)}\int_0^\infty \gamma^{\beta-1}e^{-\alpha\gamma}F_{eq}(\gamma)d\gamma. \tag{5.48}$$

5.4.2.1 Approximate ABER Using Eq. (5.39)

The ABER may be obtained by substituting (5.39) in (5.48) to give

$$\bar{P}_E = \frac{1}{2\alpha^\beta} - \frac{\Lambda_R^{N_R}\Lambda_D^{N_D}}{2\Gamma(\beta)\lambda_{RD}^{N_D+1}}\left(\lambda_{RD}T_1 + T_2 + \left(\Lambda_D + \lambda_{RD}N_D\right)T_3\right), \tag{5.49}$$

where

$$T_1 = \int_0^\infty \frac{\gamma^{\beta-1}}{\left(\gamma+\Lambda_R\right)^{N_R}}e^{-a\gamma}\psi\left(N_D+1, N_D; \frac{\gamma+\Lambda_D}{\lambda_{RD}}\right)d\gamma, \tag{5.50}$$

$$T_2 = \int_0^\infty \frac{\gamma^{\beta}}{\left(\gamma+\Lambda_R\right)^{N_R}}e^{-a\gamma}\psi\left(N_D+1, N_D+1; \frac{\gamma+\Lambda_D}{\lambda_{RD}}\right)d\gamma, \tag{5.51}$$

$$T_3 = \int_0^\infty \frac{\gamma^{\beta-1}}{\left(\gamma+\Lambda_R\right)^{N_R}}e^{-a\gamma}\psi\left(N_D+1, N_D+1; \frac{\gamma+\Lambda_D}{\lambda_{RD}}\right)d\gamma. \tag{5.52}$$

The constant a in (5.50)-(5.52) is defined as $a = \left(\frac{1}{\lambda_{SR}} + \frac{1}{\lambda_{RD}} + \alpha\right)$. Since the integrals in

(5.50)-(5.52) are in the form

$$A = \int_0^\infty \frac{x^{v-1}}{\left(x+b\right)^m}e^{-ax}\psi\left(c, c+i; gx+f\right)d\gamma, \tag{5.53}$$

where a, b, c, f, g, m, $v \geq 0$ and $i \in (-1, 0)$ are the arbitrary constants, using a Taylor

series expansion of the confluent hypergeometric function, yields [13]

$$\psi\left(c; c+i; gx+f\right) = \sum_{k=0}^\infty \frac{(c)_k}{k!}(-gx)^k \psi\left(c+k; c+i+k; f\right),$$

$$\approx \psi\left(c; c+i; f\right) - cgx\psi\left(c+1; c+i+1; f\right), \tag{5.54}$$

where for sufficiently small values of g. Only the first two terms in the series may be

considered. Using (5.54), the integral in (5.53) becomes

$$A \cong \Gamma(v)b^{v-m}\left\{\psi\left(c+1; c+i; f\right)\psi\left(v; v+1-m; ab\right)\right.$$

$$\left. - (cgbv)\psi\left(c+1; c+i+1; f\right)\psi\left(v+1; v+2-m; ab\right)\right\}. \tag{5.55}$$

Using (5.55), the ABER in (5.49) becomes

$$\bar{P}_E = \frac{1}{2\alpha^\beta} - \frac{\Lambda_R^{N_R}\Lambda_D^{N_D}}{2\Gamma(\beta)\lambda_{RD}^{N_D+1}}\left(J_1 + J_2 + J_3\right), \tag{5.56}$$

where

$$J_1 = \lambda_{RD}\Gamma(\beta)\Lambda_R^{\beta-N_R}\left[\psi\left(N_D+1;N_D;\frac{\Lambda_D}{\lambda_{RD}}\right)\psi\left(\beta;\beta+1-N_R;a\Lambda_R\right)\right.$$

$$\left. -\frac{(N_D+1)\Lambda_R}{\lambda_{RD}}\psi\left(N_D+2;N_D+1;\frac{\Lambda_D}{\lambda_{RD}}\right)\psi\left(\beta+1;\beta+2-N_R;a\Lambda_R\right)\right], \quad (5.57)$$

$$J_2 = \Gamma(\beta+1)\Lambda_R^{\beta+1-N_R}\left[\psi\left(N_D+1;N_D+1;\frac{\Lambda_D}{\lambda_{RD}}\right)\psi\left(\beta+1;\beta+2-N_R;a\Lambda_R\right)\right.$$

$$\left. -\frac{(N_D+1)\Lambda_R}{\lambda_{RD}}\psi\left(N_D+2;N_D+2;\frac{\Lambda_D}{\lambda_{RD}}\right)\psi\left(\beta+2;\beta+3-N_R;a\Lambda_R\right)\right], \quad (5.58)$$

$$J_3 = \left(\Lambda_D+\lambda_{RD}N_D\right)\Gamma(\beta)\Lambda_R^{\beta-N_R}\left[\psi\left(N_D+1;N_D+1;\frac{\Lambda_D}{\lambda_{RD}}\right)\psi\left(\beta;\beta+1-N_R;a\Lambda_R\right)\right.$$

$$\left. -\frac{(N_D+1)\Lambda_R}{\lambda_{RD}}\psi\left(N_D+2;N_D+2;\frac{\Lambda_D}{\lambda_{RD}}\right)\psi\left(\beta+1;\beta+2-N_R;a\Lambda_R\right)\right]. \quad (5.59)$$

5.4.2.2 Exact ABER for the Interference-limited Case

The exact ABER for the end-to-end SIR may be obtained by substituting (5.46) in (5.48) as

$$\bar{P}_E = \frac{1}{2\alpha^\beta} - \frac{\Lambda_R^{N_R}\Lambda_D^{N_D}\Gamma(N_R+1)\Gamma(N_D+1)}{2\Gamma(\beta)\Gamma(N_R+N_D+1)}\int_0^\infty \frac{\gamma(\gamma+1)e^{-\beta\gamma}}{(\gamma+\Lambda_R)^{N_R+1}(\gamma+\Lambda_D)^{N_D+1}}$$

$$\times {}_2F_1\left(N_R+1,N_D+1;N_R+N_D+1;1-\frac{\gamma(\gamma+1)}{(\gamma+\Lambda_R)(\gamma+\Lambda_D)}\right)d\gamma. \quad (5.60)$$

Unfortuately, a closed-form solution for the integral in (5.60) cannot be obtained, however, the result can be accurately computed by using the numerical integration in [7, (25.4.33)].

5.5 Numerical Results

In this section, some numerical and simulation results to illustrate the performance analysis for a dual-hop AF relay system in a Rayleigh fading channel in the presence of

identically distributed co-channel interferers at the relay and destination nodes are illustrated. Figure 5.2 shows a comparison of the approximate outage probability in (5.39) with the exact one given in (5.26), when the threshold γ_{th} is set at 3 dB. Assuming that there are the same number of co-channel interferers at **R** and **D** (i.e., $N_R = N_D = 0,1,2,4$) with equal powers (all INRs are set equal to 5dB). It is observed that as the number of interfering signals increases the outage probability increases, with the most dramatic performance deterioration occurring with the introduction of the first interferer. For example, when there is no interference in the system $(N_R = N_D = 0)$ and equal desired signal powers along the **S - R** and **R - D** links (i.e., $\lambda_{SR} = \lambda_{SD}$), in order the maintain the same outage performance of 10%, the transmission powers must be increased by approximately 6 dB to counter the effect of a single interferer and by 12dB for four interferers. In addition, it can be found that the numerical results based on the exact cdf of the end-to-end SINR match perfectly with computer simulation results, while the results of the approximate outage probability agrees with the simulation result when the link signals are strong (for $\lambda_{SR}, \lambda_{SD} \geq 25$ dB).

Figure 5.3 shows the outage probability for a dual-hop relay system in the presence of high-power interferers at both the relay and destination terminals. Specifically, the parameters Λ_R and Λ_D are set at 30 dB and one can observe that at low and moderate SNRs $\left(\lambda_{SR}, \lambda_{SD} \right)$, increasing the SNR improves the outage performance because AWGN is the dominate noise in this region. On the other hand, at high SNRs, an outage floor results due to the fact that the effect of co-channel interferers is independent of the SNR [45].

In Figure 5.4, the ABER in (5.56) for the case of DPSK is plotted. Similar to Figure 5.2, the ABER performance deteriorates as the number of interferers increases; also the approximation agrees with the exact ABER result (obtained from computer simulation) when the link signals are strong, i.e., $\lambda_{SR}, \lambda_{SD} \geq 20$ dB. Moreover, in Figure 5.5, the ABER of dual-hop relay system with the presence of strong SIR at both the relay and destination terminals (i.e., $\Lambda_R = \Lambda_D = 30$ dB) are provided. Similar to Figure 5.3, it can be shown that at low and moderate values of λ_{SR} and λ_{SD}, increasing the SNR improves the ABER performance because the dominate noise in this region is AWGN. On the other hand, at high SNRs, an ABER floor results as shown in [45].

Finally, an interference-limited dual hop relay system is considered. Figure 5.5 plots the outage probability of such a system, using the closed-form expression in (5.46), whereas Figure 5.6 plots the ABER of DPSK using the expression in (5.59). As expected, numerical results match perfectly with the results of the simulation. Both figures depict the performance deterioration that occurs as the number of interferers increases.
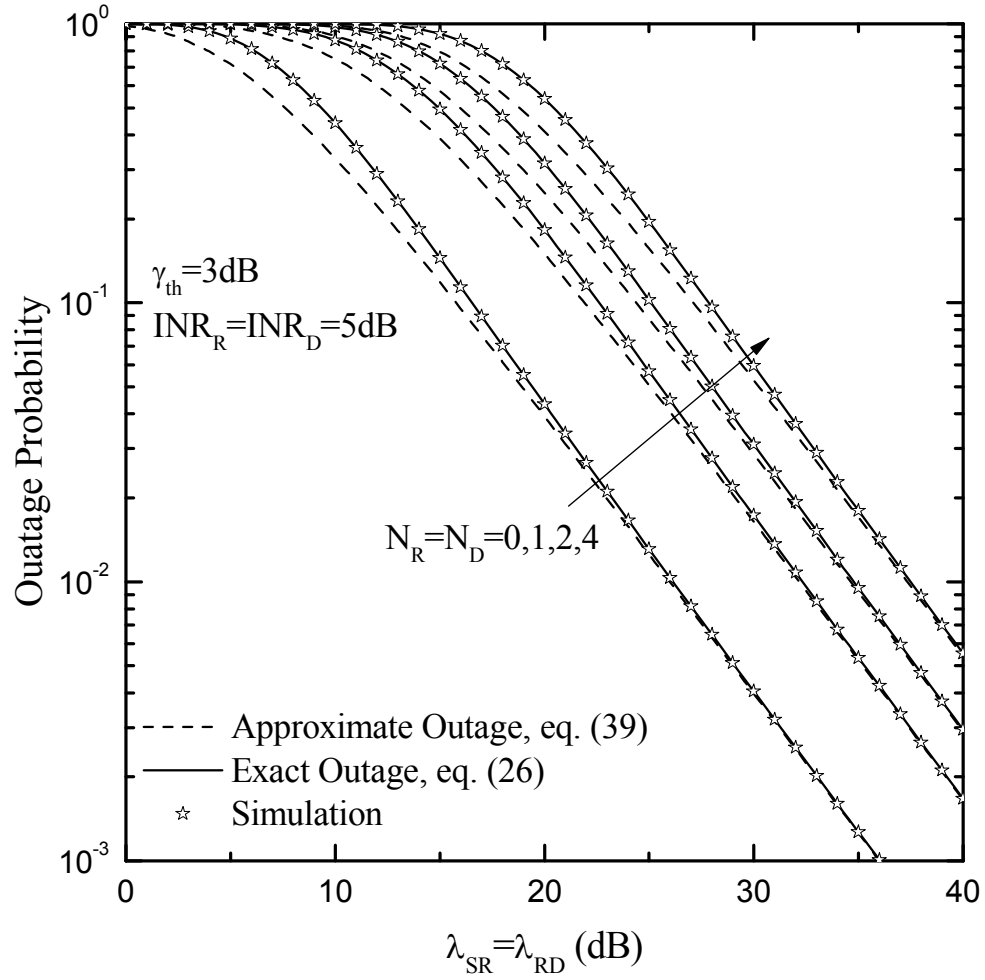
Figure 5.2 Outage probability of dual-hop relay system in the presence of equal-power

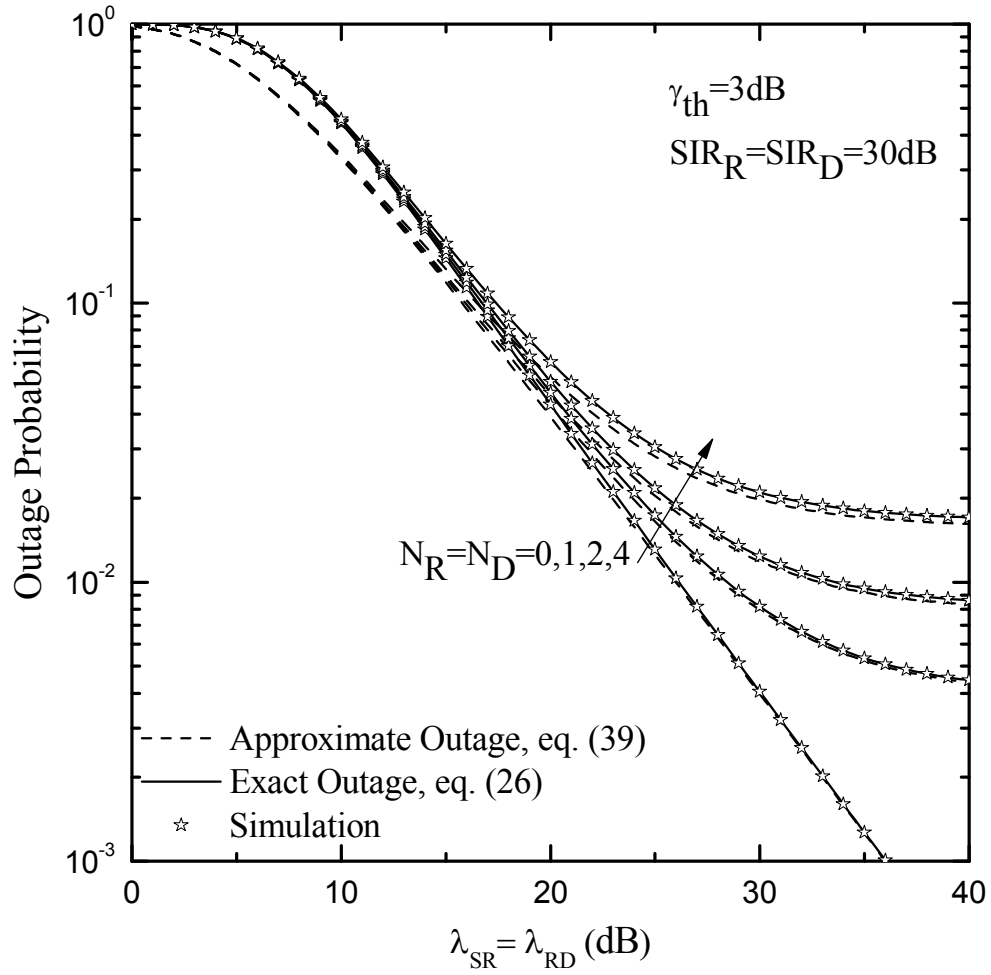interferers at the relay and destination nodes.

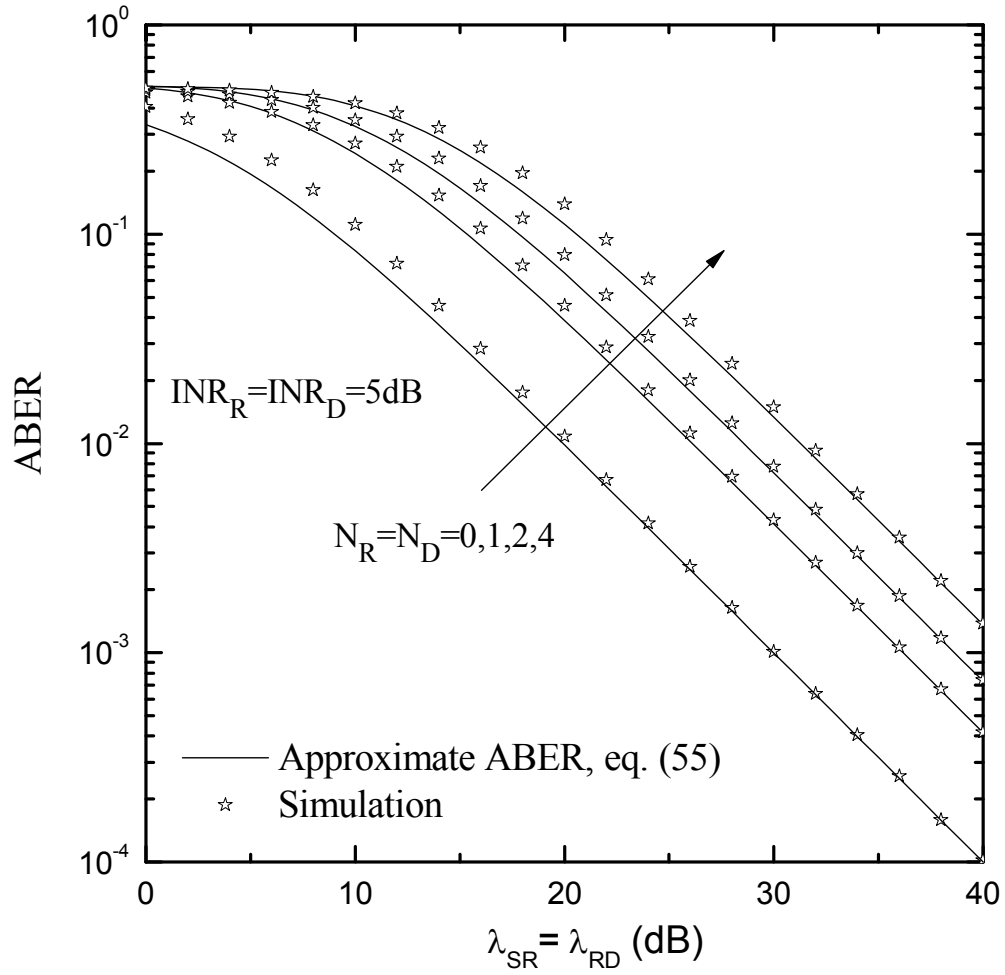**Figure 5.3** Outage probability of dual-hop relay system with high SIR at the relay and destination nodes.

Figure 5.4 ABER of dual-hop relay system in the presence of equal-power interferers at the relay and destination nodes.
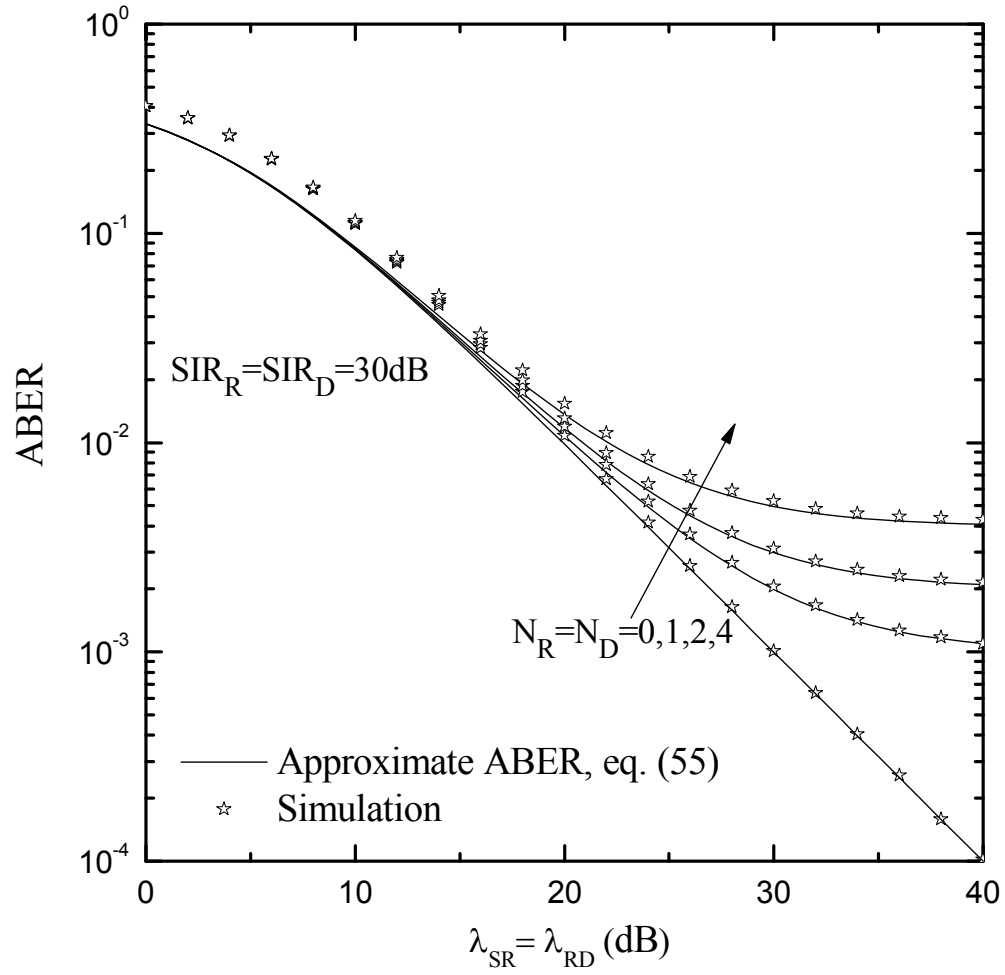
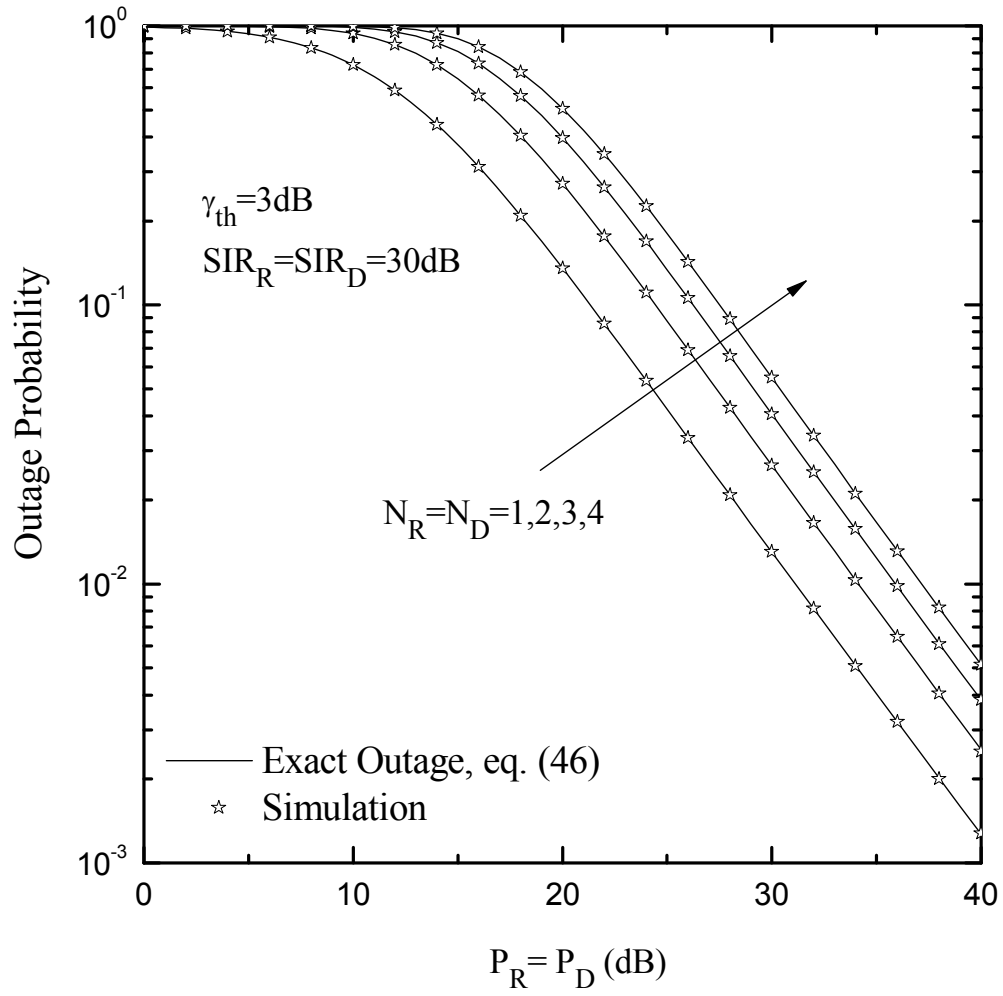**Figure 5.5** ABER of dual-hop relay system with high SIR at the relay and destination nodes.

Figure 5.6 Outage probability of interference-limited dual-hop relay system.

CHAPTER 6 MULTI-HOP RELAY SYSTEMS IN RAYLEIGH FADING CHANNELS

6.1 Introduction

Multihop relaying in which the transmitted signal propagates through cascaded nodes, with each node amplifying and forwarding the received signal from the previous node to the next, has been shown to improve the performance and extend the coverage of many communication systems [44], [65]. The performances of multihop AF and DF relaying systems in a thermal noise-limited environment have been studied extensively [40-41], [47]. In these systems, it is well known that the choice of the relay gain that maximizes the end-to-end SNR is to invert the combined instantaneous received power (i.e., sum of desired signal and noise power) at each relay node. The exact closed-form analytical expression for the end-to-end SNR for an arbitrary N-hops transmission system is derived in [41]. However, the exact performances of such system appear to be intractable for $N \geq 3$ and are usually bounded or asymptotically approximated. For example, upper bounds may be obtained for the end-to-end SNR by bounding the harmonic mean by geometric mean [47] or by bounding the end-to-end SNR by the minimum SNR of all the hops [41], [47]. It is well known that in a multihop relay network with multiple relays in series, the end-to-end SNR in an AF system in which the relay gains ignores noise is, indeed, proportional to the harmonic mean of all the per-hop SNRs. In DF relaying, on the other hand, the end-to-end SNR is dominated by the SNR of the weakest link [41].

A lot of the existing works on multihop relay transmission consider thermal noise-limited conditions in systems with no interference. However, in addition to thermal noise, many practical relay networks also encounter co-channel interference, which causes severe performance degradation. Co-channel interference is inherent in many

wireless networks due to frequency re-use that optimizes spectrum utilization in such system. Recently, considerable attention has been given to dual-hop AF relay transmission in the presence of thermal noise and co-channel interference [45], [47], [54], [76]. In most of these studies for the effect of Rayleigh interferers, the exact distribution of the end-to-end SNR has not been obtained and the analytical results are based on bounds or asymptotic approximations. However, the outage probability performance of dual-hop DF transmissions in a Rayleigh fading environment with interference has also been studied in [48], [55], [85].

In this chapter, the outage probability, the average symbol error rate and the average channel capacity performances of multi-hop relay systems with AF and DF relays are considered. Specifically, it can be shown that the well-known result of [41, eq. (2)] also holds in the presence of interference and Gaussian noise, where now, the SNR is replaced by SIR in an interference-limited system and SINR in the presence of interference and noise. This observation was also made by a number of investigators for the special case of dual-hop relaying [45], [54], [76]. Then following [41], [54], [55], two upper bounds for the end-to-end SINR; namely, the minimum SINR are investigeted along the hop links (which corresponds to DF relaying) and the harmonic mean of the per-hop SINR (which corresponds to AF relaying).

6.2 System Model

A wireless network, comprising a source **S**, several relays (R_n, $n=1,2,..,N-1$) in series and a destination ($D=R_N$) is considered. It is assumed that the desired signal at the nth relay is interrupted by L_n, $n=1,2,..,N$ co-channel interferers and the additive white Gaussian noisewith power σ_n^2, $n=1,2,..,N$, as shown in Figure 6.1.
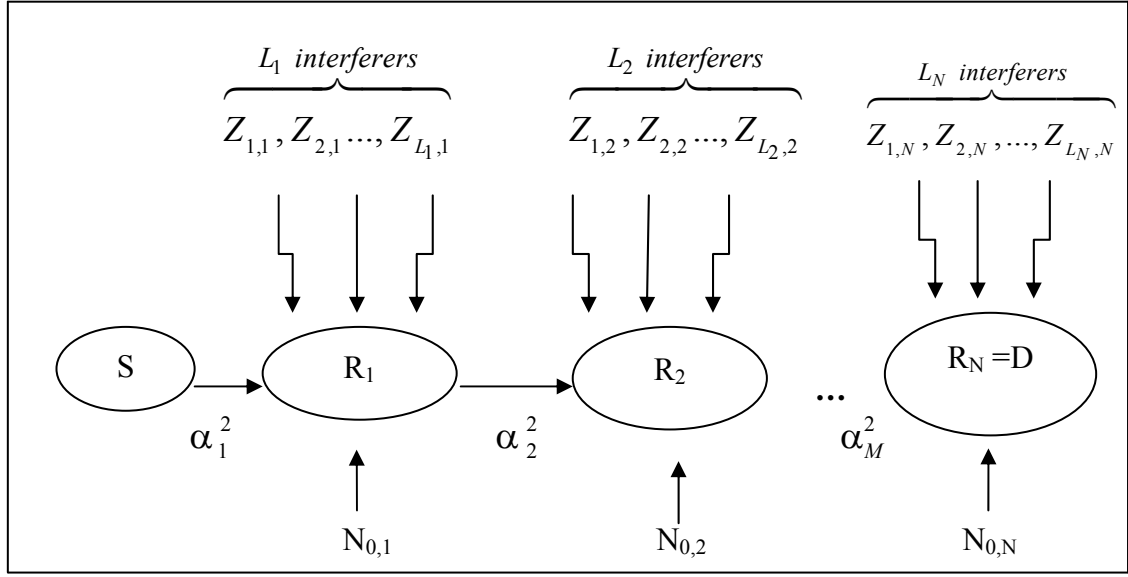
Figure 6.1 The multi-hop systems with the presence of interference and noise

In the figure, α_n is the fading amplitude of the desired signal on the communication link between relay nodes n-1 and n. In the case of AF protocol, the received signal at the relay node n is amplified by the gain G_n and forwarded to the next relay node. The total power of the desired signal at the final node in the series chain is given by

$$P_D = \left(\alpha_1^2 \alpha_2^2 ... \alpha_N^2\right)\left(G_1^2 G_2^2 ... G_{N-1}^2\right).$$ (6.1)

The instantaneous power of the i-th interferer at node n is denoted by $Z_{i,n}$, $i=1,2,...,L_n$. Therefore, the total interference power at the destination hop D is given by

$$I_D = \sum_{i=1}^{L_1} Z_{i,1}\left(G_1^2 G_2^2 ... G_{N-1}^2\right)\left(\alpha_2^2 \alpha_3^2 ... \alpha_N^2\right) + \sum_{i=1}^{L_2} Z_{i,2}\left(G_2^2 G_3^2 ... G_{N-1}^2\right)\left(\alpha_3^2 \alpha_4^2 ... \alpha_N^2\right)$$

$$+ \sum_{i=1}^{L_3} Z_{i,3}\left(G_3^2 G_4^2 ... G_{N-1}^2\right)\left(\alpha_4^2 \alpha_5^2 ... \alpha_N^2\right) + ... + \sum_{i=1}^{L_N} Z_{i,N}.$$ (6.2)

The total noise power at the destination is

$$N_D = \sigma_1^2\left(G_1^2 G_2^2 ... G_{N-1}^2\right)\left(\alpha_2^2 \alpha_3^2 ... \alpha_N^2\right) + \sigma_2^2\left(G_2^2 G_3^2 ... G_{N-1}^2\right)\left(\alpha_3^2 \alpha_4^2 ... \alpha_N^2\right)$$

$$+ \sigma_3^2\left(G_3^2 G_4^2 ... G_{N-1}^2\right)\left(\alpha_4^2 \alpha_5^2 ... \alpha_N^2\right) + ... + \sigma_N^2.$$ (6.3)

Consequently, the end-to-end instantaneous SINR is given by

$$\gamma_{eq} = \frac{P_D}{I_D + N_D},$$

$$= \frac{\prod_{n=1}^{N} \alpha_n^2 \prod_{n=1}^{N-1} G_n^2}{a \sum_{n=1}^{N} \sigma_n^2 \prod_{s=n+1}^{N} \alpha_s^2 \prod_{s=n}^{N-1} G_s^2 + b \sum_{n=1}^{N} \sum_{i=1}^{L_n} Z_{i,n} \prod_{s=n+1}^{N} \alpha_s^2 \prod_{s=n}^{N-1} G_s^2},$$

$$= \frac{\prod_{n=1}^{N} \alpha_n^2 \prod_{n=1}^{N-1} G_n^2}{\sum_{n=1}^{N} \left(a\sigma_n^2 + b \sum_{i=1}^{L_n} Z_{i,n} \right) \prod_{s=n+1}^{N} \alpha_s^2 \prod_{s=n}^{N-1} G_s^2},$$

(6.4)

where the parameters $a,b = [0,1]$ are constants introduced to account for the presence of co-channel interference and thermal noise at the relays. For example, $(a=1, b=0)$ corresponds to the case of no interferers (noise-limited system) while $(a=0, b=1)$ implies that no noise is present (interference-limited system). Next, dividing both nominator and denominator in (6.4) by $\prod_{n=1}^{N} \left(a\sigma_n^2 + b \sum_{i=1}^{L_N} Z_{i,n} \right) \prod_{n=1}^{N-1} G_n^2$, yeilds

$$\gamma_{eq} = \frac{\prod_{n=1}^{N} \dfrac{\alpha_n^2}{\left(a\sigma_n^2 + b \sum_{i=1}^{L_N} Z_{i,n} \right)}}{\sum_{n=1}^{N} \dfrac{\prod_{s=n+1}^{N} \dfrac{\alpha_s^2}{\left(a\sigma_s^2 + b \sum_{i=1}^{L_s} Z_{i,s} \right)}}{\prod_{s=1}^{n-1} G_s^2 \prod_{s=1}^{n-1} \left(a\sigma_s^2 + b \sum_{i=1}^{L_s} Z_{i,s} \right)}}.$$

(6.5)

The AF gain employed at the *n*-th relay is chosen as

$$G_n^2 = \frac{1}{\alpha_n^2 + a\sigma_n^2 + b \sum_{i=1}^{L_n} Z_{i,n}}. \tag{6.6}$$

Substituting (6.6) in (6.5) and simplifying, the equivalent end-to-end SINR is then given by

$$\gamma_{eq} = \frac{\prod_{n=1}^{N} \frac{\alpha_n^2}{\left(a\sigma_n^2 + b\sum_{i=1}^{L_N} Z_{i,n}\right)}}{\sum_{n=1}^{N} \prod_{s=n+1}^{N} \frac{\alpha_s^2}{\left(a\sigma_s^2 + b\sum_{i=1}^{L_N} Z_{i,s}\right)} \prod_{s=1}^{n-1} \left(\frac{\alpha_s^2}{\left(a\sigma_s^2 + b\sum_{i=1}^{L_n} Z_{i,s}\right)} + 1\right)},$$

$$= \left[\sum_{n=1}^{N} \frac{1}{\gamma_n} \prod_{s=1}^{n-1} \left(1 + \frac{1}{\gamma_s}\right)\right]^{-1},$$

(6.7)

which is the equivalent end-to-end SINR given in [41, eq.(3)], where now

$$\gamma_n = \frac{\alpha_n^2}{a\sigma_n^2 + b\sum_{i=1}^{L_j} Z_{i,n}}$$ (6.8)

is the generalized SINR per hop. The following special cases for the choice of the parameters a and b will be considered in the rest of this paper:

i)   Noise-Limited Systems ($a=1,\ b=0$)

$\gamma_n = \frac{\alpha_n^2}{\sigma_n^2}$ is the SNR per hop [41, eq.(2)].

ii)   Interference-limited case ($a=0,\ b=1$)

$\gamma_n = \frac{\alpha_n^2}{\sum_{i=1}^{L_n} Z_{i,n}}$ is the SIR per hop [54], [55].

iii)   In general ($a=b=1$)

$\gamma_n = \frac{\alpha_n^2}{\sigma_n^2 + \sum_{i=1}^{L_n} Z_{i,n}}$ is the SINR per hop [45], [76].

Note that replacing N=2 in (6.7), then $\gamma_{eq} = \frac{\gamma_1 \gamma_2}{\gamma_1 + \gamma_2 + 1}$ which is the end-to-end SINR of the dual-hop relay system as shown in (5.7).

6.3 Statistics of End-to-End SINR

To the best of our knowledge, the exact cdf of the end-to-end SINR in (6.7) is still unavailable due to its complicated mathematical form. Also the analytical results are usually based on obtaining bounds on the system performance. In what follows two upper bounds on the end-to-end SINR that are frequently considered in the literature for evaluating the system performance, and correspond to the end-to-end SINR for DF and AF relaying are focused. The cdf of the SINR per hop given by

$$F_{\gamma_n}(\gamma) = \Pr\left[\alpha_n^2 < \gamma\left(a\sigma_n^2 + b\tilde{Z}_n\right)\right],$$

$$= \int_0^\infty F_{x_n}\left[\gamma\left(a + b\frac{\tilde{Z}_n}{\sigma_n^2}\right)\right] f_{\tilde{Z}_n}\left(\tilde{Z}_n\right) d\tilde{Z}_n, \tag{6.9}$$

where $x_n = \alpha_n^2/\sigma_n^2$, $\tilde{Z}_n = \sum_{i=1}^{L_n} Z_{i,n}$ and a, b are the arbitrary constants. The additive white Gaussian noise at the n-th relay node has the average power σ_n^2. For Raleigh channel, the cdf of x_n is given by

$$F_{x_n}(x) = 1 - \exp\left(-\frac{x}{\Omega_{s,n}}\right), \tag{6.10}$$

where $\Omega_{s,n}$ is the average SNR of the desired signal at the n-th hop. Substituting (6.10) in (6.9) gives

$$F_{\gamma_n}(\gamma) = \int_0^\infty \left[1 - \exp\left(-\frac{\gamma}{\Omega_{s,n}}\left(a + b\frac{\tilde{Z}_n}{\sigma_n^2}\right)\right)\right] f_{\tilde{Z}_n}\left(\tilde{Z}_n\right) d\tilde{Z}_n,$$

$$= 1 - \exp\left(-\frac{a\gamma}{\Omega_{s,n}}\right) M_{\tilde{Z}_n}\left(\frac{b\gamma}{\Omega_{s,n}}\right),$$

$$= 1 - \exp\left(-\frac{a\gamma}{\Omega_{s,n}}\right) \prod_{i=1}^{L_n} M_{Z_{i,n}}\left(\frac{b\gamma}{\Omega_{s,n}}\right). \tag{6.11}$$

In the presence of Rayleigh-faded interferers, $M_{Z_{i,n}}\left(\frac{b\gamma}{\Omega_{s,n}}\right) = \left(1 + \frac{\Omega_{i,n}b\gamma}{\Omega_{s,n}}\right)^{-1}$ and (6.11) becomes

$$F_{\gamma_n}(\gamma) = 1 - \exp\left(-\frac{a\gamma}{\Omega_{s,n}}\right)\left\{\prod_{i=1}^{L_n}\left(\frac{\Lambda_{i,n}}{b\gamma + \Lambda_{i,n}}\right)\right\},\tag{6.12}$$

where $\Lambda_{i,n} = \dfrac{\Omega_{s,n}}{\Omega_{i,n}}$ is the average signal-to-interference ratio per hop.

6.3.1 DF Relaying

Since in DF relying systems, the end-to-end performance is usually dominated by that of the weakest link, it follows that the end-to-end SINR for DF is given by [41], [76]

$$\gamma_{eq} \le \gamma_{DF} = \min(\gamma_1,...,\gamma_N).$$

(6.13)

It is well known that, in this case, cdf of γ_{DF} is given by

$$F_{\gamma_{DF}}(\gamma) = \Pr\left[\min(\gamma_1,...,\gamma_N) < \gamma\right],$$

$$= 1 - \Pr\left[\gamma_1 > \gamma,...,\gamma_N > \gamma\right],$$

$$= 1 - \prod_{n=1}^{N}\left(1 - F_{\gamma_n}(\gamma)\right).\tag{6.14}$$

Substituting (6.12) in (6.14), the cdf of γ_{DF} is given by

$$F_{\gamma_{DF}}(\gamma) = 1 - \prod_{n=1}^{N}\exp\left(-\frac{a\gamma}{\Omega_{s,n}}\right)\left\{\prod_{i=1}^{L_n}\left(\frac{\Lambda_{i,n}}{b\gamma + \Lambda_{i,n}}\right)\right\},$$

$$= 1 - \exp(-a\gamma\varpi)\prod_{n=1}^{N}\left\{\prod_{i=1}^{L_n}\left(\frac{\Lambda_{i,n}}{b\gamma + \Lambda_{i,n}}\right)\right\},\tag{6.15}$$

where $\varpi = \sum_{n=1}^{N}\dfrac{1}{\Omega_{s,n}}$. Note that replacing $a=0$ (no noise), (6.15) becomes

$$F_{\gamma_{DF}}(\gamma) = 1 - \left\{\prod_{i=1}^{L_n}\left(\frac{\Lambda_{i,n}}{b\gamma + \Lambda_{i,n}}\right)\right\}.\tag{6.16}$$

When $b = 0$ (no interferers), then (6.15) becomes

$$F_{\gamma_{DF}}(\gamma) = 1 - \exp(-a\gamma\varpi).\tag{6.17}$$

In general, there are L_d distinct values of $\Lambda_{i,n}$, $i=1,...,L_n$, $n=1,...,N$ which are denoted by $\{\lambda_r\}_{r=1}^{L_d}$ with multiplicity $\{m_r\}_{r=1}^{L_d}$ such that (6.15) can be expressed as

$$F_{\gamma_{DF}}(\gamma) = 1 - \exp\left(-\sum_{j=1}^{N} \frac{a\gamma}{\Omega_{s,j}}\right) \prod_{i=1}^{L_d} \left(\frac{\lambda_r}{b\gamma + \lambda_r}\right)^{m_r},$$

$$= 1 - \exp\left(-\sum_{n=1}^{N} \frac{a\gamma}{\Omega_{s,n}}\right) \prod_{i=1}^{L_d} \left(\frac{\lambda_r}{b}\right)^{m_r} \sum_{r=1}^{L_d}\sum_{j=1}^{m_r} \Xi_{j,r}\left(\gamma + \frac{\lambda_r}{b}\right)^{-j}, \qquad (6.18)$$

where the coefficient of the partial fraction expansion is given by

$$\Xi_{j,r} = \frac{1}{(m_r - j)!}\left[d^{m_r-j}/d\gamma^{m_r-j}\right]\prod_{\substack{r=1 \\ r\neq j}}^{L_d}\left(\gamma + (\lambda_r/b)\right)^{-m_r}\Bigg|_{\gamma=-\lambda_r/b}. \qquad (6.19)$$

For the case of MGF of γ_{DF}, it can be shown that

$$M_{\gamma_{DF}}(t) = 1 - t\int_0^\infty e^{-t\gamma}\bar{F}_{\gamma_{DF}}(\gamma)d\gamma, \qquad (6.20)$$

where $\bar{F}_{\gamma_{DF}}(\gamma)$ is the complementary cdf of SINR defined by $\bar{F}_{\gamma_{DF}}(\gamma) = 1 - F_{\gamma_{DF}}(\gamma)$.

Substituting (6.18) in (6.20), thus the MGF for end-to-end SINR is given by

$$M_{\gamma_{DF}}(t) = 1 - t\prod_{i=1}^{L_d}\left(\frac{\lambda_r}{b}\right)^{m_r}\sum_{r=1}^{L_d}\sum_{j=1}^{m_r}\Xi_{j,r}\int_0^\infty \exp\left(-\gamma(a\varpi + t)\right)\left(\gamma + \frac{\lambda_r}{b}\right)^{-j}d\gamma,$$

$$= 1 - t\prod_{i=1}^{L_d}\left(\frac{\lambda_r}{b}\right)^{m_r}\sum_{r=1}^{L_d}\sum_{j=1}^{m_r}\Xi_{j,r}\left(\frac{\lambda_r}{b}\right)^{1-j}\psi\left(1, 2-j; \frac{\lambda_r}{b}(a\varpi + t)\right), \qquad (6.21)$$

where $\psi(.)$ is the confluent hypergeometric function defined in [38, eq.(9.211-4)].

Note that replacing $a=0$ (no noise), (6.21)becomes

$$M_{\gamma_{DF}}(t) = 1 - t\prod_{i=1}^{L_d}\left(\frac{\lambda_r}{b}\right)^{m_r}\sum_{r=1}^{L_d}\sum_{j=1}^{m_r}\Xi_{j,r}\left(\frac{\lambda_r}{b}\right)^{1-j}\psi\left(1, 2-j; \frac{\lambda_r}{b}t\right), \qquad (6.22)$$

which is the MGF for end-to-end SIR for interference-limited case. In addition, for $b=0$ (no interferers), substituting (6.17) in (6.20) and using [38, eq.(3.381.4)], the MGF for end-to-end SNR can be given by

$$M_{\gamma_{DF}}(t) = 1 - \frac{t}{t + a\varpi} = \frac{a\varpi}{t + a\varpi}. \tag{6.23}$$

6.3.2 AF Relaying

As stated earlier, in a multihop AF relay system, the end-to-end SINR is upper-bounded by the harmonic mean of the entire hop SINRs in the series chain. In fact, when the choice of the relay gain used in the AF protocol ignores the effect of noise and interference, i.e., $G_n^2 = 1/\alpha_n^2$, the end-to-end SINR is proportional to the harmonic mean of the per-hop SINRs.

Therefore, [41], [76]

$$\gamma_{eq} \leq \gamma_{AF} = \left[\sum_{n=1}^{N} \gamma_n^{-1} \right]^{-1}. \tag{6.24}$$

The MGF of inverse end-to-end SINR per hop (γ_n^{-1}) is provided by [14, eq.(7)]

$$M_{\gamma_n^{-1}}(t) = 1 - 2\sqrt{t} \int_0^\infty J_1(2x\sqrt{t}) M_{\gamma_n}(x^2) dx, \tag{6.25}$$

where $J_1(.)$ is the Bessel function of the first kind and first order [7], and $M_{\gamma_n}(x^2)$ is the MGF of SINR per hop given by

$$M_{\gamma_n}(x^2) = 1 - x^2 \int_0^\infty e^{-x^2\gamma} \bar{F}_{\gamma_n}(\gamma) d\gamma. \tag{6.26}$$

When the interference powers at the nth node are all equal, i.e., $\Lambda_{1,n} = ... = \Lambda_{L_n,n} = \Lambda_n$, (6.12) becomes

$$F_{\gamma_n}(\gamma) = 1 - \exp\left(-\frac{a\gamma}{\Omega_{s,n}} \right) \left(\frac{\Lambda_n}{b\gamma + \Lambda_n} \right)^{L_n}. \tag{6.27}$$

Substituting (6.27) and (6.26) in (6.25), gives

$$M_{\gamma_n^{-1}}(t) = 1 - 2\sqrt{t} \int_0^\infty J_1(2x\sqrt{t}) dx + 2\sqrt{t} \int_0^\infty \exp\left(-\frac{a\gamma}{\Omega_{s,n}} \right) \left(\frac{1}{b\gamma / \Lambda_n + 1} \right)^{L_n} \int_0^\infty x^2 e^{-x^2\gamma} J_1(2x\sqrt{t}) dx d\gamma,$$

$$= 2\sqrt{t}\int_0^\infty \exp\left(-\frac{a\gamma}{\Omega_{s,n}}\right)\left(\frac{1}{b\gamma / \Lambda_n + 1}\right)^{L_n}\int_0^\infty x^2 e^{-x^2\gamma} J_1\left(2x\sqrt{t}\right)dxd\gamma.$$

(6.28)

Next using the identity in [20, eq.(9.1.69)], then

$$J_1\left(2x\sqrt{t}\right) = x\sqrt{t}\,_0F_1\left(-;2;-x^2t\right),$$

(6.29)

where $_pF_q(.)$ is the generalized hypergeometric function [38, eq. (9.14.1)].

Substituting (6.29) in (6.28) and introducing $y=x^2$, yields [38, eq.(7.522.5)]

$$M_{\gamma_n^{-1}}(t) = t\int_0^\infty \exp\left(-\frac{a\gamma}{\Omega_{s,n}}\right)\left(\frac{1}{b\gamma / \Lambda_n + 1}\right)^{L_n}\int_0^\infty ye^{-y\gamma}\,_0F_1\left(-;2;-yt\right)dyd\gamma,$$

$$= t\int_0^\infty \gamma^{-2}\exp\left(-\frac{a\gamma}{\Omega_{s,n}}\right)\left(\frac{1}{b\gamma / \Lambda_n + 1}\right)^{L_n}\,_1F_1\left(2;2;-\frac{t}{\gamma}\right)d\gamma,$$

$$= t\left(\Lambda_n / b\right)^{L_n}\int_0^\infty \gamma^{-L_n-2}\exp\left(-\frac{a\gamma}{\Omega_{s,n}}\right)\left(\frac{1}{1 + \Lambda_n / b\gamma}\right)^{L_n}\exp(-t / \gamma)d\gamma.$$

(6.30)

Using the identity in [38, eq.(3.381.4)], then

$$\left(\Lambda_n / b\gamma + 1\right)^{-L_n} = \frac{1}{\Gamma\left(L_n\right)}\int_0^\infty x^{L_n-1}e^{-x(\Lambda_n / b\gamma+1)}dx.$$

(6.31)

Substituting (6.31) in (6.30) and using [38, eq.(3.478.4)], it can be shown that

$$M_{\gamma_n^{-1}}(t) = \frac{t}{\Gamma\left(L_n\right)}\left(\Lambda_n / b\right)^{L_n}\int_0^\infty x^{L_n-1}e^{-x}\int_0^\infty \gamma^{-L_n-2}\exp\left(-\frac{\gamma a}{\Omega_{s,n}}\right)\exp\left(-\frac{1}{\gamma}\left\{t + \frac{x\Lambda_n}{b}\right\}\right)d\gamma dx,$$

$$= \frac{t}{\Gamma\left(L_n\right)}\left(\Lambda_n / b\right)^{L_n}\int_0^\infty x^{L_n-1}e^{-x}2\left(\left\{t + \frac{x\Lambda_n}{b}\right\} / \left(\frac{a}{\Omega_{s,n}}\right)\right)^{-(L_n+1)/2}K_{-(L_n+1)}\left(2\sqrt{\frac{a}{\Omega_{s,n}}\left\{t + \frac{x\Lambda_n}{b}\right\}}\right)dx,$$

$$= \frac{t}{\Gamma\left(L_n\right)}\left(\Lambda_n / b\right)^{L_n}\int_0^\infty x^{L_n-1}e^{-x}2\left(\left(\frac{a}{\Omega_{s,n}}\right) / \left\{t + \frac{x\Lambda_n}{b}\right\}\right)^{(L_n+1)/2}K_{L_n+1}\left(2\sqrt{\frac{a}{\Omega_{s,n}}\left\{t + \frac{x\Lambda_n}{b}\right\}}\right)dx,$$

(6.32)

where $K_{L_{n+1}}(.)$ is the modified Bessel function of the second kind and $L_n + 1$ order [7].

Using [38, eq.(8.486.17)], the term $K_{L_n+1}(z)$ can be written by

$$K_{L_n+1}(z) = \frac{z}{2(L_n+1)}\left\{K_{L_n+2}(z) - K_{L_n}(z)\right\}. \tag{6.33}$$

Moreover, the modified Bessel function may be approximated as [7, eq.(9.6.9)]

$$K_q(z) \cong \frac{\Gamma(q)}{2}\left(\frac{z}{2}\right)^{-q}. \tag{6.34}$$

Then substituting (6.34) and (6.33) in (6.32), gives

$$M_{\gamma_n^{-1}}(t) \cong \frac{t}{\Gamma(L_n)}(\Lambda_n/b)^{L_n}\left\{\Gamma(L_n+1)\int_0^\infty x^{L_n-1}e^{-x}\left(t+\frac{x\Lambda_n}{b}\right)^{-(L_n+1)}dx\right.$$

$$\left. -\frac{\Gamma(L_n)}{(L_n+1)}\left(\frac{a}{\Omega_{s,n}}\right)(b/\Lambda_n)^{L_n}\int_0^\infty x^{L_n-1}e^{-x}\left\{1+\frac{x\Lambda_n}{tb}\right\}^{-L_n}dx\right\},$$

$$= \Gamma(L_n+1)\psi\left(L_n;0;\frac{tb}{\Lambda_n}\right) - \frac{\Gamma(L_n)t}{(L_n+1)}\left(\frac{a}{\Omega_{s,n}}\right)\psi\left(L_n;1;\frac{tb}{\Lambda_n}\right). \tag{6.35}$$

Note that when $a=0$ (no noise), the second term vanishes and (6.35) becomes

$$M_{\gamma_n^{-1}}(t) = \Gamma(L_n+1)\psi\left(L_n;0;\frac{tb}{\Lambda_n}\right), \tag{6.36}$$

which is the MGF of inverse SIR per hop for the interference-limited case. Under the assumption that the hops are subject to independent fading, the MGF of γ_{AF}^{-1} is given by

$$M_{\gamma_{AF}^{-1}}(t) = \prod_{n=1}^N M_{\gamma_n^{-1}}(t). \tag{6.37}$$

Substituting (6.35) in (6.37) gives

$$M_{\gamma_{AF}^{-1}}(t) = \prod_{n=1}^N \left\{\Gamma(L_n+1)\psi\left(L_n;0;\frac{bt}{\Lambda_n}\right) - \frac{\Gamma(L_n)t}{(L_n+1)}\left(\frac{a}{\Omega_{s,n}}\right)\psi\left(L_n;1;\frac{bt}{\Lambda_n}\right)\right\}. \tag{6.38}$$

In addition, the following representation may be used for the product in (6.38), i.e.,

$$M_{\gamma_B^{-1}}(t) = \prod_{n=1}^N (A_n + B_n) = \sum_{\kappa \in P_N}\prod_{n=1}^N A_n^{\kappa_n}B_n^{1-\kappa_n}, \tag{6.39}$$

where $\mathbf{P}_N := \left\{\kappa = (\kappa_1,\kappa_2,...,\kappa_N): \kappa \in \{0,1\}^N\right\}$ with

$$A_n = \Gamma(L_n + 1) \psi\left(L_n; 0; \frac{bt}{\Lambda_n}\right), \tag{6.40a}$$

$$B_n = -\frac{\Gamma(L_n)t}{(L_n + 1)}\left(\frac{a}{\Omega_{s,n}}\right) \psi\left(L_n; 1; \frac{bt}{\Lambda_n}\right). \tag{6.40b}$$

Therefore the cdf of γ_{AF} can be expressed as [41, eq.(7)]

$$F_{\gamma_{AF}}(\gamma) = 1 - \mathcal{L}^{-1}\left[\frac{\prod_{n=1}^{N} M_{1/\gamma_n}(t)}{t}\right]\bigg|_{x=1/\gamma}, \tag{6.41}$$

where $\mathcal{L}^{-1}(.)$ is the inverse Laplace transform operation. Substituting (6.39) in (6.41), the

cdf can be shown to be given by

$$F_{\gamma_{AF}}(\gamma) = 1 - \sum_{\kappa \in \mathcal{P}_N} \mathcal{L}^{-1}\left[t^{-1} \prod_{n=1}^{N} \left\{\Gamma(L_n + 1)\psi\left(L_n; 0; \frac{bt}{\Lambda_n}\right)\right\}^{\kappa_n} \left\{-\frac{\Gamma(L_n)t}{(L_n + 1)}\left(\frac{a}{\Omega_{s,n}}\right)\psi\left(L_n; 1; \frac{bt}{\Lambda_n}\right)\right\}^{1-\kappa_n}\right]\bigg|_{x=1/\gamma},$$

$$= 1 - \sum_{\kappa \in \mathcal{P}_N} \left\{\prod_{n=1}^{N} \left[\Gamma(L_n + 1)\right]^{\kappa_n} \left[-\frac{\Gamma(L_n)}{(L_n + 1)}\left(\frac{a}{\Omega_{s,n}}\right)\right]^{1-\kappa_n}\right\},$$

$$\times \mathcal{L}^{-1}\left[t^{N-1-\sum_{n=1}^{N}\kappa_n} \prod_{n=1}^{N} \left[\psi\left(L_n; 0; \frac{bt}{\Lambda_n}\right)\right]^{\kappa_n} \left[\psi\left(L_n; 1; \frac{bt}{\Lambda_n}\right)\right]^{1-\kappa_n}\right]\bigg|_{x=1/\gamma}. \tag{6.42}$$

The inverse transform in (6.42) can be evaluated using the following Laplace inversion

formula to obtain

$$\mathcal{L}^{-1}\left\{t^{c-1}\prod_{n=1}^{N} \psi(a_n, b_n; \sigma_n t)\right\} = \frac{x^{\sum_{n=1}^{N} a_n - c}}{\Gamma\left(\sum_{n=1}^{N} a_n + 1 - c\right)} \prod_{n=1}^{N} \sigma_n^{-a_n}$$

$$\times F_B^{(N)}\left(a_1,...,a_N, 1 + a_1 - b_1,...,1 + a_N - b_N; \sum_{n=1}^{N} a_n + 1 - c; \frac{-x}{\sigma_1},...,\frac{-x}{\sigma_N}\right), \tag{6.43}$$

The proof of (6.43) is provided in Appendix D.

The term $F_B^{(N)}$ in (6.43) is the Lauricella multivariate hypergeometric function of the

second kind [31]. Note that (6.43) generalizes [54, eq.(27)] and [31, eq.(3.24.6.3)] as the

inverse Laplace transform of an arbitrary number of the confluent hypergeometric function, each with arbitrary parameters. Using (6.43) and upon simplifying the resulting expression, the cdf of γ_{AF} becomes

$$F_{\gamma_{AF}}(\gamma) = 1 - \sum_{\kappa \in \square_N} \left\{ \prod_{n=1}^{N} \left(\frac{b}{\Lambda_n}\right)^{-1} \left[\Gamma(L_n+1)\right]^{\kappa_n} \left[-\frac{\Gamma(L_n)}{(L_n+1)}\left(\frac{a}{\Omega_{s,n}}\right)\right]^{1-\kappa_n} \right\} \frac{x^{\sum_{n=1}^{N} L_n + \sum_{n=1}^{N} \kappa_n - N}}{\Gamma\left(\sum_{n=1}^{N} L_n + \sum_{n=1}^{N} \kappa_n - N\right)}$$

$$\times F_B^{(N)} \left(L_1, \cdots, L_N; L_1 + \delta_{\kappa_1}, \cdots, L_N + \delta_{\kappa_N}; \sum_{n=1}^{N} L_n + \sum_{n=1}^{N} \kappa_n + 1 - N; \frac{-x\Lambda_1}{b}, \cdots, \frac{-x\Lambda_N}{b}\right)\Bigg|_{x=1/\gamma},$$

$$= 1 - \sum_{\kappa \in \mathcal{P}_N} \left\{ \prod_{n=1}^{N} \left(\frac{b}{\Lambda_n}\right)^{-1} \left[\Gamma(L_n+1)\right]^{\kappa_n} \left[-\frac{\Gamma(L_n)}{(L_n+1)}\left(\frac{a}{\Omega_{s,n}}\right)\right]^{1-\kappa_n} \right\} \frac{\gamma^{-\left(\sum_{n=1}^{N} L_n + \sum_{n=1}^{N} \kappa_n - N\right)}}{\Gamma\left(\sum_{n=1}^{N} L_n + \sum_{n=1}^{N} \kappa_n - N\right)}$$

$$\times F_B^{(N)} \left(L_1, \cdots, L_N; L_1 + \delta_{\kappa_1}, \cdots, L_N + \delta_{\kappa_N}; \sum_{n=1}^{N} L_n + \sum_{n=1}^{N} \kappa_n + 1 - N; \frac{-\Lambda_1}{b\gamma}, \cdots, \frac{-\Lambda_N}{b\gamma}\right), \qquad (6.44)$$

where $\delta_{\kappa_n} = \begin{cases} 0, & \kappa_n = 0 \\ 1, & \kappa_n = 1 \end{cases}$.

6.4 Performance Analysis

6.4.1 Outage Probability

The end-to-end outage probability is defined as the probability that the end-to-end SINR falls below a predetermined protection ratio γ_{th} and is given by $P_{out} = F_{\gamma_{eq}}(\gamma_{th})$. Therefore, for DF multihop relay system we can use $P_{out} = F_{\gamma_{DF}}(\gamma_{th})$ in (6.15) and for AF, we use $P_{out} = F_{\gamma_{AF}}(\gamma_{th})$ in (6.44), respectively.

6.4.2 Average SER

The average SER of multihop transmission over relay fading channels is an important performance metric and is defined as the averaging of the instantaneous (conditional) error probability over the pdf of the end-to-end SINR.

6.4.2.1 DF Relaying

Using the MGF-based approach, the average SER for several *M*-ary modulations can be given by

$$\bar{P}_s = \sum_{\tilde{z}=1}^{\tilde{Z}} \int_0^{\theta_{\tilde{z}}} \lambda_{\tilde{z}} M_{\gamma_{eq}} \left(\frac{\phi_{\tilde{z}}}{\sin^2 \theta} \right) d\theta, \tag{6.45}$$

where parameters $\tilde{Z}$, $\lambda_{\tilde{z}}$, $\phi_{\tilde{z}}$ and $\theta_{\tilde{z}}$ given in table 3.1. Moreover, for the special case of BPSK, making a change variable $s = \sin^2 \theta$, the infinite integral in (6.45) may be evaluated in the closed form to give (see Appendix E)

$$\bar{P}_b = \frac{1}{2} - \frac{1}{2} \left(\prod_{n=1}^{L_d} \frac{\lambda_r}{b} \right)^{m_r} \sum_{r=1}^{L_d} \sum_{j=1}^{m_r} \Xi_{j,r} \left(\frac{\lambda_r}{b} \right)^{1/2-j} \psi \left(1/2, 3/2 - j; \frac{\lambda_r}{b} (a\varpi + 1) \right). \tag{6.46}$$

6.4.2.1 AF Relaying

An approach to evaluate the average SER of multihop AF transmission over a fading channel is given by [93, eq. (6)]

$$\bar{P}_s = -\int_0^\infty Z(u) \frac{d}{du} \{ M_{1/\gamma_{AF}}(u) \} du, \tag{6.47}$$

where $Z(u)$ is the auxiliary function which represents the instantaneous (conditional) SER and is given in [93] for a variety of M-ary modulation schemes. Specifically, for a given conditional instantaneous SER $P_s(\gamma_{eq})$, the auxiliary function $Z(u)$ is defined as

$$Z(u) = \mathcal{L}^{-1} \left[\frac{P_s(1/t)}{t} \right](u). \tag{6.48}$$

Substituting (6.38) in (6.47), the average SER is given by

$$\bar{P}_s = \sum_{n=1}^{N} \int_0^{\infty} Z(u) \prod_{\substack{k=1 \\ k \neq n}}^{N} \left\{ \Gamma(L_k+1)\psi\left(L_k;0;\frac{ub}{\Lambda_k}\right) - \frac{\Gamma(L_k)u}{(L_k+1)}\left(\frac{a}{\Omega_{s,k}}\right)\psi\left(L_k;1;\frac{ub}{\Lambda_k}\right) \right\} R_n(u)du,$$

(6.49)

where

$$R_n(u) = \frac{\partial}{\partial u}\left\{ \frac{\Gamma(L_k)u}{(L_k+1)}\left(\frac{a}{\Omega_{s,k}}\right)\psi\left(L_k;1;\frac{ub}{\Lambda_k}\right) - \Gamma(L_k+1)\psi\left(L_k;0;\frac{ub}{\Lambda_k}\right) \right\},$$

$$= \frac{\Gamma(L_k)}{(L_k+1)}\left(\frac{a}{\Omega_{s,k}}\right)\psi\left(L_k;1;\frac{ub}{\Lambda_k}\right)$$

$$- \frac{u\Gamma(L_k)}{(L_k+1)}\left(\frac{L_k ab}{\Omega_{s,k}\Lambda_k}\right)\psi\left(L_k+1;2;\frac{ub}{\Lambda_k}\right) + \frac{L_k b}{\Lambda_k}\Gamma(L_k+1)\psi\left(L_k+1;1;\frac{ub}{\Lambda_k}\right).$$

(6.50)

Note that the result in (6.49) can be easily evaluated numerically. In the numerical result section, to illustrate the numerical accuracy of (6.49), the average BER for the special case of binary modulations is depicted. In this case, the auxiliary function $Z(u)$ is defined as

$$Z(u) = \frac{1}{2\Gamma(\beta)} G_{1,3}^{2,0}\left(\alpha u \left| \begin{matrix} 1 \\ \beta,0,0 \end{matrix} \right. \right),$$

(6.51)

where $\alpha = \begin{cases} 1, & \text{BPSK} \\ 1/2, & \text{BFSK} \end{cases}$ and $\beta = \begin{cases} 1, & \text{NFSK / DPSK} \\ 1/2, & \text{CFSK / CPSK} \end{cases}$.

6.4.3 Average Channel Capacity

The average channel capacity provides an upper bound for the maximum transmission rate and was initially established for the Gaussian channel. In this section, novel expressions for this metric for DF and AF relay systems operating in Rayleigh fading with co-channel interference are derived. The expression for the DF relay protocol is

given by a closed-form expression in terms of the confluent hypergeometric function $\Psi(.)$, whereas the AF is given by a single integral which can be easily implemented in most popular computing software.

6.4.3.1 DF Relaying

The average channel capacity can be given by

$$\bar{C}_{DF} = W \int_0^\infty \log_2(1+\gamma) f_{\gamma_{DF}}(\gamma) d\gamma,$$

$$= \frac{W}{\ln(2)} \int_0^\infty \frac{\bar{F}_{\gamma_{DF}}(\gamma)}{1+\gamma} d\gamma, \tag{6.52}$$

where W is the channel bandwidth. Substituting (6.12) in (6.52) gives

$$\bar{C}_{DF} = \frac{W}{\ln(2)} \prod_{i=1}^{L_d} \left(\frac{\lambda_r}{b}\right)^{m_r} \sum_{r=1}^{L_d} \sum_{j=1}^{m_r} \Xi_{j,r} \int_0^\infty \frac{\exp(-\gamma a\varpi)}{(1+\gamma)(\gamma+\lambda_r/b)^j} d\gamma.$$

(6.53)

Using the partial expansion, (6.53) becomes

$$\bar{C}_{DF} = \frac{W}{\ln(2)} \prod_{i=1}^{L_d} \left(\frac{\lambda_r}{b}\right)^{m_r} \sum_{r=1}^{L_d} \sum_{j=1}^{m_r} \Xi_{j,r} \left\{ \frac{1}{(\lambda_r/b-1)^i} \int_0^\infty \frac{\exp(-\gamma a\varpi)}{(1+\gamma)} d\gamma \right.$$

$$\left. + \sum_{k=1}^j \frac{(-1)^{i-k}}{(i-k)!}(1)_{i-k}(1-\lambda_r/b)^{k-i-1} \int_0^\infty \frac{\exp(-\gamma a\varpi)}{(\gamma+\lambda_r/b)^k} d\gamma \right\},$$

$$= \frac{W}{\ln(2)} \prod_{i=1}^{L_d} \left(\frac{\lambda_r}{b}\right)^{m_r} \sum_{r=1}^{L_d} \sum_{j=1}^{m_r} \Xi_{j,r} \left\{ \frac{1}{(\lambda_r/b-1)^i} \psi(1;1;a\varpi) \right.$$

$$\left. + \sum_{k=1}^j \frac{(-1)^{i-k}}{(i-k)!}(1)_{i-k}(1-\lambda_r/b)^{k-i-1} \left(\frac{b}{\lambda_r}\right)^{k-1} \psi(1;1;a\varpi\lambda_r/b) \right\}. \tag{6.54}$$

Note that when we replace $a = 0$ in (6.54) and using [38, eq. (3.197.5)], (6.54) becomes

$$\bar{C}_{DF} = \frac{W}{\ln(2)} \prod_{i=1}^{L_d} \left(\frac{\lambda_r}{b}\right)^{m_r} \sum_{r=1}^{L_d} \sum_{j=1}^{m_r} \Xi_{j,r} \int_0^\infty \frac{1}{(1+\gamma)(\gamma + \lambda_r / b)^j} \, d\gamma,$$

$$= \frac{W}{\ln(2)} \prod_{i=1}^{L_d} \left(\frac{\lambda_r}{b}\right)^{m_r} \sum_{r=1}^{L_d} \sum_{j=1}^{m_r} \Xi_{j,r} \, {}_2F_1\left(j,1; j+1; 1 - \frac{b}{\lambda_r}\right), \tag{6.55}$$

which is the average channel capacity for the interference-limited case.

Also for the case $b=0$ (no interferers), substituting (6.17) in (6.52), (6.52) becomes

$$\bar{C}_{DF} = \frac{W}{\ln(2)} \int_0^\infty \frac{\exp(-\gamma a \varpi)}{(1+\gamma)} d\gamma,$$

$$= \frac{W}{\ln(2)} \psi(1;1;a\varpi),$$

(6.56)

which is the average channel capacity for the noise-limited case.

6.4.3.1 AF Relaying

The average channel capacity for multihop AF relay systems can be given by [88, eq. (9)], [81]

$$\bar{C}_{AF} = \frac{W}{\log(2)} \int_0^\infty \frac{1}{t}(1 - \exp(-t)) M_{1/\gamma_{AF}}(t) \, dt. \tag{6.57}$$

Substituting (6.38) in (6.57) yields

$$C_{avg} = \frac{W}{\log(2)} \int_0^\infty \frac{1}{t}(1 - \exp(-t)) \left\{ \prod_{n=1}^N \Gamma(L_n + 1) \psi\left(L_n; 0; \frac{tb}{\Lambda_n}\right) - \frac{\Gamma(L_n)t}{(L_n+1)}\left(\frac{a}{\Omega_{s,n}}\right) \psi\left(L_n; 1; \frac{tb}{\Lambda_n}\right) \right\} dt, \tag{6.58}$$

which can be easily and accurately computed numerically.

6.5 Numerical Results

In this section, some numerical and simulation results to illustrate the performance analysis presented in the previous sections are presented. For illustration purposes multihop relay systems with N=2 and 3 hops and two equal-power interferers per hop with average INR equal to 5 dB are considered. Figure 6.2 plots the outage probability against the average SNR per hop with threshold γth=3 dB. The outage performance for the DF and AF multihop relay systems are evaluated using (6.15) and (6.44), respectively. The figure shows that the analytical results match perfectly the simulation results. It also shows that the outage probability decreases as the SNR per hop increases. Moreover, it is observed that DF relaying protocol provides a better performance than AF relaying with the performance gap between the two relaying schemes to increase at low and medium values of the average SNR as the number of hops N increases, but it diminishes at the high SNR per hop regime.

In Figure 6.3, the average BER for DF and AF relaying are plotted with BPSK given by (6.46) and (6.49), respectively. The figure shows that the analytical results and the simulation results are in excellent agreement. Similar observations to those in Figure 6.2 can be deduced from Figure 6.3, i.e., the DF relaying scheme outperforms the AF scheme, although the two performances converge at high SNRs. Finally, in Figure 6.4 the average channel capacity per unit bandwidth (W=1) for both multihop relay systems are depicted. The numerical results obtained by (6.54) for DF relaying and (6.58) for AF relaying are shown to be in excellent agreement with the simulation results obtained using γ_{DF} in (6.13) and γ_{AF} in (6.24), respectively.
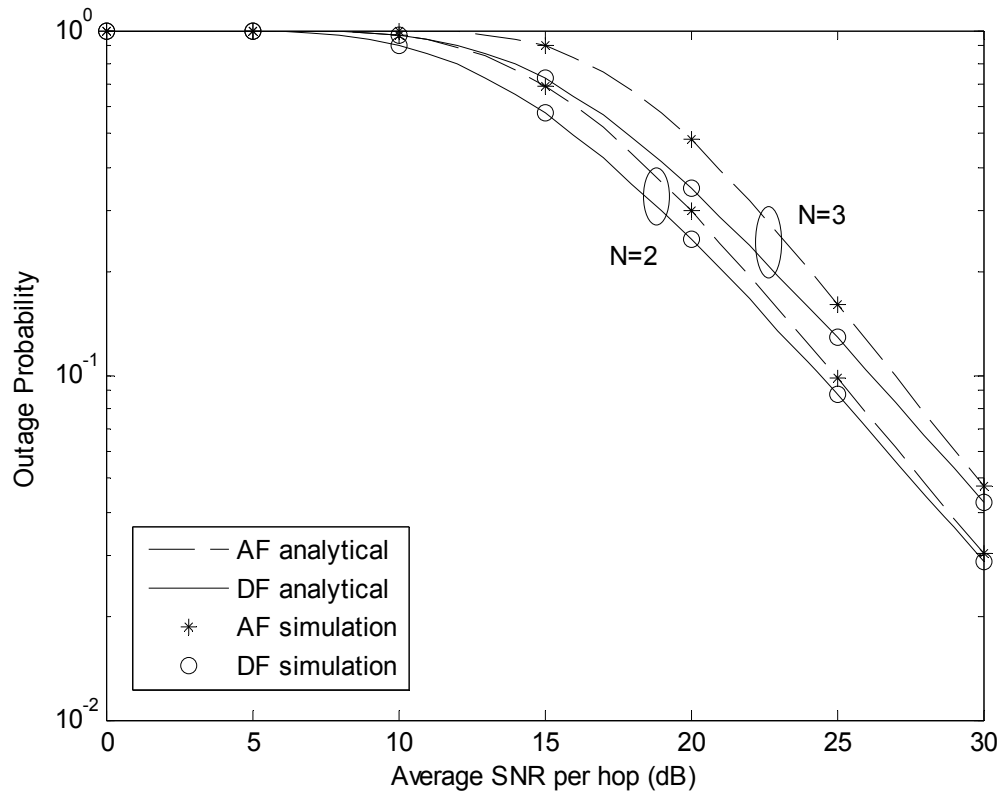
Figure 6.2 Outage probability versus average SNR per hop for AF and DF relay systems with N=2, 3 hops and two equal-power interferers per hop with average INR equal to 5 dB.
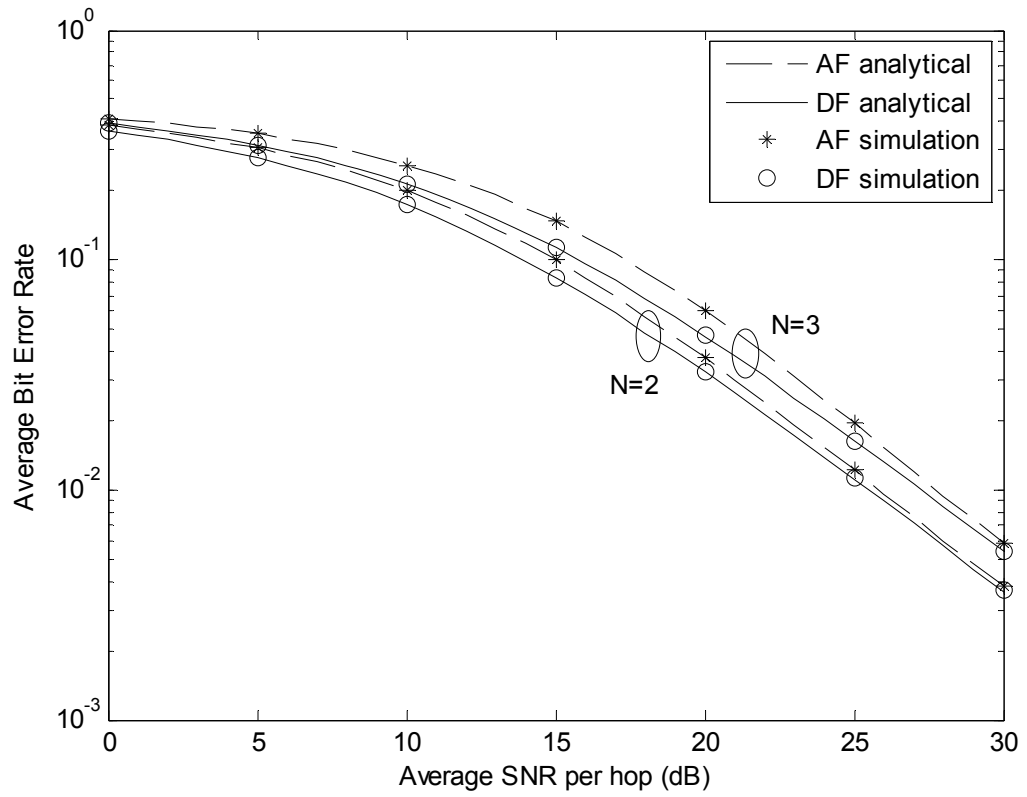
Figure 6.3   Average BER versus average SNR per hop for AF and DF relay systems with N=2, 3 hops and two equal-power interferers per hop with average INR equal to 5 dB.
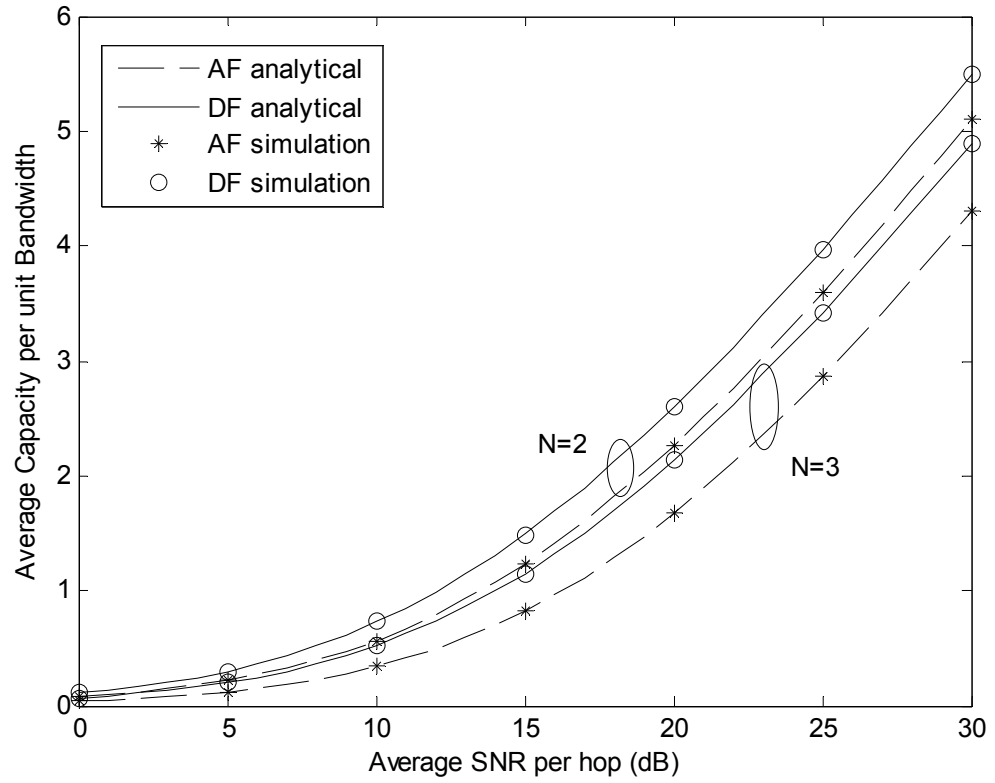
Figure 6.4 Average capacity versus average SNR per hop for AF and DF relay systems with N=2, 3 hops and two equal-power interferers per hop with average INR equal to 5 dB.

CHAPTER 7 MULTI-HOP RELAY SYSTEMS IN INTERFERENCE-LIMITED NAKAGAMI FADING CHANNELS

7.1 Introduction

The main purpose of chapter is to derive the outage probability of channel-assisted AF and DF relaying for cascaded multihop relay systems in interference-limited Nakagami fading environments. The multiple Nakagami-faded interferers at the relay and the destination nodes are considered and the closed-form expressions for the outage probability of both AF and DF relay systems are then be studied. Specifically, the Nakagami-faded interferers at a particular relay node are identically distributed but the statistics of the interferers may differ from node to node. Also the case of non-identically distributed Rayleigh-faded interferers is investigated at the relay nodes. The impact of interference on the outage performance of both DF and AF relay protocols is illustrated through analytical and simulation results.

7.2 System Model

A wireless network that comprises of a source (S), several AF relays (R_n, $n = 1,...,N-1$) and a destination ($R_N = D$) is considered with the nth ($n = 1,...,N$) relay interrupted by L_n co-channel interferers in a Nakagami fading environment. Throughout the chapter the interferers at each node are assumed to be independent. Although the interfering signals at different relay nodes may originate from the same source, the independence assumption is justified when the relays operate in different time slots and are spatially located sufficiently far from each other. In an interference-limited wireless communication system, the effect of AWGN can usually be neglected. Then the

equivalent end-to-end SIR in an AF multihop relay system may be tightly upper-bounded by [41],[45], [54]

$$\gamma_{eq}^{AF} = \left[\sum_{n=1}^{N} \frac{1}{\gamma_n} \right]^{-1},$$ (7.1)

where the instantaneous SIR at the nth hop is given by

$$\gamma_n = \frac{a_n^2}{\sum_{i=1}^{L_n} Z_{n,i}},$$ (7.2)

with a_n being the fading amplitude of the desired signal at the nth relay and $Z_{n,i}$, $i = 1,\ldots, L_n$, $n = 1,\ldots,N$, being the instantaneous power of the ith interferer at the nth hop.

7.2.1 Derivation of PDF

The probability density function of the inverse of the per hop SIR in (7.2) is given by

$$f_{\gamma_n^{-1}}(\gamma) = \int_0^\infty x f_{\tilde{Z}_n}(\gamma x) f_{a_n^2}(x) dx,$$ (7.3)

where $\tilde{Z}_n = \sum_{i=1}^{L_n} Z_{n,i}$ is the total interference power at the nth relay. For a Nakagami-m fading channel, the pdfs of a_n^2 and $\tilde{Z}_n$ are provided as

$$f_{a_n^2}(x) = \frac{1}{\Gamma(m_{s,n})} \left(\frac{m_{s,n}}{\Omega_{s,n}} \right)^{m_{s,n}} x^{m_{s,n}-1} \exp\left(-\frac{m_{s,n}}{\Omega_{s,n}} x \right),$$ (7.4)

$$f_{\tilde{Z}_n}(z) = \frac{1}{\Gamma(L_n m_{I,n})} \left(\frac{m_{I,n}}{\Omega_{I,n}} \right)^{L_n m_{I,n}} z^{L_n m_{I,n}-1} \exp\left(-\frac{m_{I,n}}{\Omega_{I,n}} z \right),$$

(7.5)

where $m_{s,n}$ and $\Omega_{s,n}$ are the Nakagami fading parameter and the average power of the desired signal at the nth hop ($n = 1, 2, \ldots, N$). Similarly, $m_{I,n}$ and $\Omega_{I,n}$ are the Nakagami fading parameter and the average power of the interfering signal at the nth

hop. In (7.5), the interferers are assumed to be independent and identically distributed (i.i.d.) at the nth hop. Substituting (7.4) and (7.5) in (7.3), then [38]

$$f_{\gamma_n^{-1}}(\gamma) = \frac{\Gamma(m_{s,n} + L_n m_{I,n})}{\Gamma(m_{s,n})\Gamma(L_n m_{I,n})}\left(\frac{m_{I,n}\Lambda_n}{m_{s,n}}\right)^{L_n m_{I,n}}\gamma^{L_n m_{I,n}-1}\left\{\frac{m_{I,n}\Lambda_n}{m_{s,n}}\gamma+1\right\}^{-(m_{s,n}+L_n m_{I,n})}, \tag{7.6}$$

where $\Lambda_n = \Omega_{s,n}/\Omega_{I,n}$ is average SIR at the nth hop. Moreover, for the case of independent non-identically distributed (i.n.i.d.) Rayleigh interferers, the pdf can be written by

$$f_{\tilde{Z}_n}(z) = \sum_{i=1}^{L_n}\frac{\pi_i}{\Omega_{i,n}}\exp\left(-\frac{z}{\Omega_{i,n}}\right), \tag{7.7}$$

where $\pi_i = \prod_{\substack{k=1 \\ k\neq i}}^{L_n}\frac{\Omega_{i,n}}{\Omega_{i,n}-\Omega_{k,n}}$. Substituting (7.4) and (7.7) in (7.3), it is easy to show that

the pdf of the inverse SIR at the nth hop with i.n.i.d. Rayleigh interferers is given by [38]

$$f_{\gamma_n^{-1}}(\gamma) = \sum_{i=1}^{L_n}\pi_i\Lambda_{i,n}\left\{1+\frac{\gamma\Lambda_{i,n}}{m_{s,n}}\right\}^{-(m_{s,n}+1)}, \tag{7.8}$$

where $\Lambda_{i,n} = \Omega_{s,n}/\Omega_{i,n}$ is the average SIR of the ith interferer at the nth hop. Similarly, the pdf of instantaneous SIR at the nth hop is provided by

$$f_{\gamma_n}(\gamma) = \int_0^\infty x f_{a_n^2}(\gamma x) f_{\tilde{Z}_n}(x)\,dx. \tag{7.9}$$

Substituting (7.4) and (7.5) in (7.9), yields [38]

$$f_{\gamma_n}(\gamma) = \frac{\Gamma(m_{s,n} + L_n m_{I,n})}{\Gamma(m_{s,n})\Gamma(L_n m_{I,n})}\left(\frac{m_{I,n}\Lambda_n}{m_{s,n}}\right)^{L_n m_{I,n}}\gamma^{m_{s,n}-1}\left\{\gamma+\frac{m_{I,n}\Lambda_n}{m_{s,n}}\right\}^{-(m_{s,n}+L_n m_{I,n})}. \tag{7.10}$$

Similarly, for the case of i.n.i.d Rayleigh interference, the pdf can be obtained by

$$f_{\gamma_n}(\gamma) = \gamma^{m_{s,n}-1} m_{s,n}\sum_{i=1}^{L_n}\pi_i\left(\frac{m_{s,n}}{\Lambda_{i,n}}\right)^{m_{s,n}}\left\{1+\frac{m_{s,n}}{\Lambda_{i,n}}\gamma\right\}^{-(1+m_{s,n})}. \tag{7.11}$$

7.2.2 Derivation of MGF

The MGF of the inverse instantaneous SIR per hop is given by

$$M_{\gamma_n^{-1}}(t) = \int_0^\infty e^{-t\gamma} f_{\gamma_n^{-1}}(\gamma) d\gamma. \tag{7.12}$$

Substituting (7.6) in (7.12), (7.12) becomes

$$M_{\gamma_n^{-1}}(t) = \frac{\Gamma(m_{s,n} + L_n m_{I,n})}{\Gamma(m_{s,n})} \psi\left(L_n m_{I,n}; 1 - m_{s,n}; \frac{m_{s,n}}{m_{I,n}\Lambda_n} t\right), \tag{7.13}$$

where $\psi(a;b;x) = \dfrac{1}{\Gamma(a)} \displaystyle\int_0^\infty t^{a-1}(1+t)^{b-a-1} e^{-xt} dt$ is the confluent hypergeometric function of the

second kind [7]. For the special case of a Rayleigh channel ($m_{s,n} = m_{I,n} = 1$), (7.13)

becomes

$$M_{\gamma_n^{-1}}(t) = \Gamma(1 + L_n) \psi\left(L_n; 0; \Lambda_n^{-1} t\right). \tag{7.14}$$

Moreover, for the case of distinct Rayleigh interfering powers, substituting (7.8) in

(7.12), the MGF of inverse instantaneous SIR per hop can be show to be given by

$$M_{\gamma_n^{-1}}(t) = m_{s,n} \sum_{i=1}^{L_n} \pi_i \Psi\left(1, 1 - m_{s,n}; \frac{m_{s,n}}{\Lambda_{i,n}} t\right). \tag{7.15}$$

Thus the MGF of end-to-end per hop SIR is given by

$$M_{\gamma_n}(t) = \int_0^\infty e^{-t\gamma} f_{\gamma_n}(\gamma) d\gamma. \tag{7.16}$$

Substituting (7.10) in (7.16) yields

$$M_{\gamma_n}(t) = \frac{\Gamma(m_{s,n} + L_n m_{I,n})}{\Gamma(L_n m_{I,n})} \psi\left(m_{s,n}, 1 - L_n m_{I,n}; \frac{m_{I,n}\Lambda_n}{m_{s,n}} t\right). \tag{7.17}$$

Similarly, for i.n.i.d Rayleigh interference, the MGF of the SIR per hop is given by

$$M_{\gamma_n}(t) = \Gamma(m_{s,n} + 1) \sum_{i=1}^{L_n} \pi_i \psi\left(m_{s,n}; 0; \frac{\Lambda_{i,n}}{m_{s,n}} t\right). \tag{7.18}$$

7.3 Outage Performance

7.3.1 AF Relaying System

Under the assumption that the hops are subject to independent fading, the cumulative density function of γ_{eq}^{AF} can be expressed as [41]

$$F_{\gamma_{eq}^{AF}}(\gamma) = 1 - \mathcal{L}^{-1}\left[\frac{\prod_{n=1}^{N} M_{1/\gamma_n}(t)}{t}\right]\Bigg|_{x=1/\gamma}, \tag{7.19}$$

where $\mathcal{L}^{-1}(.)$ is the inverse Laplace transform and $M_{1/\gamma_n}(.)$ is the MGF of the inverse SIR per hop. The cdf in (7.19) may be found with the help of Appendix D.

For the case of i.n.i.d. Nakagami desired signals and i.i.d. Nakagami interferers at each relay, the closed-form expression for the cdf of the end-to-end SIR of an N-hop AF relay network can be obtained as

$$F_{\gamma_{eq_1}^{AF}}(\gamma) = 1 - \frac{1}{\Gamma\left(1 + \sum_{n=1}^{N} L_n m_{I,n}\right)}\left\{\prod_{n=1}^{N} \frac{\Gamma\left(m_{s,n} + L_n m_{I,n}\right)}{\Gamma\left(m_{s,n}\right)}\left(\frac{m_{I,n}\Lambda_n}{m_{s,n}\gamma}\right)^{L_n m_{I,n}}\right\}$$

$$\times F_B^{(N)}\left(L_1 m_{I,1},...,L_N m_{I,N}; L_1 m_{I,1} + m_{s,1},..., L_N m_{I,N} + m_{s,N}; 1 + \sum_{i=1}^{N} L_i m_{I,i}; -\frac{m_{I,1}\Lambda_1}{m_{s,1}\gamma},...,-\frac{m_{I,N}\Lambda_N}{m_{s,N}\gamma}\right). \tag{7.20}$$

Note that the Lauricella function $F_B^{(N)}$ may be written in integral form as [31, eq. (2.3.4)]

$$F_B^{(n)}\left(a_1,...,a_n; b_1,...,b_n; \sum_{i=1}^{N} a_i + 1; x_1,...,x_n\right)$$

$$= \frac{\Gamma\left(\sum_{i=1}^{N} a_i + 1\right)}{\Gamma(a_1)...\Gamma(a_n)}\int_0^1 \frac{u_1^{a_1-1}}{(1-u_1 x_1)^{b_1}}...\int_0^{1-u_1-u_2-...u_{n-1}} \frac{u_n^{a_n-1}}{(1-u_n x_n)^{b_n}}du_1 du_2...du_n, \tag{7.21}$$

and can be accurately computed numerically with the software program Maple. An upper bound on F_B may be obtained if the upper limits of the integrals in (7.21) are replaced by one:

$$F_B^{(n)}\left(a_1,\ldots,a_n;a_1+1,\ldots,a_n+1;\sum_{i=1}^{N}a_i+1;x_1,\ldots,x_n\right) \le \Gamma\left(\sum_{i=1}^{N}a_i+1\right)\prod_{i=1}^{n}\frac{1}{\Gamma(a_i+1)(1-x_i)^{a_i}}. \qquad (7.22)$$

In the case of a Rayleigh fading environment, (7.20) reduces to

$$F_{\gamma_{eq}^{AF}}(\gamma)=1-\frac{(1/\gamma)^{L_T}}{\Gamma(L_T+1)}\left[\prod_{n=1}^{N}\Gamma(L_n+1)\Lambda_n^{L_n}\right]F_B^{(N)}\left(L_1,\ldots,L_N,1+L_1,\ldots,1+L_N;L_T+1;\frac{-\Lambda_1}{\gamma},\ldots,\frac{-\Lambda_N}{\gamma}\right),$$

$$(7.23)$$

where $L_T=\sum_{n=1}^{N}L_n$. Moreover, for i.n.i.d Rayleigh interferers, inserting (7.15) in (7.19), after some mathematical manipulations, the cdf can be given by

$$F_{\gamma_{eq}^{AF}}(\gamma)=1-\left[\prod_{n=1}^{N}m_{s,n}\right]$$

$$\times\sum_{k_1=1}^{L_1}\cdots\sum_{k_N=1}^{L_N}\frac{\gamma^{-N}\left[\prod_{n=1}^{N}\pi_{k_n}\frac{\Lambda_{k_n,n}}{m_{s,n}}\right]}{\Gamma(N+1)}F_B^{(N)}\left(1,\ldots,1;m_{s,1}+1,\ldots,m_{s,N}+1;N+1;-\frac{\Lambda_{k_1,1}}{m_{s,n}\gamma},\ldots,\frac{\Lambda_{k_N,N}}{m_s\gamma}\right).$$

$$(7.24)$$

Note that for the special case of $N=2$ (dual-hop system), (7.23) reduces to

$$F_{\gamma_{eq}^{AF}}(\gamma)=1-\frac{\Gamma(L_1+1)\Gamma(L_2+1)}{\Gamma(L_1+L_2+1)}\left(\frac{\Lambda_1}{\gamma}\right)^{L_1}\left(\frac{\Lambda_2}{\gamma}\right)^{L_2}F_3\left(L_1,L_2;L_1+1,L_2+1;L_1+L_2+1;-\frac{\Lambda_1}{\gamma},-\frac{\Lambda_2}{\gamma}\right),$$

$$(7.25)$$

where $F_3(.)$ is the Appell's double hypergeometric function of the third kind [18]. Also using [38, eq. (9.182.4)] and [38, eq. (9.131.1)], and after some algebra, we can show that

$$F_3\left(a_1,a_2;1+a_1,1+a_2;a_1+a_2+1;\frac{-x}{\sigma_1},\frac{-x}{\sigma_2}\right)$$

$$=\left(\frac{x+\sigma_1}{\sigma_1}\right)^{-a_1}\left(\frac{x+\sigma_2}{\sigma_2}\right)^{-a_2}{}_2F_1\left(a_1,a_2;a_1+a_2+1;\frac{x(x+\sigma_1+\sigma_2)}{(x+\sigma_1)(x+\sigma_2)}\right).$$

$$(7.26)$$

Substituting (7.26) in (7.23), then

$$F_{\gamma_{eq}^{AF}}(\gamma) = 1 - \frac{\Gamma(L_1+1)\Gamma(L_2+1)}{\Gamma(L_1+L_2+1)}\left(\frac{\gamma}{\Lambda_1}+1\right)^{-L_1}\left(\frac{\gamma}{\Lambda_2}+1\right)^{-L_2} {}_2F_1\left(L_1,L_2;L_1+L_2+1;\frac{1+\gamma/\Lambda_1+\gamma/\Lambda_2}{(1+\gamma/\Lambda_1)(1+\gamma/\Lambda_2)}\right),$$

(7.27)

which agrees with the cdf of the end-to-end SIR for the dual-hop relay system given in [54, eq. (11)]. It then follows that the outage probability for the N-hop AF relaying system with identical interferers at each relay is given by $P_{out}^{AF}(\gamma_{th}) = F_{\gamma_{eq}^{AF}}(\gamma_{th})$.

7.3.2 DF Relaying System

For the multihop DF relaying system, the cdf of the end-to-end SIR is given by

$$F_{\gamma_{eq}^{DF}}(\gamma_{th}) = \Pr\left[\min(\gamma_1,...,\gamma_N) < \gamma_{th}\right] = 1 - \prod_{n=1}^{N}\left(1 - F_{\gamma_n}(\gamma_{th})\right)$$

(7.28)

where the cdf of SIR per hop is given by $F_{\gamma_n}(\gamma_{th}) = \mathcal{L}^{-1}\left[\frac{M_{\gamma_n}(t)}{t}\right]\Big|_{x=\gamma_{th}}$. Then, using the

inverse Laplace transform in (7.17) yields

$$F_{\gamma_n}(\gamma_{th}) = \frac{\Gamma(m_{s,n}+L_n m_{I,n})}{\Gamma(L_n m_{I,n})\Gamma(m_{s,n}+1)}\left(\frac{m_{s,n}\gamma_{th}}{m_{I,n}\Lambda_n}\right)^{m_{s,n}} F_B^{(1)}\left(m_{s,n},m_{s,n}+L_n m_{I,n};m_{s,n}+1;-\frac{m_{s,n}\gamma_{th}}{m_{I,n}\Lambda_n}\right),$$

$$= \frac{\Gamma(m_{s,n}+L_n m_{I,n})}{\Gamma(L_n m_{I,n})\Gamma(m_{s,n}+1)}\left(\frac{m_{s,n}\gamma_{th}}{m_{I,n}\Lambda_n}\right)^{m_{s,n}} {}_2F_1\left(m_{s,n},m_{s,n}+L_n m_{I,n};m_{s,n}+1;-\frac{m_{s,n}\gamma_{th}}{m_{I,n}\Lambda_n}\right),(7.29)$$

where ${}_2F_1(.)$ is the Gauss hypergeometric function. Substituting (7.29) in (7.28), (7.28)

becomes

$$F_{\gamma_{eq}^{DF}}(\gamma_{th}) = 1 - \prod_{n=1}^{N}\left\{1 - \frac{\Gamma(m_{s,n}+L_n m_{I,n})}{\Gamma(L_n m_{I,n})\Gamma(m_{s,n}+1)}\left(\frac{m_{s,n}\gamma_{th}}{m_{I,n}\Lambda_n}\right)^{m_{s,n}} {}_2F_1\left(m_{s,n},m_{s,n}+L_n m_{I,n};m_{s,n}+1;-\frac{m_{s,n}\gamma_{th}}{m_{I,n}\Lambda_n}\right)\right\}.$$

(7.30)

For the case of the Rayleigh fading channel ($m_{s,n} = m_{I,n} = 1$), (7.30) reduces to

$$F_{\gamma_{eq}^{DF}}(\gamma_{th}) = 1 - \prod_{n=1}^{N}\left(1 - \frac{L_n\gamma_{th}}{\Lambda_n}{}_2F_1\left(1+L_n,1;2;-\frac{\gamma_{th}}{\Lambda_n}\right)\right).$$

(7.31)

By using the fact that ${}_2F_1(v+1,1;2;-x) = \frac{1}{vx}\left\{1-(1+x)^{-v}\right\}$, (7.31) becomes

$$F_{\gamma_{eq}^{DF}}\left(\gamma_{th}\right)=1-\prod_{n=1}^{N}\left(\frac{\Lambda_n}{\Lambda_n+\gamma_{th}}\right)^{L_n}.\qquad(7.32)$$

In addition, for the case of i.n.i.d Raleigh interference, the cdf can be written by

$$F_{\gamma_{eq}^{DF}}\left(\gamma_{th}\right)=1-\prod_{n=1}^{N}\left\{1-\sum_{i=1}^{L_n}\pi_i\left(\frac{m_{s,n}\gamma_{th}}{\Lambda_{i,n}}\right)^{m_{s,n}}{}_2F_1\left(m_{s,n},1+m_{s,n};1+m_{s,n};-\frac{m_{s,n}\gamma_{th}}{\Lambda_{i,n}}\right)\right\}$$

$$=1-\prod_{n=1}^{N}\left\{1-\sum_{i=1}^{L_n}\pi_i\left(\frac{\Lambda_{i,n}}{m_{s,n}\gamma_{th}+\Lambda_{i,n}}\right)^{m_{s,n}}\right\}.\qquad(7.33)$$

Finally, we observe that, in the case Rayleigh fading channel with identical interferers at the relay nodes, using the upper bound in (7.22) and comparing with (7.33), it is observed that the outage performance of DF relaying is better than that of AF relaying.

7.4 Numerical Results

In this section the numerical and simulation results to verify the derived results are presented. In the figures, outage threshold γ_{th} is set at 3 dB and the impact of varying the Nakagami parameters for the desired and interfering signals, the number of cooperating relay nodes, and the number of interferers are investigated. Figure 7.1 plots the outage probability against the average SIR per hop for $N=3$ and $\{L_n\}_{n=1}^{N}=\{2,2,3\}$, assuming i.i.d Nakagami fading with $\{m_{s,n}\}_{n=1}^{N}=2.5$, $\{m_{I,n}\}_{n=1}^{N}=1.5$ and i.n.i.d. Nakagami fading channels with $\{m_{s,n}\}_{n=1}^{N}=\{2.5,3.5,2\}$ $\{m_{I,n}\}_{n=1}^{N}=\{1.5,2,1\}$. This figure shows that the analytical results match the simulation results perfectly. It also shows the effect that Nakagami fading parameters have on the outage performance. Moreover, it is observed that the DF relaying protocol provides better performance than the AF method, with the performance gap between the two relaying schemes to increase at low and medium values of the average SIR, but it diminishes at the high SIR per hop regime. In Figure

7.2, the outage probability versus the average SIR of the first interferer $\Lambda_{1,1}$ for $N=2$ and 3 hops are plotted by assuming identical Nakagami fading channels $\{m_{s,n}\}_{n=1}^{N} = 2$ and two i.n.i.d Rayleigh interferers per hop, with average SIRs in dB given by $\left\{\left[\Lambda_{i,n}\right]_{i=1}^{L_n}\right\}_{n=1}^{N} = \left\{\left[\Lambda_{1,1}, \Lambda_{1,1}+3\right], \left[\Lambda_{1,1}+2, \Lambda_{1,1}+4\right], \left[\Lambda_{1,1}+3, \Lambda_{1,1}+6\right]\right\}$. The figure shows that the outage probability deteriorates as the number of hops N increases. Finally, Figure 7.3 shows the outage probability for $N=2$ hops with AF and DF relaying schemes versus the number of identical interferers with $\{m_{s,n}\}_{n=1}^{N} = 2$, $\{m_{I,n}\}_{n=1}^{N} = 1$ and $\{\Lambda_n\}_{n=1}^{N} = 20, 25, \text{and} 30 \, \text{dB}$. Again, the analytical results and the simulation results are in excellent agreement. From this figure we can quantify the performance degradation that occurs as the number of interferers increases. The DF relaying system outperforms the AF relaying system with the performance gap between the two schemes decreasing as the total SIR per hop increases.
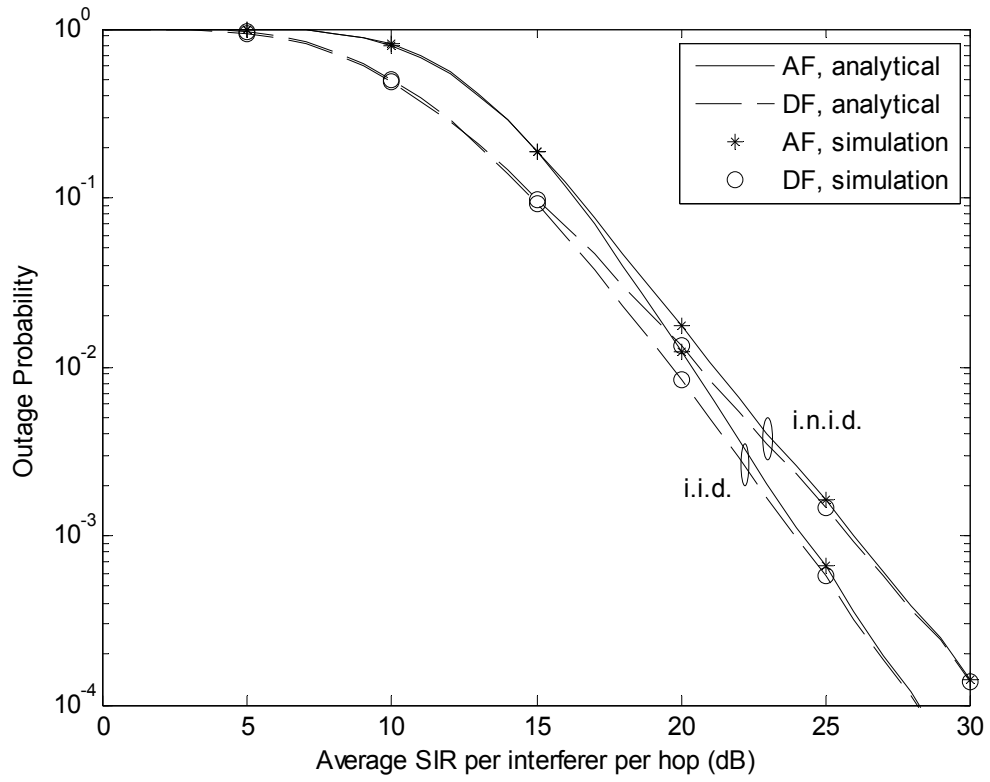
Figure 7.1 Outage probability of 3-hop DF and AF relay systems in Nakagami-*m* fading channels.
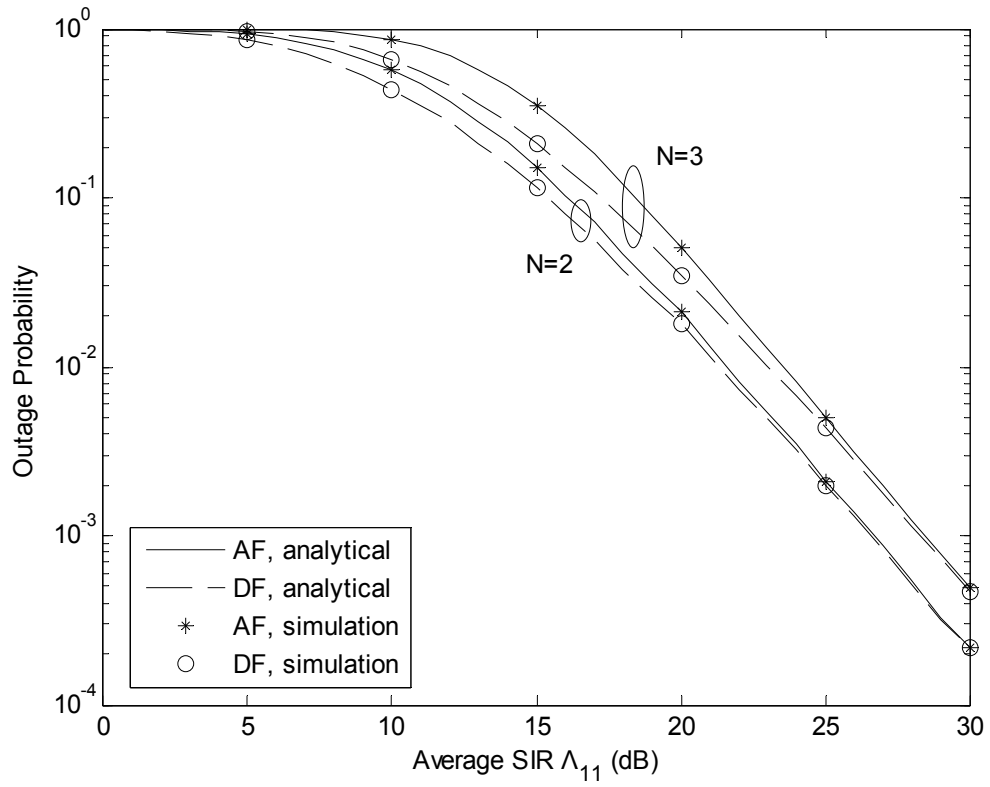
Figure 7.2 Outage probability of DF and AF relay systems with N=2 and 3 hops in Rayleigh fading channels with distinct powers.
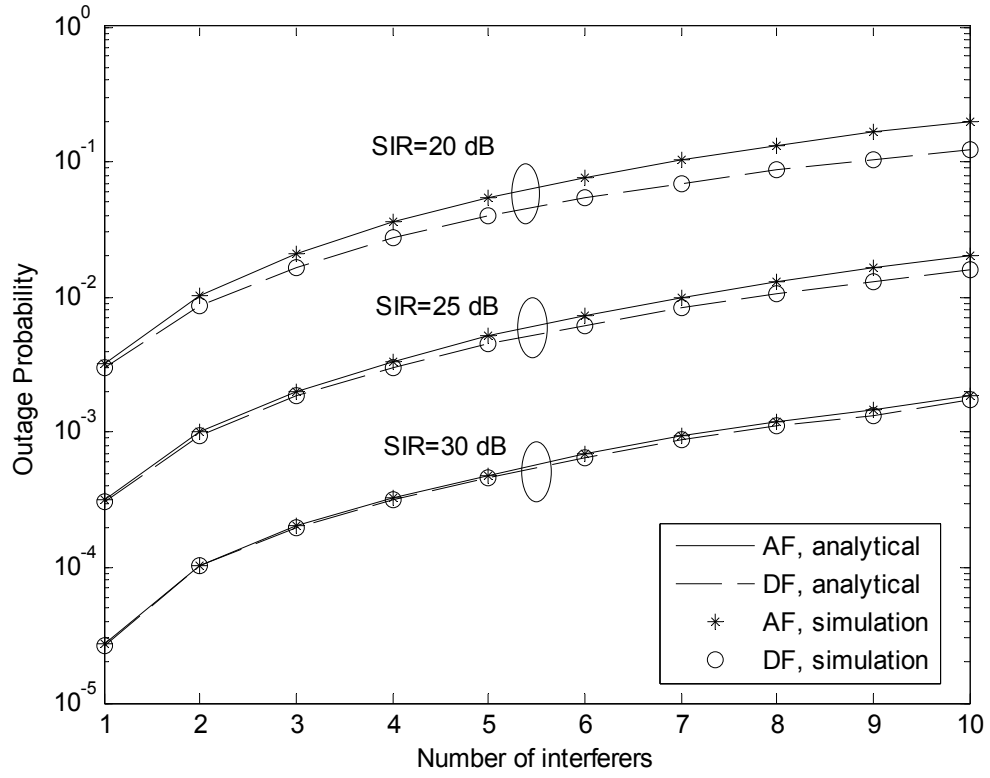
Figure 7.3 Outage probability of DF and AF for 2-hop relay systems with $\left\{m_{s,n}\right\}_{n=1}^{2} = 2$ and Λ =20, 25, 30 dB per interferer in Rayleigh fading channels.

CHAPTER 8 CONCLUSIONS AND FUTURE WORK

8.1 Conclusions

The main contributions and conclusion remarks of this work are provided as follows:

8.1.1 Optimum Combining

- In this dissertation, the analytical performance of OC diversity system in the presence of multiple equal mean-power interferers has been investigated. Both the desired signal and interference experience a spherically invariant random process (SIRP) fading while the background noise is neglected. The important performance measures such as outage probability, MGF, and ASER are then derived in terms of the Meijer-G function which can be accurately computed by the software programs such as MAPLE or MATHEMATICA.

8.1.2 Multihop Relay Systems

- The performance of multi-hop relay transmission systems that operate in a Rayleigh fading environment in the presence of co-channel interference and thermal noise is studied. Both amplify-and-forward (AF) and decode-and-forward (DF) relaying protocols are considered and analytical expressions for useful performance measures such as the outage probability, the average symbol error rate, and the average channel capacity are then obtained. The accuracy of the analytical results is verified by computer simulation.

- In addition, the effect of co-channel interference on multihop AF and DF interference-limited relaying systems operating in Nakagami-m fading channels is also investigated. For these transmission schemes, the case of interference-limited relays with gains based on the inverse of the fading amplitude of the desired signal in the previous link. For arbitrary but fixed number of Nakagami-distributed interferers per hop, A closed-form expression for the outage of an

N-hop AF relay system is given in terms of the multivariate Lauricella function $F_B^{(N)}$ that can be evaluated with commonly available computer software. Moreover, the outage performance of DF relay systems is also derived in closed form and their performance are compared. Simulation results are also provided to demonstrate the accuracy of the analytical expressions.

8.2 Future Research Directions

Extensions of this dissertation are possible in the following directions**:**

- Until recently the performance for multihop relay nodes together with multiple antennas is limited to systems that are noise-limited (no interferers). Therefore, it would be interesting to extend the results in this dissertation to obtain the performance of the system with the presence of co-channel interference and noise.

- In this dissertation, the assumption of independent interferers is justified when the relays operate in different time slots and are spatially located sufficiently far from each other at different relay. However since all the relays are forwarding information to the same destination, they may be operating at the same frequency and will suffer from the same interferers or at least correlated interferers in different time slots. In this case, some analytical results for correlated interferers would be also studied to make the results in this dissertation more generic.

- The performance various cooperation protocols such as AF, DF, DAF, EF, and PF could be established based on different performance goals, such as minimization of the download time, spectral efficiency, minimization of interference, etc.

REFERENCES

1. Aalo, V. A. and Chayawan, C., 2000, "Outage Probability of Cellular Radio using Maximal Ratio Combining in Rayleigh Fading Channels with Multiple Interferers", **Electronics Letters**, Vol. 36, No. 15, pp. 1314-1315.

2. Aalo, V.A. and Zhang, J., 2000, "Performance of Antenna Array Systems with Optimum Combining in a Rayleigh Fading Environment", **IEEE Transactions on Communications**, Vol. 4, pp. 387-389.

3. Aalo, V.A., Efthymoglou, G.P., Piboongungon T. and Iskander, C.D., 2007, "Performance of Diversity Receivers in Generalized Gamma Fading Channels", **IET Communications**, Vol. 1, pp. 341–347.

4. Aalo, V.A., Piboongungon, T., and Iskander, C.D., 2005, "Bit-error Rate of Binary Digital Modulation Schemes in Generalized Gamma Fading Channels", **IEEE Communications Letters**, Vol. 9, No. 2, pp. 139–141.

5. Abate, J. and Whitt, W., 1995, "Numerical Inversion of Laplace Transforms of Probability Distributions", **ORSA Journal on Computing**, Vol. 7, No.1, pp. 36-43.

6. Abdi, A. and Kaveh, M., 1998, "K Distribution: An Appropriate Substitute for Rayleigh-lognormal Distribution in Fading-Shadowing Wireless Channels" **Electronics Letters**, Vol. 34, No. 9, pp. 851-852.

7. Abramowitz M. and Stegun, I., 1980, **Handbook of Mathematical Functions**, 3rd ed., Dover Publications, New York, pp. 1-600.

8. Adamchik, V.S. and Marichev,O. I., 1990, "The Algorithm for Calculating Integrals of Hypergeometric Type Functions and Its Realization in Reduce System", **Symbolic and Algebraic Computation International Conference**, pp. 212-224.

9. Agrest, M. M. and Maksimov, M. S., 1971, **The Theory of Incomplete Cylinder Functions and Their Applications**, Springer Press, New York, pp. 1-345.

10. Agustin, A. and Vidal, J., 2008, "Amplify-and-forward Cooperation under Interference-limited Spatial Reuse of the Relay Slot", **IEEE Transactions on Wireless Communications**, Vol. 7, No.5, pp. 1952-1962.

11. Alouini, M.S., and Simon, M.K., 1999, "Performance of Coherent Receivers with Hybrid SC/MRC over Nakagami-m Fading Channels', **IEEE Transactions on Vehicular Technology**, Vol. 48, No. 4, pp. 1155–1164.

12. Anastassopoulos,V., Lampropoulos,G.A., Drosopoulos,A., and Rey, M., 1999, "High Resolution Radar Clutter Statistics", **IEEE Transactions on Aerospace And Electronics Systems**, Vol. 35, No.1, pp. 43–60.

13. Andrew, L.C., 1985, **Special Functions for Engineers and Applied Mathematicians**, Macmillan Publishing Company, New York, pp.1-129.

14. Asghari, V., Maaref, A. and Aissa, S., 2010, "Symbol Error Probability Analysis for Multihop Relaying over Nakagami Fading Channels", **IEEE Wireless Communications and Networking Conference**, Vol.1, pp. 1-6.

15. Bao X. and Li, J., 2007, "Efficient Message Relaying for Wireless User Cooperation: Decode-amplify-forward (DAF) and Hybrid DAF and Coded-cooperation", **IEEE Transactions on Wireless Communications**, Vol. 6, No. 11, pp. 3975-3984.

16. Barts, R.M. and Stutsman, 1992, "Modeling and Simulation of Mobile Satellite Propagation", **IEEE Transactions on Antennas Propagation**, Vol. 40, pp.375-382.

17. Beaulieu, N.C. and Abu-Dayya, A., 1991, "Analysis of Equal Gain Diversity on Nakagami Fading Channels', **IEEE Transactions on Communications**, Vol. 39, No. 2, pp. 225–234.

18. Beckmann, P., 1967, **Probability in Communication Engineering**, Brace & World Press, Harcourt, pp. 41-69.

19. Bithas, P.S., Sagias, N.C. and Mathiopoulos, P.T., 2009, " The Bivariate Generalized-K Distribution and Its Application to Diversity Receivers", **Transactions on Communications**, Vol. 57, No. 9, pp. 2655-2662.

20. Bletsas, A., Dimitriou, A. G. and Sahalos, J. N., 2010, "Interference-limited Optimistic Relaying with Reactive Sensing", **IEEE Transactions on Wireless Communications**, Vol. 9, No.1, pp. 14-20.

21. Boyer, J., Falconer, D. D. and Yanikomaroglou, H., 2004, "Multihop Diversity in Wireless Relaying Channel", **Transactions on Communications**, Vol. 52, No.10, pp. 1820-1830.

22. Chaudhry, M. A. and Zubair, S. M., 2002, **On a Class of Incomplete Gamma Functions with Applications**, Chapman & Hall/CRC Press, Boca Raton, pp.1-222.

23. Chayawan, C., and Aalo, V. A. , 2002, "On the Outage Probability of Optimum Combining and Maximal Ratio Combining Schemes in An Interference-limited Rice Fading Channel", **IEEE Transactions on Communications**, Vol. 50, No. 4, pp. 532-535.

24. Chayawan, C., and Aalo, V. A. , 2002, "Performance Study of MRC Systems with Multiple Cochannel Interferers in A Non-Gaussian Multipath Fading Environment", **IEEE Vehicular Technology Conference**, Vol. 3, pp. 1720-1724.

25. Chen, S., Zhang, X., Liu, F. and Yang, D., 2010 "Outage Performance of Dual-hop Relay Network with Co-channel Interference", **IEEE Vehicular Technology Conference**, Vol.1, pp.1-5.

26. Cheng, J., Tellambura, C., and Beaulieu, N.C., 2004, "Performance of Digital Linear Modulations on Weibull Slow-fading Channels", **IEEE Transactions on Communications**, Vol. 52, No. 8, pp. 1265–1268.

27. Corazza, G.E. and Vatalalo, F., 1994, "A Statistical Model for Land Mobile Satellite Channels an Its Application to Nongeostationary Orbit Systems", **IEEE Transactions on Vehicular Technology**, Vol. 43, No. 3, pp. 738-742.

28. Coulson, A.J., Williamson, A.G., and Vaughan, R.G., 1998, "Improved Fading Distribution for Mobile Radio", **IEE Communications**, Vol. 145, No. 13, pp. 197–202.

29. Cui, J., Falconer, D.D. and Sheikh, A.U., 1997, " Performance Evaluation of Optimum Combining and Maximal Ratio Combining in the Presence of Co-channel Interference and Channel Correlation for Wireless Communication Systems", **Mobile Networks and Applications**, Vol. 2, pp. 315-324.

30. Erdelyi, A., et al., 1973, **Table of Integral Transforms**, 2nd ed., McGraw-Hill Press, New York, pp. 1-999.

31. Exton, H., 1976, **Multiple Hypergeometric Functions and Applications**, John Wiley Press, New York, pp.1-312.

32. Fante, R.L., 2001, "Central Limit Theorem: Use with Caution", **IEEE Transactions on Aerospace and Electronics Systems**, Vol. 37, No.2, pp. 739-740.

33. Farhadi, G. and Beaulieu, N. C., 2010, "A General Framework for Symbol Error Probability Analysis of Wireless Systems and Its Application in Amplify-and-

Forward Multihop Relaying", **IEEE Transactions on Vehicular Technology**, Vol. 59, No. 3, pp. 1505-1511.

34. Gao, H., Smith, P.J., and Clark, M.V., 1998, "Theoretical Reliability of MMSE Linear Diversity Combining in Rayleigh-fading Additive Interference Channels", **IEEE Transactions on Communications**, Vol. 46, pp. 666-672.

35. Gao, H., Smith, P.J. and Clark, M.V., 1999, "Exact SINR Calculations for Optimum Linear Combining in Wireless Systems", **Probability Engineering Information Sciences**, pp. 23-61.

36. Goldsmith, A.J., 2005, **Wireless Communications**, 2nd ed., Cambridge University Press, Cambridge, pp.1-454.

37. Gomadam, K. S. and Jafar, S. A., 2007 "Optimal Relay Functionality for SNR Maximization in Memory Relay Networks", **IEEE Journal on Selected Areas in Communications**, Vol. 25, No. 2, pp. 390-401.

38. Gradshteyn, I. S., Ryzhik. I. M., 2007, **Tables of Integrals, Series and Products**, 7th ed., Academic Press, New York, pp. 1-1159.

39. Hansen, F. and Meno, F.I., 1997, "Mobile Fading-Rayleigh and Lognormal Superimposed", **IEEE Transactions on Vehicular Technology**, Vol. 26, No. 4, pp. 332-335.

40. Hasna, M. O. and Alouini, M. S., 2003 "End-to-end Performance of Transmission Systems with Relays over Rayleigh-fading Channels", **IEEE Transactions on Wireless Communications**, Vol. 2, No.6, pp. 1126-1131.

41. Hasna, M. O. and Alouini, M. S., 2003 "Outage Probability of Multihop Transmission over Nakagami Fading Channels", **IEEE Communications Letters**, Vol. 7, No.5, pp. 216-218.

42. Hasna, M. O. and Alouini, M.-S., 2004, "A Performance Study of Dual-hop Transmissions with Fixed Gain relays," **IEEE Transactions on Wireless Communications**, Vol. 3, No.6, pp. 1963-1968.

43. Ho, M. J. and Stuber, G.L., 1999, "Co-channel Interference of Microcellular Systems on Shadowed Nakagami Fading Channels", **IEEE Vehicular Technology Conference,** Vol. 3, pp. 2308-2312.

44. Hossain, E., Kim, D.I. and Bhargava, 2011, **Cooperative Cellular Wireless Network**, 1st ed., Cambridge University Press, New York, pp. 1-514.

45. Ikki, S. S. and Aissa, S., 2010, "Performance Analysis of Dual-hop Relaying Systems in the Presence of Co-channel Interference", **IEEE Global Telecommunications Conferences**, Vol. 1, pp.1-5.

46. Karagiannidis, G. K., 2006, "Performance Bounds of Multihop Wireless Communications with Blind Relays over Generalized Fading Channels", **IEEE Transactions on Wireless Communications**, Vol. 5, No.3, pp. 498-503.

47. Karagiannidis, G. K., Tsiftsis, T.A. and Mallik, R. K., 2006 "Bounds for Multihop Relayed Communications in Nakagami-*m* Fading", **IEEE Transactions on Wireless Communications**, Vol. 54, No.1, pp. 18-22.

48. Kim, J. B. and Kim, D., 2010, "Exact and Closed-form Outage Probability of Opportunistic Decode-and-forward Relaying with Unequal-power Interferers", **IEEE Transactions on Wireless Communications**, Vol. 9. No.12.

49. Kourtis, S., and Tafazolli, R., 2002, "Modelling Cell Residence Time of Mobile Terminals in Cellular Radio Systems", **Electronics Letters**, Vol. 38, No.1, pp. 52–54.

50. Krikidis, I., Thompson, J. S., Mclaighlin, S. and Goertz, N., 2009, "Max-Min Relay Selection for Legacy Amplify-and-forward Systems with Interference",

IEEE Transactions on Wireless Communications, Vol. 8, No. 6, pp. 3016-3027.

51. Laneman J. N. and Wornell, G. W., 2000, "Energy-efficient Antenna Sharing and Relaying for Wireless Networks", **IEEE Wireless Communications and Networking Conference**, Vol.1, pp. 7-12.

52. Laneman, J. N., Tse, D. N. C., and Wornell, G. W., 2004, "Cooperative Diversity in Wireless Networks: Efficient Protocols and Outage Behavior", **IEEE Transactions Information Theory**, Vol. 50, pp. 3062-3080.

53. Lebedev, N. N., 1972, **Special Functions & Their Applications**, Dover Publications, New York, pp.1-343.

54. Lee, D. and Lee, J. H., 2010, "Outage Probability for Dual-hop Relaying Systems with Multiple Interferers over Rayleigh Fading Channels", **IEEE Transactions on Vehicular Technology**, Vol. 59, No. 9, pp. 333-338.

55. Lee, D. and Lee, J. H., 2011, "Outage Probability of Decode-and-forward Optimistic Relaying in a Multicell Environment", **IEEE Transactions on Vehicular Technology**, Vol. 60, No.4, pp.1925-1930.

56. Lee, I. H. and Kim, D., 2007, "Coverage Extension and Power Allocation in Dual-hop Space-Time Transmission with Multiple Antennas in Each Node", **IEEE Transactions on Vehicular Technology**, Vol. 56, No. 6, pp. 3524-3532.

57. Lutz, E., Cygan, D., Dippold, M., Dolainsky, F and Papke, W., 1991, "The Land Mobile Satellite Communication Channel: Recording, Statistics, and Channel Model", **IEEE Transactions on Vehicular Technology**, Vol. 40, pp.375-386.

58. Michel, K.O., 1990, **Applied Probability and Stochastic Processes in Engineering and Physical Sciences,** Wiley Press, New York, pp.1-486

59. Miller A. R. and Moskowitz, I. S., 1991 "Incomplete Weber Integrals of Cylindrical Functions", **Journal of Franklin Institute**, Vol. 328, No. 4, pp.445-457.

60. Miller, A. R., 2000, "Reduction of Generalized Incomplete Gamma Function, Related Kampe De Feriet Functions, and Incomplete Weber integrals", **Rocky Mountain Journal of Mathematics**, Vol. 39, No. 2, pp. 703-714.

61. Penfold, R., Vanden-Broeck, J. and Grandison, S., 2007, "Monotonicity of Some Modified Bessel Function Products", **Integral Transforms and Special Functions**, Vol. 18, No. 2, pp.139-144.

62. Peppas, K. P., 2009, "Performance Evaluation of Triple-branch GSC Diversity Receivers over Generalized-K Fading Channels," **IEEE Communications Letters**, Vol.13, No.11, pp. 829-831.

63. Proakis, J.G., 1989, **Digital Communications**, 2nd ed., McGraw-Hill, New York, pp. 27-98.

64. Rangaswamy, M., Weiner, D. and Ozturk, A., 1995, "Computer Generation of Correlated Non-Gaussian Radar Clutter", **IEEE Transactions on Aerospace And Electronics Systems**, Vol. 31, pp. 106-116.

65. Ray Liu, K.J., Sadek, K., Su, W. and Kwasinski, A., 2009, **Cooperative Communications and Networking**, 1st ed., Cambridge University Press, New York, pp. 1-623.

66. Sagias, N.C., and Mathiopoulos, T., 2005, "Switched Diversity Receivers over Generalized Gamma Fading Channels', **IEEE Communications Letters**, Vol. 9, No.10, pp. 871–873.

67. Sagias, N.C., Karagiannidis, G.K., Zogas, D.A., Mathiopoulos, P.T. and Tombras, G.S., 2004, "Performance Analysis of Dual Selection Diversity in

Correlated Weibull Fading Channels", **IEEE Transactions on Communications**, Vol. 52, No.7, pp. 1063–1067.

68. Sagias, Nikos C., Karagiannidis, G. K., Mathiopoulos, P. T., and Tsiftsis, T. A., 2006, "On the Performance Analysis of Equal-Gain Diversity Receivers over Generalized Gamma Fading Channels", **IEEE Transactions on Wireless Communications**, Vol. 5, No. 10, pp. 2967-2975.

69. Sahu, P.R., and Chaturvedi, A.K., 2005, "Performance Analysis of Predetection EGC Receiver in Weibull Fading Channel", **Electronics Letters**, Vol. 41, No. 2, pp. 85–86.

70. Salo, J., El-Sallabi, H. M. and Vainikainen, P., 2006, "Statistical Analysis of the Multiple Scattering Radio Channel", **IEEE Transactions on Antennas and Propagation**, pp. 3114-3124.

71. Senaratne, D. and Tellambura, C., 2010, "Unified Exact Performance Analysis of two-Hop Amplify-and-forward Relaying in Nakagami Fading", **Transactions on Vehicular Technology**, Vol. 59, No. 3, pp. 1529-1534.

72. Shah, A., and Haimovich, A. M., 2002, "Performance Analysis of Maximal Ratio Combining and Comparison with Optimum Combining for Mobile Radio Communications with Multiple Cochannel Interference", **IEEE Transactions on Vehicular Technology**, Vol. 49, pp. 1454-1463.

73. Shah, A., Haimovich, A. M., 1998, "Performance Analysis of Optimum Combining in Wireless Communications with Rayleigh Fading and Cochannel Interference," **IEEE Transactions on Communications**, Vol. 46, No. 4, pp. 473-479.

74. Shin, J.W., Chang, J.-H., and Kim, N.S., 2005, "Image Probability Distribution Based on Generalized Gamma function', **IEEE Signal Processing Letters**, 2005, Vol. 12, No. 4, pp. 325–328

75. Shin, J.W., Chang, J.-H., Kim, N.S., and Mitra, S.K., 2005, "Statistical Modeling of Speech Signals based on Generalized Gamma distribution', **IEEE Signal Processing Letters**, Vol. 12, No. 3, pp. 258–261.

76. Si, J. B., Li, Z. and liu, Z., 2010, "Outage Probability of Opportunistic Relaying in Rayleigh Fading Channels with Multiple Interferers", **IEEE Signal Processing Letters**, Vol. 17, No. 5, pp. 445-448.

77. Simon, M.K., and Alouini, M.S., 2006, **Digital Communications over Fading Channels**, 2nd ed., Wiley&Sons Press, New York, pp.1-345.

78. Stacy, E. W., 1962, "A Generalization of The Gamma Distribution", **Annual of Mathematical Statistics**, Vol. 33, No. 3, pp. 1187–1192.

79. Stuber, G.L., 2001, **Principles of Mobile Communications**, 2nd ed. Kluwer, Dordrecht.

80. Suraweera, H. A., Garg, H. K. and Nallanathan, A., 2010, "Performance Analysis of Two Hop Amplify-and-forward Systems with Interference at the Relay", **IEEE Communications Letters**, Vol. 14, No. 8, pp. 692-694.

81. Suraweera, H.A., Smith, P.J. and Shafi, M., 2010, "Capacity Limits and Performance Analysis of Cognitive Radio with Imperfect Channel Knowledge", **IEEE Transactions on Vehicular Technology**, Vol. 59, No. 4, pp.1811–1822.

82. Suzuki, H., 1977, "A Statistical Model for Urban Multipath Propagation", **IEEE Transactions on Communications**, Vol. 25, pp. 673-680.

83. Theodore, S.R., 1996, **Wireless Communications Principles and Practice**, Simon & Schuster Press, New Jersey, pp. 25-30.

84. Tian, S., Li, Y. and Vucetic, B., 2011, "Piecewise-and-forward Relaying in Wireless Relay Networks", **IEEE Signal Processing Letters**, Vol. 18, no. 5, pp.323-326.

85. Vakil, S. and Liang, B., 2008, "Cooperative Diversity in Interference Limited Wireless Networks", **IEEE Transactions on Wireless Communications**, Vol. 7, No. 8, pp. 3155-3195.

86. Weiner, M. M., 2006, **Adaptive Antenna and Receivers**, 1st ed. CRC Press, New York, pp.1-259.

87. Win, M. Z., Chrisikos, G. and Winters, J. H., 2000, "MRC Performance of M-ary Modulation in Arbitrarily Correlated Nakagami Fading Channels", **IEEE Communications Letters**, Vol. 4, No. 10, pp. 301–303.

88. Win, M. Z., Mallik, R. K. and Chrisikos G., 2003 "Higher Order Statistics of Antenna Subset Diversity", **IEEE Transactions on Wireless Communications**, Vol. 2, pp. 871–875.

89. Winter, J.H.,1984,"Optimum Combining in Digital Mobile Radio with Cochannel Interference", **IEEE Journal on Selected Areas in Communications**, Vol. 2, No. 4, pp. 528-539.

90. Yacoub, M.D., 2002, "The a-u Distribution: A General Fading Distribution", **IEEE International Symposium on Personal, Indoor and Mobile Radio Communications**, Vol. 2, pp. 629–633.

91. Yang, Q. and Kwak, K. S., 2009, "Outage Probability of Cooperative Relaying with Dissimilar Nakagami-m Interferers in Nakagami-m Fading", **IET Communications**, Vol. 3, No. 7, pp. 1179-1185.

92. Yao, K., 1973, "A Representation Theorem and Its Applications to Spherically Invariant Random Processes", **IEEE Transactions on Information Theory**,

Vol. 19, pp. 600–608.

93. Yilmaz, F., Kucurand O., Alouini, M.-S., 2010, "A Novel Framework on Exact Average Symbol Error Probabilities of Multihop Transmission over Amplify-and-Forward Relay Fading Channels", **IEEE International Symposium on Wireless Communication Systems**, Vol.1, pp. 546-550.

94. Zhong, C., Jin, S. and Wong, K. K., 2010, "Dual-hop Systems with Noisy Relay and Interference-limited Destination," **IEEE Transactions on Communications**, Vol. 58, No.3, pp. 764-768.

95. Zonoozi, M.M., and Dassanayake, P., 1997, "User Mobility Modeling and Characterization of Mobility Patterns", **IEEE Journal on Selected Areas in Communications**, Vol.15, No. 7, pp. 1239–1252.

APPENDIX A.

DERIVATION OF EQUATION (5.22)

In this section, we derive the closed form expressions for that the partial derivatives given in (5.22). From basic calculus in [13, eq.(2.34)], it can be shown that

$$D_x^n \left\{ (x^v) \right\} \Big|_{x=-b} = \frac{\Gamma(v+1)}{\Gamma(v-n+1)} x^{v-n} = (-1)^n (v+1)_n x^{v-n} \tag{A-1}$$

and

$$D_x^n (x+a)^{-u} = (-1)^n \frac{\Gamma(u+n)}{\Gamma(u)} x^{-u-n} = (-1)^n (u)_n (x+a)^{-u-n} \tag{A-2}$$

Substituting (A-1) and (A-2) in [38, eq.(0.42)], yields

$$D_x^n \left\{ \frac{x^v}{(x+a)^u} \right\} \Bigg|_{x=-b} = \frac{\Gamma(v+1)}{\Gamma(v-n+1)} x^{v-n} (x+a)^{-u} \sum_{k=0}^{n} \binom{n}{k} \frac{(-1)^k (u)_k}{(v-n+1)_k} \left(\frac{x}{x+a} \right)^k \Bigg|_{x=-b}$$

$$= \frac{\Gamma(v+1)}{\Gamma(v-n+1)} (-b)^{v-n} (a-b)^{-u} \sum_{k=0}^{n} \binom{n}{k} \frac{(-1)^k (u)_k}{(v-n+1)_k} \left(\frac{-b}{a-b} \right)^k$$

$$= \frac{\Gamma(v+1)}{\Gamma(v-n+1)} (-b)^{v-n} (a-b)^{-u} \sum_{k=0}^{n} \binom{n}{k} \frac{(-1)^k (u)_k}{(v-n+1)_k} \left(\frac{b}{b-a} \right)^k \tag{A-3}$$

The coefficients in (5.22) are given, respectively, by

$$\Xi_{1k} = \frac{1}{(N_R-k)!} \frac{d^{N_R-k}}{dx^{N_R-k}} \frac{x^{N_R+1} \left(x+\gamma+\Lambda_D + \lambda_{RD} N_D \right)}{\left(x+\gamma+\Lambda_D \right)^{N_D+1}} \Bigg|_{x=-\frac{\gamma(\gamma+1)}{\gamma+\Lambda_R}}$$

$$= \frac{1}{(N_R-k)!} \frac{d^{N_R-k}}{dx^{N_R-k}} \left\{ \frac{x^{N_R+2}}{\left(x+\gamma+\Lambda_D \right)^{N_D+1}} \Bigg|_{x=-\frac{\gamma(\gamma+1)}{\gamma+\Lambda_R}} \right.$$

$$\left. + \left(\gamma+\Lambda_D + \lambda_{RD} N_D \right) \frac{d^{N_R-k}}{dx^{N_R-k}} \frac{x^{N_R+1}}{\left(x+\gamma+\Lambda_D \right)^{N_D+1}} \right\} \Bigg|_{x=-\frac{\gamma(\gamma+1)}{\gamma+\Lambda_R}} \tag{A-4}$$

$$\Xi_{2k} = \frac{1}{(N_D+1-k)!} \frac{d^{N_D+1-k}}{dx^{N_D+1-k}} \frac{x^{N_R+1} \left(x+\gamma+\Lambda_D + \lambda_{RD} N_D \right)}{\left(x+\frac{\gamma(\gamma+1)}{\gamma+\Lambda_R} \right)^{N_R}} \Bigg|_{x=-(\gamma+\Lambda_D)}$$

$$= \frac{d^{N_R-k}}{dx^{N_R-k}} \left\{ \frac{x^{N_R+2}}{\left(x+\gamma+\Lambda_D \right)^{N_D+1}} \Bigg|_{x=-\frac{\gamma(\gamma+1)}{\gamma+\Lambda_R}} \right.$$

$$\left. + \left(\gamma+\Lambda_D + \lambda_{RD} N_D \right) \frac{d^{N_R-k}}{dx^{N_R-k}} \frac{x^{N_R+1}}{\left(x+\gamma+\Lambda_D \right)^{N_D+1}} \right\} \Bigg|_{x=-\frac{\gamma(\gamma+1)}{\gamma+\Lambda_R}} \tag{A-5}$$

Finally, using (A-3) in (A-4) and (A-5) results in the closed-form expressions for Ξ_{1k} and Ξ_{2k} given in (5.22a) and (5.22b), respectively.

APPENDIX B.

SPECIAL CASES OF INCOMPLETE WEBER INTEGRAL

In this appendix, we shown some special cases of the incomplete Weber integral given

by

$$K_{e^2_{u,v}}(p,x) = \int_0^x t^u e^{-pt^2} K_v(t)dt. \tag{B-1}$$

For the special cases of interest, it is shown that $K_{e^2_{u,v}}(p,x)$ may be written as the

follows:

(i) When $x \to \infty$, we have [38]

$$K_{e^2_{u,v}}(p,\infty) = \int_0^\infty t^u e^{-pt^2} K_v(t)dt$$

$$= \frac{1}{2^{(v+2)} p^{(u+v+1)/2}} \Gamma\left(\frac{u+v+1}{2}\right) \Gamma\left(\frac{u-v+1}{2}\right) \psi\left(\frac{u+v+1}{2}, 1+2v; \frac{1}{4p}\right) \tag{B-2}$$

(ii) When $p = 0$ we have [59, eq.(2.1)]

$$K_{e^2_{u,v}}(0,x) = \int_0^x t^u K_v(t)dt$$

$$= \frac{x^{u+1}}{(u-v+1)} \left\{ K_v(x)\,_1F_2\left(1; \frac{u-v+3}{2}, \frac{u+v+1}{2}; \frac{x^2}{4}\right) + \frac{xK_{v-1}(x)}{(u+v+1)}\,_1F_2\left(1; \frac{u-v+3}{2}, \frac{u+v+3}{2}; \frac{x^2}{4}\right) \right\} \tag{B-3}$$

(iii) When $u = v+1$ and $p = (2x)^{-1}$, we have [18], [60]

$$K_{e^2_{v+1,v}}\left((2x)^{-1},x\right) = -\frac{1}{2}(-x)^{v+1} e^{-(1/2)x} \left[(-1)^v v! e^x \Gamma\left(-v, \frac{x}{2}\right) - K_0(x) - 2\sum_{n=1}^v (-1)^n K_n(x) \right] \tag{B-4}$$

where $v = 0,1,2,3,...$ is an integer.

APPENDIX C.

DERIVATION OF EQUATION (5.43)

In this appendix, we derive the closed form expression for cdf of γ_1 and γ_2 given in (5.43). The cdf of γ_1 is given by [73, eq.(16)]

$$F_{\tilde{\gamma}_1}\left(\gamma_1\right) = \frac{N_R\gamma_1}{\Lambda_R}\,_2F_1\left(N_R+1,1;2;-\frac{\gamma_1}{\Lambda_R}\right) \tag{C-1}$$

where the Gauss hypergeometric function is defined as

$$_2F_1\left(v+1,1;2;-x\right) = \sum_{n=0}^{\infty}\frac{\left(v+1\right)_n\left(1\right)_n}{\left(2\right)_n\,n!}\left(-x\right)^n \tag{C-2}$$

with $v, x \neq 0$, and $(v)_n = \frac{\Gamma(v+n)}{\Gamma(v)}$. Using the fact that $(1)_n = n!$ and $(2)_n = (n+1)!$, and introducing $k = n+1$, (C-2) becomes

$$_2F_1\left(v+1,1;2;-x\right) = \frac{1}{v\left(-x\right)}\sum_{k=1}^{\infty}\frac{\left(v\right)_k}{k!}\left(-x\right)^k$$

$$= \frac{1}{vx}\left\{1-\sum_{k=0}^{\infty}\frac{\left(v\right)_k}{k!}\left(-x\right)^k\right\}$$

$$= \frac{1}{vx}\left\{1-\left(1+x\right)^{-v}\right\} \tag{C-3}$$

where we have used [38, eq.(9.121)]. Using (C-3), the closed-form expression for $F_{\tilde{\gamma}_1}\left(\gamma_1\right)$ is given in (5.43a). Similar to $F_{\tilde{\gamma}_1}\left(\gamma_1\right)$, the closed-form expression for $F_{\tilde{\gamma}_2}\left(\gamma_2\right)$ is given in (5.43b).

APPENDIX D.

DERIVATION OF EQUATION (6.43)

In this section, we provide a proof for (6.43). The confluent hypergeometric function of the second kind may be written in contour integral form as [38, eq. (13.2.10)]

$$\Psi(a,b;x) = \frac{1}{2\pi j} \int_{-j\infty}^{j\infty} \frac{\Gamma(-s)\Gamma(a+s)\Gamma(1+a-b+s)}{\Gamma(a)\Gamma(1+a-b)} x^{-(a+s)} ds, \tag{D-1}$$

where $j = \sqrt{-1}$, and the contour must separate the poles of $\Gamma(-s)$ from those $\Gamma(a+s)\Gamma(1+a-b+s)$. Using (D-1), the left hand side of (6.43) becomes

$$\mathcal{L}^{-1}\left\{t^{c-1}\prod_{n=1}^{N}\psi(a_n,b_n;\sigma_n t)\right\}$$

$$= \frac{1}{(2\pi j)^N} \int_{-j\infty}^{j\infty} \cdots \int_{-j\infty}^{j\infty} \mathcal{L}^{-1}\left\{t^{c-1-\left(\sum_{n=1}^{N} s_n+a_n\right)}\right\} \prod_{n=1}^{N}\left[\sigma_n^{-(s_n+a_n)} \frac{\Gamma(-s_n)\Gamma(a_n+s_n)\Gamma(1+a_n-b_n+s_n)}{\Gamma(a_n)\Gamma(1+a_n-b_n)}\right] ds_n,$$

$$\tag{D-2}$$

where the nth contour in (D-2) is chosen to separate the poles of $\Gamma(-s_n)$ from those of $\Gamma(a+s_n)\Gamma(1+a-b+s_n)$. The inverse transform in the brackets may be obtained from [38, eq. (17.13.3)] as

$$\mathcal{L}^{-1}\left\{t^{c-1-\sum_{n=1}^{N}(s_n+a_n)}\right\} = \frac{x^{\sum_{n=1}^{N}(s_n+a_n)-c}}{\Gamma\left(\sum_{n=1}^{N}(s_n+a_n)+1-c\right)}. \tag{D-3}$$

Substituting (D-3) in (D-2), we have

$$\mathcal{L}^{-1}\left\{t^{c-1}\prod_{n=1}^{N}\psi(a_n,b_n;\sigma_n t)\right\}$$

$$= \frac{1}{(2\pi j)^N} \int_{-j\infty}^{j\infty} \cdots \int_{-j\infty}^{j\infty} \frac{x^{\sum_{n=1}^{N}(s_n+a_n)-c}}{\Gamma\left(\sum_{n=1}^{N}(s_n+a_n)+1-c\right)} \prod_{n=1}^{N}\left[\sigma_n^{-(s_n+a_n)} \frac{\Gamma(-s_n)\Gamma(a_n+s_n)\Gamma(1+a_n-b_n+s_n)}{\Gamma(a_n)\Gamma(1+a_n-b_n)}\right] ds_n$$

$$= \frac{1}{(2\pi j)^N} \int_{-j\infty}^{j\infty} \cdots \int_{-j\infty}^{j\infty} \frac{x^{-c}}{\Gamma\left(\sum_{n=1}^{N}(s_n+a_n)+1-c\right)} \prod_{n=1}^{N}\left[\left(\frac{x}{\sigma_n}\right)^{(s_n+a_n)} \frac{\Gamma(-s_n)\Gamma(a_n+s_n)\Gamma(1+a_n-b_n+s_n)}{\Gamma(a_n)\Gamma(1+a_n-b_n)}\right] ds_n$$

$$\tag{D-4}$$

Note that the contour integrals in (D-4) may be converted into infinite series as [38]

$$\mathcal{L}^{-1}\left\{t^{c-1}\prod_{n=1}^{N}\psi(a_n,b_n;\sigma_n t)\right\}$$

$$=\sum_{i_1=0}^{\infty}\cdots\sum_{i_N=0}^{\infty}\frac{x^{\sum_{n=1}^{N}(i_n+a_n)-c}}{\Gamma\left(\sum_{n=1}^{N}(i_n+a_n)+1-c\right)}\prod_{n=1}^{N}\left[\sigma_n^{-(i_n+a_n)}\frac{\Gamma(a_n+i_n)\Gamma(1+a_n-b_n+i_n)}{\Gamma(a_n)\Gamma(1+a_n-b_n)\,(-i_n)!}\right]$$

$$=\frac{x^{a_T-c}\left[\prod_{n=1}^{N}\sigma_n^{-a_n}\right]}{\Gamma\left(\sum_{n=1}^{N}a_n+1-c\right)}\sum_{i_1=0}^{\infty}\cdots\sum_{i_N=0}^{\infty}\frac{1}{\left(\sum_{n=1}^{N}a_n+1-c\right)_{i_T}}\prod_{n=1}^{N}\left[(a_n)_{i_n}(1+a_n-b_n)_{i_n}\frac{(-x/\sigma_n)^{i_n}}{i_n!}\right]\quad\text{(D-5)}$$

where $a_T=\sum_{n=1}^{N}a_n$ and $i_T=\sum_{n=1}^{N}i_n$. Finally, the multiple infinite series in (D-5) may be

expressed in terms of the Lauricella function [31], to give the result in (6.43).

APPENDIX E.

DERIVATION OF EQUATION (6.46)

Substituting (6.26) in (6.45), the ABER for multihop DF relay system can be given by

$$\bar{P}_b = \frac{1}{2\pi} \int_0^1 s^{-1/2} (1-s)^{-1/2} \, ds$$

$$- \frac{1}{2\pi} \left(\prod_{n=1}^{L_d} \frac{\lambda_r}{b} \right)^{m_r} \sum_{r=1}^{L_d} \sum_{j=1}^{m_r} \Xi_{j,r} \int_0^\infty \exp(-\gamma a \varpi) \left(\gamma + \frac{\lambda_r}{b} \right)^{-j} \int_0^1 s^{-3/2} (1-s)^{-1/2} \exp\left(-\gamma / s\right) ds \, d\gamma$$

$$(\text{E-1})$$

To obtain the result of (E-1), in this appendix we consider the integral term given by

$$\Re = \int_0^\infty \exp(-A\gamma)(B\gamma + 1)^{-C} \int_0^1 s^{-3/2} (1-s)^{-1/2} \exp\left(-\gamma / s\right) ds \, d\gamma \qquad (\text{E-2})$$

where $A, C \geq 0$, $B > 0$ are the arbitrary constants.

Next, use the identity in [15] to give

$$\exp(-\gamma / s) = G_{0,1}^{1,0} \left(\frac{\gamma}{s} \bigg| \frac{-}{0} \right) = G_{1,0}^{0,1} \left(\frac{s}{\gamma} \bigg| \frac{1}{-} \right) \qquad (\text{E-}$$

3)

where $G_{m,n}^{p,q}(.)$ is the Meijer-G function [38]. Substituting (E-3) in (E-2) and using [38, eq. (7.811.2), eq. (9.31.1)], yields

$$\Re = \int_0^\infty \exp(-\gamma A)(B\gamma + 1)^{-C} \int_0^1 s^{-3/2} (1-s)^{-1/2} G_{1,0}^{0,1} \left(\frac{s}{\gamma} \bigg| \frac{1}{-} \right) ds \, d\gamma$$

$$= \Gamma(1/2) \int_0^\infty \exp(-\gamma A)(\gamma B + 1)^{-C} G_{2,1}^{0,2} \left(\frac{1}{\gamma} \bigg| \frac{3/2,1}{1} \right) d\gamma$$

$$= \Gamma(1/2) \int_0^\infty \exp(-\gamma A)(\gamma B + 1)^{-C} G_{1,0}^{0,1} \left(\frac{1}{\gamma} \bigg| \frac{3/2}{-} \right) d\gamma \qquad (\text{E-4})$$

Next using the properties of Meijer-G function in [38, eq. (9.31.2), eq.(9.31.5)], (E-4) may be shown to be given by

$$\Re = \Gamma(1/2) \int_0^\infty \exp(-\gamma A)(\gamma B + 1)^{-C} G_{0,1}^{1,0} \left(\gamma \bigg| \frac{-}{-1/2} \right) d\gamma$$

$$= \Gamma(1/2) \int_0^\infty \gamma^{-1/2} \exp(-\gamma A)(\gamma B + 1)^{-C} G_{0,1}^{1,0} \left(\gamma \left| \begin{matrix} - \\ 0 \end{matrix} \right. \right) d\gamma$$

$$= \Gamma(1/2) \int_0^\infty \gamma^{-1/2} (\gamma B + 1)^{-C} \exp(-\gamma \{A+1\}) d\gamma$$

$$= \Gamma(1/2) \Gamma(1/2) B^{-1/2} \psi \left(1/2; 3/2 - C; \frac{\{A+1\}}{B} \right). \tag{E-5}$$

Using (E-5), the ABER for multi-hop DF relay system is shown in (6.46).

CURRICULUM VITAE

NAME: Lt. Termpong Soithong

DATE OF BIRTH: 27 March 1982

EDUCATIONAL RECORD:

High School Armed Forces Academies Preparatory School, 2000.

Bachelor's Degree Bachelor of Engineering

(Electrical Engineering) with the Second Class Honors

Royal Thai Naval Academy, 2004.

Master's Degree Master of Engineering

(Electrical and Information Engineering)

King Mongkut's University of Technology Thonburi,

2007.

Doctoral Degree Doctor of Philosophy

(Electrical and Computer Engineering)

King Mongkut's University of Technology Thonburi,

2011.

WORKING EXPERIENCE

- Communications Officer, Naval Communications Department, Royal Thai Navy, 2004-Present.
- Visiting Researcher, Department of Computer & Electrical Engineering and Computer Science,   Florida Atlantic University, Boca Raton, USA, August 1 – December 31, 2010.

PUBLICATIONS

Journal Papers

[1] T. Soithong, V. A. Aalo, G. P. Efthymoglou, and C. Chayawan, "Performance of Multihop Relay Systems with Co-channel Interference in Rayleigh Fading Channels," **IEEE Communications Letters***,* Vol.15, No.8, pp. 836-838, 2011.

[2] T. Soithong, V. A. Aalo, G. P. Efthymoglou, and C. Chayawan, "Outage Analysis of Multihop Relays Systems in Interference-limited Nakagami Fading Channels," **IEEE Transactions on Vehicular Technology**, Vol.61, No.3, pp. 1451-1457, 2012.

Conference Papers

[3] T. Soithong and C. Chayawan, " Performance Analysis of Optimum Combining with Multiple Co-Channel Interferers in Non-Gaussian Fading Channels," **70th IEEE Vehicular Technology Conference (VTC)**, Vol.1 pp.1-5, USA, 2009.

[4] T. Soithong, V. A. Aalo, G. P. Efthymoglou, and C. Chayawan, "End-to-End Performance of Multihop Transmission Systems in a Rayleigh Fading Environment," **IEEE Global Telecommunications Conferences (GLOBECOM)**,Vol.1.pp.1-6, Texas USA, 2011.